Stabilization and Synchronization of Networked Mechanical Systems

Sujit S. Nair

A Dissertation

Presented to the Faculty

of Princeton University

in Candidacy for the Degree

of Doctor of Philosophy

Recommended for Acceptance

by the Department of

Mechanical & Aerospace Engineering

April, 2006

Abstract

The main theme of this thesis is coordination and stabilization of a network of mechanical systems or rigid bodies to achieve synchronized behaviour. The idea is to use controls derived from potentials to couple the systems such that the closed-loop system is also a mechanical system with a Lagrangian structure. This permits the closed-loop Hamiltonian to be used as a Lyapunov function for stability analysis.

It is a big challenge to develop a provable, systematic methodology to control and coordinate a network of systems to perform a given task. The control law should be robust enough to handle environment uncertainties, avoid obstacles and collisions and keep the system formation going. The fact that these systems may even have unstable dynamics makes the problem even more interesting and exciting both from a theoretical and applied point of view. This work investigates the coordination problem when each individual system has its own (maybe unstable) dynamics; this distinguishes this work from many other recent works on coordination control where the individual system dynamics are assumed to be single/double integrators.

We build coordination techniques for three kinds of systems. The first one consists of underactuated Lagrangian systems with Abelian symmetry groups lacking gyroscopic forces. Asymptotic stabilization is proved for two cases, one which yields convergence to synchronized motion restricted to a constant momentum surface and one in which the system converges asymptotically to a relative equilibrium.

Next we consider rigid body systems where the configuration space of each individual body is the non Abelian Lie group $SO(3)$ or $SE(3)$. In the $SO(3)$ case, the

asymptotically stabilized solution corresponds to each rigid body rotating about its unstable middle axis and all the bodies synchronized and pointing in a particular direction in inertial space. In the $SE(3)$ case, the asymptotically stabilized solution corresponds to each rigid body rotating about its unstable middle axis and translating along its middle axis and the whole network synchronized and moving along a particular direction in inertial space.

We conclude with a brief summary of the results and with a note on numerous directions in which this work can be extended.

Acknowledgements

Firstly, I would like to thank my advisor, Professor Naomi Leonard for her support, inspiration and patience during my graduate school years. I also thank her for giving me the freedom and flexibility on my research topic and for putting immense trust in me. I am also thankful to her for allowing me to take the numerous mathematics courses I have taken in Princeton.

I would like to acknowledge my thesis readers Professor Clancy Rowley and Professor Craig Woolsey for their valuable time and comments. Their insights helped improve the dissertation considerably.

I would like to thank everyone in the MAE department and acknowledge all the staff members who have helped me all along.

Princeton University has provided a very pleasant and vibrant environment for my work. Apart from the academics, it has also provided a very good forum for exchange of various cultural experiences and outlooks. A special thanks goes to my friends in Association of South Asians in Princeton, Princeton Peace Network, Drishti, Princeton Association for India's Development and the International Centre. I would also like to thank all my past roommates for enriching my experience in Princeton.

I am grateful to my teachers at IIT Bombay, who shaped my outlook towards science. Some have left a lasting impression on me.

Many good times were spent with my sister Swarni and brother-in-law Biju. Their company has been a pleasant break from my work. I would also like to thank Matthew, Anu, Babu and Roy for their hospitality and for always keeping their doors open for

me.

I am indebted to my parents, Usha and Sreenivasan, for their love and care. Finally, a special thanks goes to my wife Rajani for her understanding, love and patience over the years of my graduate school life.

Contents

List of Figures

Chapter 1

Introduction

1.1 Theme

Coordinated control of vehicles has gained a lot of interest in recent times. Advances in computational power, practical applications like ocean sampling and interferometry have contributed towards increasing the focus on the coordination problem. Mobile sensor networks are expected to provide better data about a distributed environment if the sensors can be made to cooperate towards optimal coverage and efficient coordination [18, 7]. Networks of communicating, sensor-equipped autonomous vehicles are of interest in a growing number of applications; for example, a fleet of underwater gliders was used collectively for adaptive ocean sampling in Monterey Bay, California in August 2003 [21]. Formation control of UAVs is considered in [27, 20].

It is a big challenge in control theory to come up with control laws for such problems. The control law should not only be able to coordinate these vehicles but should also be robust enough to noise and environmental uncertainties. The control law should also take care that the vehicles are able to avoid collisions with each other and obstacles in their pathways.

The coordination problem becomes more difficult when the vehicle dynamics are considered and the control is underactuated. Underactuated control refers to the case

in which the number of control inputs is fewer than the number of degrees of freedom of the system. The theme of this thesis is coordination of vehicles when they have unstable dynamics and are also possibly underactuated. Many of the recent works in the coordination literature are not directly applicable in this setting. In our approach, we consider the stabilization part of the problem and the coordination part together. We show that it might not even be possible to separate these two sides of the problem under certain circumstances. A central role in this thesis is played by energy-based control and geometric mechanics tools. We show how these techniques can be used to achieve stabilization and coordination simultaneously.

1.2 Background

Much of the recent work in coordinated control explores coordination and cooperative control with very simple dynamical systems, e.g., single or double integrator models (e.g., [26, 40, 41]). Double integrator models along with gyroscopic forces are considered in [17] to tackle the problem of coordination with collision avoidance. Nonholonomic models are studied in [19]. A network of kinematic models with steering controls is considered in [44] and closed-loop convergence to different types of organized motion is studied.

These authors deliberately choose to focus on the coordination issues independent of stabilization issues. Some of these problems were motivated by a search for theoretical explanation of models for swarm behaviour in biological systems or an interest in designing steering laws to generate realistic-looking coordinated motion for computer graphics purposes.

On the other hand, for networks of autonomous systems such as unmanned helicopters or underwater vehicles, stability issues are important, and it may not always be possible (or desirable) to decouple the stabilization problem from the coordination problem. In [23], an extension to a previous work ([22]) on UAV motion planning is

presented for identical multiple-vehicle stabilization and coordination. The single vehicle motion planning was based on the interconnection of a finite number of suitably defined motion primitives. The problem was set in such a way that multiple-vehicle motion coordination primitives are obtained from the single-vehicle primitives. The technique is applied to motion planning for a group of small model helicopters.

1.3 Thesis Contributions

In this thesis, the two main design objectives are as follows:

1. Stabilize individual vehicles and coordinate a group of such vehicles.

2. For the stabilization part, design controls which respect the mechanical nature of the system.

We now discuss these points in more detail. In many problems, it might not be desirable or possible to separate the stabilization problem from the coordination problem. For example, consider the case of a network of planar, inverted-pendulum-on-a-cart systems with underactuated dynamics. In this system, the only control input is the force input on the cart and there is no torque input to the swinging pendulum. The goal is to stabilize the individual pendulum in its upright position and to synchronize the dynamics across the network. Here, it is not possible to choose controls which cancel the dynamics of the system to get a double integrator model as a result. Hence, none of the methods in the references given above are directly applicable to this problem as they assume that the individual system is a single or double integrator system. Hence, for example, a network of planar pendulum/cart system cannot be stably synchronized using their methodology. It also becomes critical that the coordination control, while trying to synchronize the network, does not destabilize the individual systems.

A related problem of coordinating rigid bodies is considered in [25]. However, in that paper, the focus is on the reduction of the coupled multibody dynamics. Controls

are derived from a potential that depends on the relative attitudes and positions of the individual systems. Semi-direct product reduction theory is applied and reduced equations of motion are derived. Stability is proved only for certain restricted cases due to the lack of availability of Casimir functions.

In [46], the authors consider the problem of synchronizing a group of satellites. However, their control law cancels all the natural dynamics of the individual rigid bodies. In our work, we do not destroy the Hamiltonian structure of the system, thereby allowing us to use the readily available Hamiltonian energy function for stability analysis. In [46], the authors also land up having a fully actuated system in order to cancel the dynamics, whereas, in our approach we can achieve the same goal with an underactuated system. This is the main advantage of using an energy-based control. Since the closed-loop system is Hamiltonian, we are also able to use the Energy-Momentum method, amended potentials and other such tools to study the stability of relative equilibria of the network [33].

For systems like the planar inverted pendulum on a cart, we make further developments that build on on the method of Controlled Lagrangians (CL) to stabilize and synchronize the network. The method of Controlled Lagrangians and the equivalent Interconnection Damping Assignment - Port Based Control (IDA-PBC) method are energy-based methods to stabilize underactuated mechanical systems (see [10, 8, 42]). The former technique is used to design controls to stabilize a class of underactuated mechanical systems by shaping its Lagrangian. For a mechanical system, Dirichlet's theorem implies that an equilibrium is stable if the energy is an extremum at the equilibrium point. In a number of important and challenging physical examples with instabilities, the kinetic energy is positive definite and potential energy is negative definite at the equilibrium point. The method of CL gives an algorithm to design controls such that the closed loop system has a negative definite kinetic energy at the equilibrium point, which implies from Dirichlet's theorem that the equilibrium is stabilized.

1.4 Outline of Thesis

In Chapter 2, we briefly review some mathematical concepts and tools which will be used in the later parts of the thesis. This chapter also serves to set the notation for later chapters.

In Chapter 3, we review the method of CL in more detail and demonstrate how to achieve stabilization for a network of mechanical systems by introducing additional potential terms to couple the individual systems. The systems we consider belong to the class of mechanical systems satisfying the Simplified Matching Conditions (SMC). Briefly, SMC systems have Abelian symmetry and lack gyroscopic coupling between the symmetry and non symmetry directions. We show that it is possible to choose coupling potentials carefully so that the closed-loop network is also a SMC system. The control gains are chosen so that the individual system is stabilized and synchronization is achieved for the network. Next, dissipation is added to achieve two kinds of asymptotic stability. One corresponds to synchronization of the network on a constant momentum surface. The other corresponds to asymptotic stability of a synchronized relative equilibrium for the network. We will illustrate our results with the example of a network of three inverted pendulum cart systems.

In Chapter 4, we demonstrate how to derive the reduced equations of motion using Lagrangian reduction for a network of systems with individual configuration spaces as the Lie groups $SO(3)$ or $SE(3)$. We consider n such systems and couple them using potentials. The reduced equations are also derived in [25] using semi-direct product reduction theory. Using the notion of a connection on a bundle, we derive the reduced equations on the Lagrangian side using the theory developed in [14].

In Chapter 5, we demonstrate how to achieve synchronization of a network of rigid bodies, each of which belongs to the non Abelian Lie groups $SO(3)$ or $SE(3)$. We introduce coupling using potentials that depend only on the relative attitudes and position vectors among bodies. The bodies we consider are models for rigid spacecraft in free space and underwater vehicles in potential flow with coincident

centre of gravity and centre of buoyancy. We discuss the Energy Momentum method and its interpretation for the rigid bodies. Stability is proved for the following kinds of synchronization motions:

1. For the $SO(3)$ network, the solution we stabilize is the case when the bodies are all aligned and rotating about their unstable middle axis, which itself is pointing in a prescribed direction in free space.

2. For the $SE(3)$ network, the solution we stabilize is the case when the bodies are aligned in orientation and position, each one is rotating about and translating along its unstable middle axis which in turn is pointing in a particular direction in inertial space.

In Chapter 6, we add dissipation terms to asymptotically stabilize the solutions we stabilized in Chapter 5. The relevant theory is developed to make rigorous the proof of asymptotic stability. We will illustrate the results with a simulation for a network of three rigid bodies in $SO(3)$ or $SE(3)$.

We conclude in Chapter 7 by discussing major contributions of this thesis and the various directions this work can be taken in the future.

Chapter 2

Mathematical Background

This chapter gives a basic introduction to mathematical tools which are used throughout the thesis. It also serves to set the notation used in the rest of the chapters. We define and illustrate relevant notions from differential geometry and geometric mechanics including differentiable manifolds, symmetry, momentum maps and locked inertia tensors. We will keep the discussion in this chapter at an informal level. References for contents in this chapter are [45, 12, 3, 2, 1, 34, 39].

Many of the models used in the cooperative control literature can be put into two categories, kinematic models and dynamical models. In our work, we use dynamical models, by which we mean equations that follow Newton's second law relating force and acceleration in an inertial frame. Our motivation in using dynamical models stems from the fact that in our work, we concentrate on stabilizing and coordinating a group of mechanical systems using external forces or torques.

2.1 Variational Principle

Throughout this thesis, we study mechanical systems with differential equations of motion that arise from the *action principle* in classical mechanics. The resulting differential equation is called the Euler-Lagrange equation. What the action principle

says is the following. There is a function, called the *action function*, which depends upon time, the system state, the time derivatives of the system state and the path followed in configuration space from one point to another. All these parameters are assumed to be smooth. For simple mechanical systems, the *action function* is usually the difference between the kinetic and potential energies. The path which the system takes in its configuration space is such that the action function is minimized. Making these ideas mathematically rigourous leads us into notions of differentiable manifolds and in particular Riemannian geometry.

2.2 Smooth Manifolds and Riemannian Geometry

The set of all configurations of a system is called the *configuration space*. For example, the set of all configurations of a pendulum with one end fixed is the circle S^1. The set of all configurations of a point mass in space is the three-dimensional Euclidean space denoted by $\mathbb{R}^3$. The configuration space of a double pendulum is the torus T^2 and that of an inverted pendulum on a cart is $\mathbb{R} \times S^1$. The configuration space of a typical mechanical system has the structure of what is called a differentiable manifold. $S^2, \mathbb{R}^3, T^2$ and $\mathbb{R} \times S^1$ are all very good illustrative examples of what are called differentiable manifolds. We now look at this idea more formally.

An *$n-$dimensional topological manifold* without boundary M is a topological Hausdorff space which locally looks like an $n-$dimensional Euclidean space, i.e., for each point p in M, there is a neighbourhood U_p of p in M and a continuous map with continuous inverse $\phi : U_p \to \mathbb{R}^n$. ϕ is called a *homeomorphism* from U_p to $\mathbb{R}^n$ and each such neighbourhood U_p is called a *chart* for this manifold and is denoted by (U_p, ϕ). On this manifold, it makes sense to talk of continuity of a function $f : M \to \mathbb{R}$ from M to the real line $\mathbb{R}$ as M is itself a topological space. But despite the fact that M locally looks like $\mathbb{R}^n$, it does not make sense to talk of differentiability using such charts without further restrictions. For example, suppose that we define

f to be differentiable at a point p if for a chart U_p, the map $f \circ \phi^{-1} : \mathbb{R}^n \to R$ is differentiable. This definition of differentiability runs into problem if we consider for example another nieghbourhood V_p of p with the homeomorphism $\psi : V_p \to \mathbb{R}^n$. Now, $f \circ \psi^{-1} = f \circ \phi^{-1} \circ (\phi \circ \psi^{-1})$. Therefore, $f \circ \psi^{-1}$ is differentiable only if $\phi \circ \psi^{-1}$ is differentiable. This need not hold true for any two charts. Whenever this does hold, such charts are called *smoothly compatible* with each other. A family of smoothly compatible charts covering M is called an *atlas* for M. A particular chart (U_p, ϕ) is also called a coordinate system on M around point p. It can be shown that each such atlas is contained in a unique maximal atlas for M obtained by adding all charts of M which are smoothly compatible to the charts already contained in the original atlas. We denote this unique maximal atlas by A.

Definition 2.2.1 *A* differentible manifold *or a* smooth manifold *is a pair* (M, A) *where* A *is a maximal atlas for* M*.*

The atlas for M is also referred to as the differentiable structure for M. If the dimension of M is m, we will sometimes denote this manifold by M^m.

Examples of smooth manifold

1. $(\mathbb{R}^3, A_{\text{id}})$ is a smooth manifold with the maximal atlas A_{id} containing the trivial chart $\{(\mathbb{R}^3, \text{id})\}$ and all charts smoothly compatible with it. Here, id is the identity map.

2. $(\mathbb{R}, A)$ is a smooth manifold with the maximal atlas A containing the chart $\{(\mathbb{R}, x \mapsto x^3)\}$ together with all charts smoothly compatible with it.

Definition 2.2.2 *A map* $F : M^m \to N^n$ *is called a* smooth map *at a point* $p \in M$ *if* $\psi \circ F \circ \phi^{-1}$ *is smooth as a map from* $\mathbb{R}^m$ *to* $\mathbb{R}^n$ *for any coordinate chart* (U_p, ϕ) *and* $(V_{F(p)}, \psi)$ *around* p *and* $F(p)$ *respectively.*

If F is smooth for one pair of coordinate systems, it is seen to be true for any other pair.

Definition 2.2.3 *A map $F : M \to N$ is smooth if it is smooth at each point $p \in M$.*

Two smooth manifolds (M, A) and (N, B) are called diffeomorphic if there is a one-one onto smooth map $F : M \to N$ such that the inverse map F^{-1} is also smooth. The manifolds $(\mathbb{R}, A_{\text{id}})$ and $(\mathbb{R}, A)$ in example 2 above can be shown to be diffeomorphic.

Submanifold: A submanifold of M is a subset $S \subset M$ with the property that for each $s \in S$ there is a chart (U_s, ϕ) in M with the property $\phi : U_s \to \mathbb{R}^k \times \mathbb{R}^{n-k}$ and $\phi(U_s \cap S) = \phi(U_s) \cap (\mathbb{R}^k \times 0)$

It is a well known theorem of Whitney [45] that any abstract manifold is diffeomorphic to a submanifold of $\mathbb{R}^N$ for some N. Hence, for understanding purposes at least, any manifold can be thought of as a subset of some Euclidean space.

Consider a point moving in $\mathbb{R}^3$. Let its position at time t be $\boldsymbol{x}(t) = (x(t), y(t), z(t))$. Its velocity vector is given by $\dot{\boldsymbol{x}}(t) = (\dot{x}(t), \dot{y}(t), \dot{z}(t))$. Recall that the derivative $\dot{\boldsymbol{x}}(t)$ is calculated by taking the limit $\lim_{h\to 0} \dfrac{\boldsymbol{x}(t+h) - \boldsymbol{x}(t)}{h}$. Since $\boldsymbol{x}(t+h)$ and $\boldsymbol{x}(t)$ belong to the same vector space $\mathbb{R}^3$, we are able to compute their difference in the calculation above. However, in general, if x, y, z are local coordinates for an arbitrary manifold, it is not obvious how we make sense of the above operations in a coordinate independent way. For this, we need to define tangent vectors to a smooth manifold at a particular point.

To each point p of a differentiable manifold M, one can attach a *tangent space*, a real vector space which intuitively contains all possible velocity vectors when one passes through the point p in all possible directions. Elements of the tangent space at p are called *tangent vectors* at p. Here is one of the many ways in which tangent vectors can be defined.

Consider a smooth manifold M and a point p in it. Two smooth curves $c_i : (-1, 1) \to M,\ i = 1, 2$ passing through the point p, i.e., $c_i(0) = p$ are called equivalent

if given any chart (U_p, ϕ) around p,

$$\frac{d}{dt}(\phi \circ c_1)(0) = \frac{d}{dt}(\phi \circ c_2)(0).$$

A tangent vector v at p is an equivalence class of such smooth curves. It can be shown that this equivalence relation is independent of the coordinate chart we use.

Definition 2.2.4 *The set of all tangent vectors at p is called the* tangent space *of M at p and is denoted by T_pM.*

The tangent space at p is a real vector space with dimension the same as that of M. Any vector belonging to the tangent space at a point p acts on a smooth function and gives the directional derivative of the function in the direction of the vector. Thus, to each tangent vector, we can associate in an unambiguous way a function operator. If the local coordinates around p are denoted by $x : U_p \to \mathbb{R}^n$, i.e., if $q \in M$, then $x(q) \in \mathbb{R}^n$, then the basis for the tangent space at p is spanned by $\frac{\partial}{\partial x^i} \mid_p$ for $i = 1, \ldots, n$. Here, the notation $\frac{\partial}{\partial x^i} \mid_p$ denotes the operator which takes a smooth function on the manifold and gives a real number as follows $\frac{\partial}{\partial x^i} \mid_p (f) = \frac{\partial f}{\partial x^i} \mid_p$. Similarly, we can denote a basis element of the cotangent space, which is the dual to the tangent space by $dx^i \mid_p$. Its action on a basis element $\frac{\partial}{\partial x^j} \mid_p$ is given by $dx^i \mid_p \left(\frac{\partial}{\partial x^j} \mid_p \right) = 1$ if $i = j$ and 0 if $i \neq j$.

Definition 2.2.5 *The tangent bundle of M, denoted by TM is defined as*

$$TM = \{(p, v) \mid p \in M, v \in T_pM\}$$

The tangent bundle TM is itself a smooth manifold with dimension equal to twice the dimension of M.

When one introduces the notion of length, volume and angle to a manifold, one gets what is called a *Riemannian manifold.* A Riemannian manifold is obtained by assigning a metric to each tangent space T_pM which varies smoothly as p varies

smoothly over M. Before getting into details, it will help to briefly look into the theory of tensors over vector spaces.

Tensors are generalization of quantities like scalars and vectors. They are geometrical objects with intrinsic meanings, i.e., properties which do not depend upon the coordinates or the frame of reference. Hence, tensors along with their derivaties are used in formulating physical laws so that the results have physical meaning. Scalars, vectors and covectors are very good illustrative examples of tensors. Tensors can be combined with each other using tensor products to generate new higher dimensional tensors. A *metric tensor* is a symmetric bilinear positive form over a vector space. As a map, it takes two vectors and gives a real number in a bilinear manner. Tensors are denoted by the components along with their indices. For example, a vector is denoted by v^i and a covector by u_i. Scalars being tensors of rank zero have no indices on them. Tensor notations helps provide a concise way to write vector identities. For example, the scalar obtained by the action of a covector u_i on a vector v^i is written as $u_i v^i$, where the repeated indices means we are summing over it. Metric tensors are indicated by g_{ij} and one appreciates the tensor notation when the scalar obtained by the action of the metric tensor on two vectors v^i and w^i is written as $g_{ij}v^i w^j$. The summation convention holds here as well.

Tensor components change when one changes the coordinate system. For example, if V denotes a vector space and $T : V \to V$ denotes a linear coordinate change a vector $\boldsymbol{v}$ in original coordinates (written as a column vector) will have new components given by $T\boldsymbol{v}$ and a covector $\boldsymbol{u}$ in original coordinates (also written as a column vector) will have new components $T^{-T}\boldsymbol{u}$. Tensors which transform like a vector are called *contravariant tensors* and those which transform like a covector are called *covariant tensors*. A metric tensor is a covariant tensor of rank two.

If we take an arbitrary manifold and assign a tensor in a smooth way over each point of the manifold, we get a *tensor field*. The vectors and covectors on which a tensor acts at each point belong to the tangent space and its dual space respectively at

that particular point. A vector field on a manifold is a very good illustrative example. For example, a weather map showing horizontal wind velocity at each point on the Earth's surface is an example of a vector field on the curved surface of the Earth. Note that the "acceleration" quantity, with components in q-coordinates usually denoted by $\ddot{q}^i$ is *not* a tensor even though its denoted with a superscript index[1] . One way to see this would be to note that if $\ddot{q}^i = 0$ in q-coodinates, it is not necessarily true that after a smooth change of coodinates given by $q = q(s)$, the quantity $\ddot{s}^i$ is zero. A metric tensor field on a manifold is a smooth assignment of a metric tensor to each point in the manifold. Once a manifold is assigned a metric field, it makes sense to talk of length of smooth curves, angle made by intersection of two smooth curves etc. In local coordinates around a point p given by x, the metric field is denoted by $g_{ij}(x)dx^i dx^j$.

In mechanical problems, one usually uses the kinetic energy as a metric on the configuration space M. This turns M into a Riemannian manifold. For example, consider a point mass system in R^3 with global coordinates given by x, y, z. Its velocity is given by components $\dot{x}, \dot{y}, \dot{z}$. The kinetic energy is $\frac{1}{2}m\,(\dot{x}^2 + \dot{y}^2 + \dot{z}^2)$. This is a metric on R^3 which turns R^3 into a Riemannian manifold.

2.3 Symmetry and Lie Groups

A very important tool in the study of mechanical systems is the concept of a Lie group. Lie groups are mathematical objects which quantifies the notion of a symmetry. An equilateral triangle, a square, a cube, sphere are all examples of symmetric objects. Similarly, certain differential equations also "look" the same under rotations and translations. In both these cases, symmetry acts on the object (square, cube or differential equation) and gives an object (square, cube or differential equation) which

[1]However, one can define a quantity given by $\ddot{q}^i + \Gamma^i_{jk}\dot{q}^j\dot{q}^k$, which is the true acceleration vector, i.e., it transforms like a vector. Here, Γ^i_{jk} are the Riemann-Christoffel symbols associated to a Riemannin manifold. For Euclidean space $\mathbb{R}^n$, the Γ^i_{jk} coefficients are zero.

"looks" the same as the original object.

Definition 2.3.1 *A* group[2] *G is a set endowed with a binary operation $\cdot$ such that for any $f, g, h \in G$:*

1. $f \cdot (g \cdot h) = (f \cdot g) \cdot h$
2. $\exists e \in G$ *such that* $e \cdot a = a \cdot e = a \ \ \forall a \in G$
3. $\forall a \in G, \exists a^{-1} \in G$ *such that* $a \cdot a^{-1} = a^{-1} \cdot a = e$

Definition 2.3.2 *A* Lie group *is a group G which is also a smooth manifold with a smooth structure such that the operations*

$$(a, b) \mapsto a \cdot b$$
$$a \mapsto a^{-1}$$

from $G \times G \to G$ and $G \to G$, respectively, are smooth.

From now on, we will denote the composition of two group elements f, g by fg instead of $f \cdot g$.

Definition 2.3.3 *The Lie algebra $\mathfrak{g}$ of a Lie group G is the tangent space to the group at the identity together with a bracket operation induced by bracket operation of left invariant vector fields.*

See [45] for a proof of the fact that the tangent space to the identity can be given a Lie algebra structure.

We now discuss what we mean by symmetries of a differential equation. A symmetry of a differential equation is a transformation which leaves intact its family of solutions. For example, consider the Euler vector field in the plane R^2 with coordinates (x_1, x_2) given by $x_1 \dfrac{\partial}{\partial x_1} + x_2 \dfrac{\partial}{\partial x_2}$. The rotation of the plane about the origin is

[2] See page 58 of [4] to see how the definition of a group can be motivated by first looking at the transformation group of a set and then by ignoring the set that is transformed.

a symmetry for this vector field and so is the dilation $(x_1, x_2) \mapsto \lambda(x_1, x_2)$. It can be shown that the set of all the symmetries of a given field form a group. In the Euler field case, the Lie group is $GL(2, \mathbb{R})$.

$\mathbb{R}^n$ is one of the simplest examples of a Lie group with the operation being the usual vector addition. Consider the configuration space which represents a dynamical system and hence is also a differentiable manifold. The notion of a symmetry of a dynamical system is captured mathematically using what are called *actions of a Lie group* on a smooth manifold and its induced action on the tangent bundle of that manifold.

Definition 2.3.4 *A* (left) action of a Lie group G *on a smooth manifold* M *is a smooth mapping* $\Phi : G \times M \to M$ *such that*

$$\begin{aligned} \Phi(e, x) &= x \text{ for all } x \in M \\ \Phi(g, \Phi(h, x)) &= \Phi(gh, x) \text{ for all } g, h \in G \text{ and } x \in M \end{aligned}$$

Here e *is the* identity element *of* G.

For example, the Lie group $\mathbb{R}^n$ acts on the smooth manifold $\mathbb{R}^n$ by $\Phi : \mathbb{R}^n \times \mathbb{R}^n \to \mathbb{R}^n$ where $\Phi(a, x) = a + x$.

For a group action on a manifold, there is an associated induced action of the same group on the tangent bundle of the manifold given by

$$g \cdot (x, v) = (g \cdot x, \frac{d}{dt}(g \cdot c(t)))$$

where $c(t)$ is a smooth curve on the manifold passing through x such that $c(0) = x$ and $c'(0) = v$. It can be shown that this definition does not depend upon the choice of the curve $c(t)$ used to define the induced action. Since the Lagrangian for a mechanical system is a real valued function on the tangent bundle of the configuration space, this induced action is useful to analyze symmetry of a Lagrangian system and to reduce the system degrees of freedom.

2.4 Momentum Map and Locked Inertia Tensor

For a Lagrangian system, symmetries lead to conservation laws by Noether's theorem. The quantity that is conserved is called the *momentum map* and is defined as follows [33].

Definition 2.4.1 *The momentum map $J_L : TQ \to \mathfrak{g}^*$ corresponding to the Lagrangian $L : TQ \to R$ is defined by $J_L(v_q) \cdot \xi = \langle\langle v_q, \xi_Q(q) \rangle\rangle$.*

Here, Q is the configuration space, $q \in Q$, $v_q \in T_qQ$, and $\mathfrak{g}^*$ is the dual of the Lie algebra $\mathfrak{g}$ of the symmetry group G. The notation $\langle\langle \cdot, \cdot \rangle\rangle$ denotes the $G-$invariant metric on Q which gives the kinetic energy $K(v_q) = \frac{1}{2}\langle\langle v_q, v_q \rangle\rangle$ and ξ_Q is the infinitesimal generator corresponding to $\xi \in \mathfrak{g}$, i.e., $\xi_Q(q) = \frac{d}{dt}(\exp(t\xi)q)|_{t=0}$. For each $q \in Q$, the *locked inertia tensor* $I(q) : \mathfrak{g} \mapsto \mathfrak{g}^*$, is defined as

$$\langle I(q)\xi, \eta \rangle = \langle\langle \xi_Q(q), \eta_Q(q) \rangle\rangle \tag{2.4.1}$$

where $\langle \cdot, \cdot \rangle$ is the natural pairing between elements of $\mathfrak{g}$ and $\mathfrak{g}^*$. For a mechanical system consisting of rigid links with joints, the locked inertia tensor is equal to the inertia tensor when all the joints are locked, hence the nomenclature. The locked inertial tensor is used in defining the amended potential which in turn is used to prove stability of relative equilibri.

The momentum map and locked inertia tensor can be related using the mechanical connection $A : TQ \mapsto \mathfrak{g}$ defined as follows:

$$J_L(v_q) = I(q)A(v_q). \tag{2.4.2}$$

The mechanical connection can be used to derive the reduced Lagrangian equations in an intrinsic manner as is described in Chapter 4.

2.5 Example

We now discuss an example to illustrate the concepts stated above. Consider a point mass moving in the Euclidean space $\mathbb{R}^3$ under the influence of a potential V given by $V = k(y^2 + z^2)$ where (x, y, z) are coordinates for $\mathbb{R}^3$. If the mass of the body is m, its kinetic energy is given by $K = \frac{1}{2}m(\dot{x}^2 + \dot{y}^2 + \dot{z}^2)$. In this case, the configuration space manifold is just $\mathbb{R}^3$ and the tangent bundle is $T\mathbb{R}^3 = \mathbb{R}^3 \times \mathbb{R}^3$. Coordinates for the tangent bundle are given by $(x, y, z, \dot{x}, \dot{y}, \dot{z})$. The velocity vector at the point (x, y, z) is a vector in $\mathbb{R}^3$ located at (x, y, z) and pointing in the direction $(\dot{x}, \dot{y}, \dot{z})$ as pictured in Figure 2.5.1. The kinetic energy can be used as a metric for $\mathbb{R}^3$, i.e.,

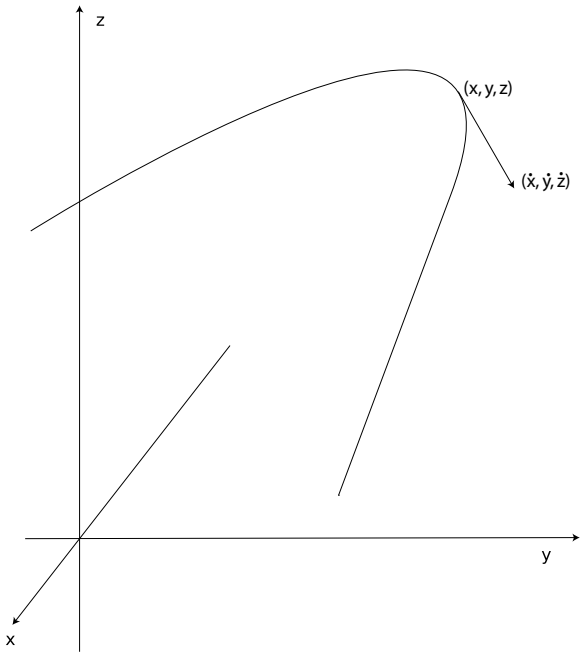

Figure 2.5.1: Motion of a particle in $\mathbb{R}^3$.

$$\begin{aligned} \langle\langle v_q, v_q \rangle\rangle &= \langle\langle (x, y, z, \dot{x}, \dot{y}, \dot{z}), (x, y, z, \dot{x}, \dot{y}, \dot{z}) \rangle\rangle \\ &= m(\dot{x}^2 + \dot{y}^2 + \dot{z}^2). \end{aligned}$$

This turns $\mathbb{R}^3$ into a Riemannian manifold. The Lagrangian for the system is $L = K - V$. It is easily seen that the Lagrangian does not depend upon the x coordinate of

the body, i.e., the Lagrangian has a symmetry in the x-direction. The symmetry group is just the real line $\mathbb{R}$ with the action given by $c \cdot (x, y, z, \dot{x}, \dot{y}, \dot{z}) = (x + c, y, z, \dot{x}, \dot{y}, \dot{z})$. The Lie algebra of the Lie group $\mathbb{R}$ is again $\mathbb{R}$. Given a Lie algebra element $\xi \in \mathbb{R}$, the infinitesimal generator is computed as

$$\begin{aligned} \xi_{\mathbb{R}^3}(x, y, z) &= \frac{d}{dt}(\exp(t\xi)(x, y, z))|_{t=0} \\ &= \frac{d}{dt}(x + \xi t, y, z)|_{t=0} \\ &= (\xi, 0, 0) \end{aligned}$$

The corresponding conserved momentum map lies in the vector space dual to $\mathbb{R}$ which can again be identified with $\mathbb{R}$. It can be found as follows using the definition stated in the previous section:

$$\begin{aligned} \langle J_L(x, y, z, \dot{x}, \dot{y}, \dot{z}), \xi \rangle = & \quad \langle\langle (x, y, z, \dot{x}, \dot{y}, \dot{z}), \xi_{\mathbb{R}^3}(x, y, z) \rangle\rangle \\ = & \quad \langle\langle (x, y, z, \dot{x}, \dot{y}, \dot{z}), (x, y, z, \xi, 0, 0) \rangle\rangle \\ = & \quad m\dot{x}\xi \\ = & \quad \langle m\dot{x}, \xi \rangle \end{aligned}$$

Therefore,

$$J_L(x, y, z, \dot{x}, \dot{y}, \dot{z}) = m\dot{x}, \tag{2.5.1}$$

which is the linear momentum in the $x-$direction. That this quantity is a conserved quantity for the motion can be easily checked by computing its time derivatie along the flow Euler-Lagrange equations of motion. The locked inertia tensor in this case is the mass m. This can be obtained as follows:

$$\begin{aligned} \langle I(x, y, z)\xi, \eta \rangle &= \langle\langle \xi_{\mathbb{R}^3}(x, y, z), \eta_{\mathbb{R}^3}(x, y, z) \rangle\rangle \\ &= \langle\langle (x, y, z, \xi, 0, 0), (x, y, z, \eta, 0, 0) \rangle\rangle \\ &= m\xi\eta \\ &= \langle m\xi, \eta \rangle \end{aligned}$$

Therefore,

$$I(x, y, z) = m. \tag{2.5.2}$$

Using (2.4.2), (2.5.1) and (2.5.2), we get that the mechanical connection for our example is given by

$$A(x, y, z, \dot{x}, \dot{y}, \dot{z}) = \dot{x}. \tag{2.5.3}$$

Chapter 3

Stable Synchronization of Mechanical Systems: The Simplified Matching Case

This chapter focuses on the stabilization and coordination problem for a class of systems which satisfy the *simplified matching conditions*, henceforth denoted by *SMC systems*. *SMC* systems have Abelian symmetry group in their kinetic energy term and the control inputs are in the direction of the symmetry. For example, the planar pendulum/cart system has the cart position as its Abelian symmetry direction and for this system, we consider the underactuated case in which the control inputs are force inputs in the cart direction. For a planar pendulum/cart system on an inclined plane, the kinetic energy term still has Abelian symmetry. The Method of Controlled Lagrangians [10, 8, 11] gives an algorithm to derive a control law to asymptotically stabilize an equilibrium for an individual *SMC* system in full state space. We consider n such systems and couple them using potentials. We demonstrate stabilization of individual dynamics and synchronization across the network. The closed-loop network is Lagrangian and energy methods are used to prove Lyapunov stability and two cases of asymptotic stability. This chapter is based on an expanded discussion of [38].

3.1 Introduction

The Method of Controlled Lagrangians is an energy based method used for stabilization of underactuated mechanical systems [10, 8, 11] . By a mechanical system, we mean a Riemannin manifold where the Riemannian metric represents the kinetic energy and a function on the manifold which represents the potential energy with the system dynamics being the Euler-Lagrange equations. The control prescribed by this method is such that the closed-loop system is a Lagrangian system, i.e., the closed-loop system follows the Euler-Lagrange equations with the Lagrangian depending upon the control law parameters. In particular, the kinetic and potential energy of the closed-loop system can be "shaped" using the control law parameters. One of the main advantages of this approach is that we can use techniques like Dirichlet's theorem to prove stability of the closed-loop system once we choose controls to shape the closed loop kinetic and potential energy appropriately. This is an important tool since for the closed-loop system, after adding dissipative terms, not all the eigenvalues of the linearized system lie in the strict left half plane. Hence, to prove stability of the closed-loop system, the energy corresponding to the closed-loop Lagrangian (which is a readily available candidate for Lyapunov function) is crucial along with a LaSalle argument. Having a Lyapunov function also makes possible estimates of region of attraction. We point out that the Method of Controlled Lagrangians is also equavalent to the Interconnection Damping Assignment - Port Based Control (IDA-PBC) method (see [8, 42] and references therein).

For a class of mechanical systems satisfying the simplified matching conditions or SMCs, the Method of Controlled Lagrangians can be made algorithmic, i.e., we get formulas for the closed-loop Lagrangian and control law directly [10, 8]. These are the systems we consider in this chapter. As mentioned in the introduction to this chapter, *SMC* systems have Abelian symmetry group with controls in the symmetry direction and which satisfy a set of conditions which we state explicitly in §3.3. For a derivation of these conditions, see [10, 8]. We will also give physical interpretations of

these conditions in the same section. This class of SMC systems includes the planar or spherical inverted pendulum on a (controlled) cart. The goal in this chapter is to stabilize unstable dynamics for each individual mechanical system in the network and stably synchronize the actuated configuration variables across the network. For individual stabilization, the approach is based on the theory developed in [8]. Coupling potentials are then added with the goal of synchronizing the network. We will show that it is possible to choose the coupling potentials such that the closed-loop system also satisfies the SMC conditions. By choosing the coupling potentials to depend upon relative positions, the closed-loop system is made to have an Abelian symmetry group. Routh's criterion is then used to prove Lyapunov stability of the closed-loop synchronized network. As an example, for a network of pendulum/cart systems, the problem is to stabilize each pendulum in the upright position while synchronizing the motion of the carts.

To achieve asymptotic stability, additional dissipative control terms are added. Depending upon the Lyapunov function we use to design dissipation, we get two cases of asymptotic stability. These two cases correspond to stably synchronized constant momentum motion and stably synchronized relative equilibrium. For the inverted pendulum on a cart system, the former case corresponds to a synchronized motion of the carts such that all the carts move together with a common velocity that is the sum of a constant plus an oscillation. Likewise, the pendula synchronize and oscillate at the same frequency as the carts. The oscillation frequency for the carts and pendula can be tuned using the control parameters. For the pendulum/cart system, the latter case corresponds to steady, synchronized motion of n carts, with each balancing its inverted pendulum.

The organization of this chapter is as follows. In §3.2 we define notation and the different kinds of stabilization studied. In §3.3, we give a brief background on the method of Controlled Lagrangians and mechanical systems that satisfy the *simplified matching conditions*. We discuss how unstable dynamics are stabilized with feedback

control that preserves Lagrangian structure. In §3.4, we study a network of n systems, each of which satisfies the simplified matching conditions. We choose coupling potentials in §3.5, and we prove stability and coordination of the network. Asymptotic stabilization is investigated in §3.6 and §3.7. We illustrate the theory with the example of n planar, inverted pendulum/cart systems in §3.8.

3.2 Notation and Definitions

In this section, we set the notation for the rest of the chapter and define the various kinds of equilibrium solutions for which stability is proved. Consider an underactuated mechanical system with an $(m+r)$-dimensional configuration space $Q \times \mathbb{R}^r$. Let x^α denote the coordinates for the unactuated directions Q, with index α going from 1 to m. θ^a denotes the coordinates for the actuated directions $\mathbb{R}^r$, which are also the Abelian symmetry directions of the kinetic energy of the system, with index a going from 1 to r[1] . In the case of a network of n mechanical systems, each with the same $(m+r)$-dimensional configuration space, x_i^α and θ_i^a are the corresponding coordinates for the ith mechanical system, $i = 1, \ldots, n$.

The goal of coordination is to synchronize the actuated variables θ_i^a with the variables θ_j^a for all $i, j = 1, \ldots, n$. We define stable synchronization of these variables as stabilization of $\theta_i^a - \theta_j^a = 0$ for all $i \neq j$.

For a mechanical system which has a symmetry both in the kinetic energy as well as potential energy term, a relative equilibrium is a motion which is a group orbit as well as a solution of the Euler-Lagrange equations. For a planar pendulum/cart example, this corresponds to the motion where the cart is moving with a constant velocity and the pendulum is in its upright position.

We define the following stability notions for the mechanical system network.

Definition 3.2.1 (SSRE) *A relative equilibrium of the mechanical system network*

[1]The actuated directions can also be the r-dimensional torus T^r or the space $\mathbb{R}^s \times T^{r-s}$ for some non-zero $s < r$ as we are considering systems whose kinetic energy has an Abelian symmetry.

dynamics is a Stable Synchronized Relative Equilibrium (SSRE) *if it is defined by* $\theta_i^a - \theta_j^a = 0$ *for all* $i \neq j$, $x_i^\alpha = 0$ *for all* i *and if it is Lyapunov stable. This implies that the unactuated dynamics are stable and the actuated dynamics are stably synchronized.*

Definition 3.2.2 (ASSRE) *A relative equilibrium of the mechanical system network dynamics is an* Asymptotically Stable Synchronized Relative Equilibrium (ASSRE) *if it is SSRE and asymptotically stable.*

Definition 3.2.3 (ASSM) *An asymptotically stable solution of the mechanical system network dynamics is an* Asymptotically Stable Synchronized Motion (ASSM) *if it is defined by* $x_i^\alpha - x_j^\alpha = 0$ *and* $\theta_i^a - \theta_j^a = 0$ *for all* $i \neq j$ *and the dynamics of the network evolve on a constant momentum surface.*

We will now discuss what the above three different kinds of motion means for a network of inverted pendulum/cart systems. More details along with simulation plots are given in §3.8. Such a system is illustrated in Figure 3.2.1. In this figure, x denotes the angle made by the pendulum with the vertical and θ denotes the position of the cart on the track. Consider n such systems, each of whose configuration is denoted

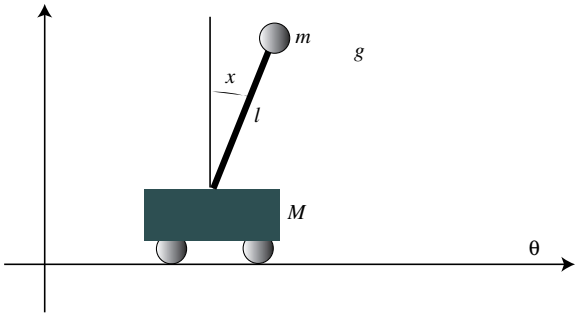

Figure 3.2.1: The planar pendulum on a cart.

by (x_i, θ_i) for $i = 1, \ldots, n$. Then, the SSRE case corresponds to the motion where the cart positions are synchronized and each individual pendulum is in its upright position. SSRE also requires such a solution to be Lyapunov stable. The ASSRE case

corresponds to the motion where the cart positions are asymptotically synchronized and the individual pendulum position asymptotically tend to the upright position. The ASSM case corresponds to the motion where the cart positions are asymptotically synchronized and the pendulum positions are also asymptotically synchronized. The ASSM case for the inverted pendulum/cart network give a periodic orbit for the angle made by each pendulum with the vertical line, with the velocity of the cart oscillating about a constant velocity with the same frequency as the pendulum oscillation.

Recall that as mentioned in §3.1, for a network of planar inverted pendulum-on-a-cart systems, ASSRE corresponds to the carts moving together at the same constant speed with each pendulum at rest in the upright position. And for this network, ASSM corresponds to stable synchronized motion, with the carts moving with a common velocity with additional oscillation and at the same time, the pendulums also have synchronized oscillations about the vertical with the same frequency. In §3.8 we will state explicitly the corresponding control laws required to achieve this motion.

3.3 Controlled Lagrangians and Simplified Matching Conditions

We review here Controlled Lagrangians and *simplified matching conditions* as described in [10, 8]. Let the Lagrangian for an individual mechanical system be given by

$$L(x^\alpha, \theta^a, \dot{x}^\beta, \dot{\theta}^b) = \frac{1}{2} g_{\alpha\beta} \dot{x}^\alpha \dot{x}^\beta + g_{\alpha a} \dot{x}^\alpha \dot{\theta}^a + \frac{1}{2} g_{ab} \dot{\theta}^a \dot{\theta}^b - V(x^\alpha, \theta^a)$$

where summation over indices is implied, g is the kinetic energy metric and V is the potential energy. We will assume that $g_{\alpha\beta}, g_{\alpha a}, g_{ab}$ are independent of θ^a, i.e., the kinetic energy is independent of θ^a coordinates. The actuation for this system is along the θ^a directions only. The planar pendulum/cart system satisfies this but the pendulum/cart system on a circular track does not satisfy this. The equations of

motion for the mechanical system with control inputs u_a along the θ^a directions are given by

$$\begin{aligned} EL(x^\alpha) &= 0 \\ EL(\theta^a) &= u_a \end{aligned} \tag{3.3.1}$$

where $EL(q)$ denotes the Euler-Lagrange expression corresponding to a Lagrangian L and generalized coordinates q, i.e.,

$$EL(q) = \frac{d}{dt}\frac{\partial L}{\partial \dot{q}} - \frac{\partial L}{\partial q}. \tag{3.3.2}$$

The idea behind Controlled Lagrangians (CL) is to choose u_a such that the closed-loop system can be derived from a Lagrangian, which we denote by L_c. Assume the closed-loop equations are as follows:

$$\begin{aligned} EL_c(x^\alpha) &= 0 \\ EL_c(\theta^a) &= 0. \end{aligned}$$

For general systems, u_a and L_c can be found by solving a set of PDEs [16]. These PDEs can be highly nontrivial and there is no general procedure to solve them [6, 24, 15]. The method of CL gives an algorithm to solve these PDEs by restricting the problem to a class of systems called the *simplified matching condition (SMC)* systems. A system is said to be an SMC system if it satisfies the following conditions:

SMC1 $g_{ab} =$ constant

SMC2 $\dfrac{\partial g_{\alpha a}}{\partial x^\beta} = \dfrac{\partial g_{\beta a}}{\partial x^\alpha}$

SMC3 $\frac{\partial^2 V}{\partial x^\alpha \partial \theta^a} g^{ad} g_{\beta d} = \frac{\partial^2 V}{\partial x^\beta \partial \theta^a} g^{ad} g_{\alpha d}$.

With these assumptions, it is shown in [8] that it is possible to choose controls $u_a = u_a^{\text{cons}}$ to shape the kinetic and potential energy of the system. The closed-loop system is a Lagrangian system depending upon control parameters. The planar inverted

pendulum on a cart satisfies the SMC conditions but the inverted pendulum on a rotating arm, also called the Furuta pendulum [5, 37] does not satisfy SMC conditions. In particular, the Furuta pendulum does not satisfy SMC1. A free rigid body in space does not satisfy SMC2. For the Euler equations of a rigid body, the right hand side terms arise due to failure of SMC2.

Let us go over the interpretation of the SMC conditions. SMC1 and SMC2 imply that SMC systems lack gyroscopic coupling terms in their equations of motion. By that we mean that the Euler-Lagrange equations of motion for the x^α variable without external control terms have no $\dot{\theta}^a$ terms, i.e., the equations of motion for the x^α variables are

$$\frac{d}{dt}(g_{\alpha\beta}\dot{x}^\beta) + g_{\alpha a}\ddot{\theta}^a - \frac{1}{2}g_{\beta\gamma,\alpha}\dot{x}^\beta\dot{x}^\gamma + \frac{\partial V}{\partial x^\alpha} = 0$$

For systems with θ^a symmetry, the "no gyroscope force" condition also means that there are no "magnetic terms" in the reduced equations of motion given by the Routhian, i.e., the *mechanical connection* of the system has zero curvature. See [33] for an expression of the reduced equations of motion. SMC3 is automatically satisfied when the original system has θ^a variables as symmetry not only in the kinetic energy term, but also for the potential energy. For systems in which θ^a is not a symmetry for the potential energy, the closed-loop potential, denoted by V_ϵ, where ϵ is a real parameter, must satisfy the following PDE [8]:

$$-\left(\frac{\partial V}{\partial \theta^a} + \frac{\partial V_\epsilon}{\partial \theta^a}\right)(\kappa + \frac{\rho - 1}{\rho})g^{ad}g_{\alpha d} + \frac{\partial V_\epsilon}{\partial x^\alpha} = 0. \tag{3.3.3}$$

This PDE arises when one matches the non-velocity terms in the original system with controls with the non-velocity terms in the closed-loop system. SMC3 is a necessary and sufficient condition for the existence of solution V_ϵ in (3.3.3). In [8], it is shown that the closed-loop Lagrangian can be chosen to be

$$\begin{aligned} L_c(x^\alpha, \theta^a, \dot{x}^\beta, \dot{\theta}^b) &= \frac{1}{2}\left(g_{\alpha\beta} + \rho(\kappa+1)(\kappa + \frac{\rho-1}{\rho})g_{\alpha a}g^{ab}g_{b\beta}\right)\dot{x}^\alpha\dot{x}^\beta + \rho(\kappa+1)g_{\alpha a}\dot{x}^\alpha\dot{\theta}^a \\ &\quad + \frac{1}{2}\rho g_{ab}\dot{\theta}^a\dot{\theta}^b - V(x^\alpha, \theta^b) - V_\epsilon(x^\alpha, \theta^b). \end{aligned} \tag{3.3.4}$$

where ρ and κ are real constant parameters. The expression for the control law such that the closed-loop system is Lagrangian with Lagrangian given by L_c is given by [8]

$$u_a = u_a^{\text{cons}} = -\kappa \left\{ g_{\beta a,\gamma} - g_{\delta a} A^{\delta\alpha} \left[g_{\alpha\beta,\gamma} - \frac{1}{2} g_{\beta\gamma,\alpha} - (1+\kappa) g_{\alpha d} g^{da} g_{\beta a,\gamma} \right] \right\} \dot{x}^\beta \dot{x}^\gamma + \kappa g_{\delta a} A^{\delta\alpha} \frac{\partial V}{\partial x^\alpha} + \frac{\partial V}{\partial \theta^a} - \frac{1}{\rho} \left(1 + \kappa g_{\delta a} A^{\delta\alpha} g_{\alpha d} g^{db}\right) \frac{\partial V'_\epsilon}{\partial \theta^a} \tag{3.3.5}$$

where

$$A_{\alpha\beta} = g_{\alpha\beta} - (1+\kappa) g_{\alpha d} g^{da} g_{\beta a}.$$

The control law is obtained as follows. From (3.3.1), $u_a^{\text{cons}} = EL(\theta^a)$. The expression $EL(\theta^a)$ contains coordinates, velocities and acceleration terms. To express u_a^{cons} in terms of coordinates and velocities, we can solve for the acceleration terms using the closed-loop equations corresponding to the closed-loop Lagrangian L_c and substitute it in $EL(\theta^a)$ to get (3.3.5). Note that the closed loop Lagrangian L_c depends upon the (control) parameters ρ, κ and ϵ. In [8], it is shown how to choose these parameters such that the system is stabilized in the full state space. If we assume that the equilibrim point is a *maximum* of the original potential energy V (the case when the origin is a minimum can be handled similarly), then the parameter ϵ is chosen so as to make the closed-loop potential also a maximum at the equilibrium point. The inverted pendulum systems fall into this category. For this case, the parameter κ should be "sufficiently positive" and $\rho < 0$. The energy function E_c for the controlled Lagrangian has a maximum at the origin of the full state space. Asymptotic stability is obtained by adding a dissipative term u_a^{diss} to the control law, i.e.,

$$u_a = u_a^{\text{cons}} + \frac{1}{\rho} u_a^{\text{diss}}$$

which drives the controlled system to the maximum value of the energy E_c. The equations of motion after adding the dissipation term are:

$$EL_c(x^\alpha) = (\kappa + \frac{\rho - 1}{\rho}) g^{ad} g_{\alpha d} u_a^{\text{diss}} \tag{3.3.6}$$

$$EL_c(\theta^a) = u_a^{\text{diss}}. \tag{3.3.7}$$

Using SMC1, SMC2 and the Poincaré Lemma [34] for the form $g^{ac}g_{\alpha c}dx^{\alpha}$ for each $a = 1, \ldots, r$, there exists a function $h^a(x^\alpha)$ defined on an open subset of the configuration space of the unactuated variables such that

$$\frac{\partial h^a}{\partial x^\alpha} = \left(\kappa + \frac{\rho - 1}{\rho}\right) g^{ac} g_{\alpha c}, \quad h^a(0) = 0. \tag{3.3.8}$$

In [8], it is shown how to use $h^a(x^\alpha)$ to define new coordinates as follows:

$$(x^\alpha, y^a) = (x^\alpha, \theta^a + h^a(x^\alpha)).$$

These coordinate are useful to prove asymptotic stability of the equilibrium point after adding dissipation. For the system with dissipation, all the eigenvalues of the linearized system do not lie in the strict left half plane. This is because, dissipation is added only in the θ^a direction. Hence, these new coordinates become important in proving asymptotic stability using energy methods. If the origin is an equilibrium in the original coordinates it is also an equilibrium in the new coordinates. In these coordinates, the closed-loop Lagrangian takes the form (with abuse of notation for L_c)

$$\begin{aligned} L_c &= \frac{1}{2}\left(g_{\alpha\beta} - (\kappa + \frac{\rho-1}{\rho}) g_{\alpha a} g^{ab} g_{b\beta}\right)\dot{x}^\alpha \dot{x}^\beta + g_{\alpha a}\dot{x}^\alpha \dot{y}^a + \frac{1}{2}\rho g_{ab}\dot{y}^a \dot{y}^b \\ &\quad -V(x^\alpha, y^a - h^a(x^\alpha)) - V_\epsilon(y^a) \\ &= \frac{1}{2}\tilde{g}_{\alpha\beta}\dot{x}^\alpha \dot{x}^\beta + \tilde{g}_{\alpha a}\dot{x}^\alpha \dot{y}^a + \frac{1}{2}\tilde{g}_{ab}\dot{y}^a \dot{y}^b - V(x^\alpha, y^a - h^a(x^\alpha)) - V_\epsilon(y^a), \end{aligned} \tag{3.3.9}$$

where

$$\begin{aligned} \tilde{g}_{\alpha\beta} &= \left(g_{\alpha\beta} - (\kappa + \frac{\rho-1}{\rho}) g_{\alpha a} g^{ab} g_{b\beta}, \right) \\ \tilde{g}_{\alpha a} &= g_{\alpha a}, \\ \tilde{g}_{ab} &= \rho g_{ab}\,. \end{aligned} \tag{3.3.10}$$

Further, after adding dissipation u_a^{diss}, the Euler-Lagrange equations given by (3.3.6) and (3.3.7) are transformed, in terms of the new coordinates, to

$$\begin{pmatrix} EL_c(x^\alpha) \\ EL_c(y^a) \end{pmatrix} = \frac{\partial(x^\alpha, y^a)}{\partial(x^\alpha, \theta^a)} \begin{pmatrix} \frac{\partial h^a}{\partial x^\alpha} u_a^{\text{diss}} \\ u_a^{\text{diss}} \end{pmatrix} = \begin{pmatrix} 0 \\ u_a^{\text{diss}} \end{pmatrix} \tag{3.3.11}$$

where $\dfrac{\partial(x^\alpha, y^a)}{\partial(x^\alpha, \theta^a)}$ is the inverse transpose of the Jacobian matrix of the coordinate transformation and is given by

$$\frac{\partial(x^\alpha, y^a)}{\partial(x^\alpha, \theta^a)} = \begin{pmatrix} I_{m\times m} & -\dfrac{\partial h^a}{\partial x^\alpha} \\ 0 & I_{r\times r} \end{pmatrix}. \tag{3.3.12}$$

3.4 Matching for Network of SMC Systems

The goal in this section is to couple a network of n systems, each of which satisfies SMC conditions, using potentials which depend upon their relative position coordinates in such a way that the total closed-loop Lagrangian system is also an SMC system. We will derive the most general form that the coupling potential can take in this section and work with a particular class of such potentials in the next section to prove stability for the stabilized and synchronized network of vehicles. Having the closed-loop system be a SMC system enables us to exploit the SMC structure in proving stability of the synchronized motion.

Let the ith SMC system have dynamics described by Lagrangian L_i where

$$L_i(x_i^\alpha, \theta_i^a, \dot{x}_i^\beta, \dot{\theta}_i^b) = \frac{1}{2} g^i_{\alpha\beta} \dot{x}_i^\alpha \dot{x}_i^\beta + g^i_{\alpha a} \dot{x}_i^\alpha \dot{\theta}_i^a + \frac{1}{2} g^i_{ab} \dot{\theta}_i^a \dot{\theta}_i^b - V_i(x_i^\alpha, \theta_i^a), \tag{3.4.1}$$

and the index i on every variable refers to the ith system. Note that we do not mean to sum over i in this expression, i.e., $g^i_{\alpha\beta}$ is not a $\binom{1}{2}$ tensor, but rather a $\binom{0}{2}$ tensor.

The Lagrangian for the total system before adding control term is

$$L = \sum_{i=1}^{n} L_i = \frac{1}{2} \dot{\boldsymbol{x}}^T M \dot{\boldsymbol{x}} - \sum_{i=1}^{n} V_i(x_i^\alpha, \theta_i^a), \tag{3.4.2}$$

where $\boldsymbol{x} = (x_1^\alpha, \ldots, x_n^\beta, \theta_1^a, \ldots, \theta_n^b)^T$, and

$$M = \left(\begin{array}{ccc|ccc} g^1_{\alpha\beta} & & 0 & g^1_{\alpha a} & & 0 \\ & \ddots & & & \ddots & \\ 0 & & g^n_{\alpha\beta} & 0 & & g^n_{\alpha a} \\ \hline g^1_{a\alpha} & & 0 & g^1_{ab} & & 0 \\ & \ddots & & & \ddots & \\ 0 & & g^n_{a\alpha} & 0 & & g^n_{ab} \end{array}\right).$$

Since we are assuming that each system is an SMC system, $g^i_{ab} =$ constant for each $i = 1, \ldots, n$. It can be easily verified that the simplified matching conditions are satisfied for the total system L, since they are satisfied for each individual system.

For the Lagrangian given by (3.4.2), the symmetry coordinates are $(\theta_1^a, \ldots, \theta_n^b)$. As shown in [8], there exists a control law and a change of coordinates given by

$$\boldsymbol{x} = (x_1^\alpha, \ldots, x_n^\beta, \theta_1^a, \ldots, \theta_n^b) \mapsto \boldsymbol{x}' = (x_1^\alpha, \ldots, x_n^\beta, y_1^a, \ldots, y_n^b)$$

such that the closed-loop system is also a Lagrangian system with Lagrangian L_c' given by

$$L_c' = \frac{1}{2}(\dot{\boldsymbol{x}}')^T M_c \dot{\boldsymbol{x}}' - V_\epsilon'(\boldsymbol{x}') \tag{3.4.3}$$

and

$$M_c = \left(\begin{array}{ccc|ccc} \tilde{g}^1_{\alpha\beta} & & 0 & \tilde{g}^1_{\alpha a} & & 0 \\ & \ddots & & & \ddots & \\ 0 & & \tilde{g}^n_{\alpha\beta} & 0 & & \tilde{g}^n_{\alpha a} \\ \hline \tilde{g}^1_{a\alpha} & & 0 & \tilde{g}^1_{ab} & & 0 \\ & \ddots & & & \ddots & \\ 0 & & \tilde{g}^n_{a\alpha} & 0 & & \tilde{g}^n_{ab} \end{array}\right) := \left(\begin{array}{c|c} M_{11} & M_{12} \\ \hline M_{12}^T & M_{22} \end{array}\right), \tag{3.4.4}$$

$$V_\epsilon' = \sum_{i=1}^n \Big(V_i(x_i^\alpha, y_i^a - h_i^a(x_i^\alpha)) + V_{\epsilon i}(x_i^\alpha, y_i^a) \Big)$$

with an abuse of notation for V_i. For the i^{th} system, $\tilde{g}^i_{\alpha\beta}$, $\tilde{g}^i_{\alpha a}$, and $\tilde{g}^i_{\alpha a}$ are defined by (3.3.10). At this stage, there is still no coupling between the systems.

Using the choice of control gains κ_i and ρ_i and control potentials $V_{\epsilon i}$ chosen so as to be a maximum at the origin as prescribed in [8], the mass matrix M_c can be made negative definite and the potential V_ϵ' can be made a maximum when the configuration of each system, i.e., (x_i^α, θ_i^a), is at the origin. The control law asymptotically stabilizes the origin for each individual system independently, i.e., the system is still completely decoupled.

We will now make the following assumption about the potential for the individual SMC systems. This will enable us to state explicitly the form which the closed-loop potential $V_{\epsilon i}$ can take.

> **AS1.** *The potential energy for each system in the original coordinates satisfies* $V_i(x_i^\alpha, \theta_i^a) = V_{1i}(x_i^\alpha) + V_{2i}(\theta_i^a)$.

Examples of systems which satisfy this assumption are the planar pendulum/cart system on a level and on an inclined plane and the spherical pendulum on a level and on an inclined plane.

Under the assumption **AS1**, $V_{\epsilon i}$ can be chosen to be

$$V_{\epsilon i}(x_i^\alpha, y_i^a) = -V_{2i}(y_i^a - h_i^a(x_i^\alpha)) + \bar{V}_{\epsilon i}(y_i^a)$$

where $\bar{V}_{\epsilon i}$ is an arbitrary function and $h_i^a(x_i^\alpha)$ is as in (3.3.8) for each $i = 1, \ldots, n$:

$$\frac{\partial h_i^a}{\partial x_i^\alpha} = \left(\kappa_i + \frac{\rho_i - 1}{\rho_i}\right) g_i^{ac} g_{\alpha c}^i, \quad h_i^a(0) = 0. \tag{3.4.5}$$

Refer to [8] for more details on this. We now show that a more general form of potential satisfies the simplified matching condition. This will enable us to make a particular choice of potential to couple the systems.

Proposition 3.4.1 *Under assumption* **AS1**, *the potential* $V + V_\epsilon$ *satisfies the sim-*

plified matching condition with

$$V = \sum_{i=1}^{n} \Big(V_{1i}(x_i^\alpha) + V_{2i}(y_i^a - h_i^a(x_i^\alpha)) \Big)$$
$$V_\epsilon = -\left(\sum_{i=1}^{n} V_{2i}(y_i^a - h_i^a(x_i^\alpha)) \right) + \tilde{V}_\epsilon(y_1^a, \ldots, y_n^a) \tag{3.4.6}$$

and $\tilde{V}_\epsilon$ an arbitrary function.

Proof. Recall that the potential $V + V_\epsilon$ given by (3.4.6) satisfies the simplified matching condition if (3.3.3) holds. From [8], we can use the definition of $h_i^a(x_i^\alpha)$ given by (3.4.5) to rewrite the simplified matching condition (3.3.3) for the potential in the following form:

$$\frac{\partial V_\epsilon}{\partial x_i^\alpha} = \frac{\partial V}{\partial y_i^a} \frac{\partial h_i^a(x_i^\alpha)}{\partial x_i^\alpha}, \quad i = 1, \ldots, n\,. \tag{3.4.7}$$

Now, if $v_i^a = y_i^a - h_i^a(x_i^\alpha)$, then using (3.4.6) we get

$$\frac{\partial V_\epsilon}{\partial x_i^\alpha} = \frac{\partial V_{2i}}{\partial v_i^a} \frac{\partial v_i^a}{\partial x_i^\alpha} \tag{3.4.8}$$

Again, using (3.4.6) we get

$$\frac{\partial V}{\partial y_i^a} \frac{\partial h_i^a(x_i^\alpha)}{\partial x_i^\alpha} = \frac{\partial V_{2i}}{\partial v_i^a} \frac{\partial v_i^a}{\partial x_i^\alpha} \tag{3.4.9}$$

From (3.4.8) and (3.4.9), we see that (3.4.7) is satisfied. ∎

The closed-loop dynamics are now Lagrangian satisfying the SMC conditions. The more flexibility we have in choosing $\tilde{V}_\epsilon$ enables us to introduce coupling between the vehicles. Depending upon our choice of $\tilde{V}_\epsilon$, we have different degrees of coupling for the network, i.e., we can obtain a completely connected system on the one hand and on the other hand a completely uncoupled systems. Using a particular choice for $\tilde{V}_\epsilon$, we show in the next section how to obtain stable coordination for the network.

For the closed-loop system, the mass matrix is made negative definite. The part of the potential term given by $\sum_{i=1}^{n}(V_{1i}(x_i^\alpha))$ is maximum at the origin. Hence, we will choose $\tilde{V}_\epsilon(y_1^a, \ldots, y_n^a)$ to couple the system in such a way that its also maximum at the desired configuration.

3.5 Stable Coordination of SMC Network

In this section, we achieve stability of SSRE coordination as defined in §3.2 for a network of n SMC systems. From Proposition 3.4.1, $\tilde{V}_\epsilon$ can be chosen to be an arbitrary function of y_i. This means that by choosing coupling potentials to be a function of $y_i^a - y_j^a = 0$, for all $i \neq j$, we can try to achieve stable synchronization of y_i^a coordinates of the network.

Since we have assumed the potential for our original system to be maximum at the origin, we will choose $\tilde{V}_\epsilon$ such that the closed-loop potential V_ϵ', defined in Proposition 3.4.1, has a maximum when $x_i^\alpha = 0$ and $y_i^a - y_j^a = 0$ for all $i \neq j$. This is made possible by choosing $\tilde{V}_\epsilon$ to be quadratic in $(y_i^a - y_j^a)$ with maximum at $y_i^a - y_j^a = 0$ for all $i \neq j$. Figure 3.5.1 illustrates a communication topology for a 4 vehicle network where the edges between nodes i and j represents the term $(y_i^a - y_j^a)$ appearing in the quadratic function $\tilde{V}_\epsilon(y_1^a - y_2^a, y_2^a - y_3^a, y_3^a - y_4^a)$. For such a communication topology, V_ϵ' has a strict maximum when $x_i^\alpha = 0$ and $y_i^a - y_j^a = 0$ for all $i \neq j$. In general, if the communication topology is connected, i.e., there is a path between the i^{th} and j^{th} vehicle for all $i, j \in \{1, \ldots, n\}$, then V_ϵ' has a strict maximum when $x_i^\alpha = 0$ and $y_i^a - y_j^a = 0$ for all $i \neq j$. In our problem setting, we choose a particular $\tilde{V}_\epsilon$ and fix the topology for the network for the analysis.

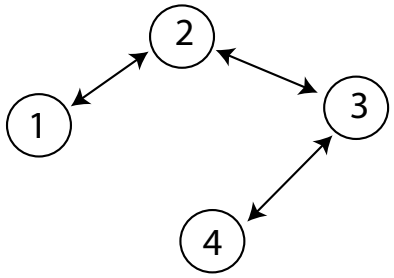

Figure 3.5.1: Connected, undirected communication graph for four vehicles.

The closed-loop network has a translational symmetry since the coupling potential depends only on $y_i^a - y_j^a$ and hence, if we translate y_i^a and y_j^a variables by the same constant, the Lagrangian remains invariant. To exploit this symmetry, we will

consider the following new set of coordinates given by

$$(x_1^\alpha, \ldots, x_n^\beta, z_1^a, \ldots, z_n^b) = (x_1^\alpha, \ldots, x_n^\beta, y_1^a - y_2^a, \ldots, y_1^b - y_n^b, y_1^c + \ldots + y_n^c). \quad (3.5.1)$$

The reason we make this coordinate transformation is because in these coordinates, z_n^a is the symmetry variable, i.e., the closed-loop potential depends only upon

$$(x_1^\alpha, \ldots, x_n^\beta, z_1^a, \ldots, z_{n-1}^b).$$

In this coordinate system, the controlled Lagrangian for the total system (with abuse of notation for V_ϵ') is

$$\tilde{L}_c = \frac{1}{2}\dot{\boldsymbol{x}}_c^T \tilde{M}_c \dot{\boldsymbol{x}}_c - V_\epsilon'(\boldsymbol{x}_r) \quad (3.5.2)$$

where $\boldsymbol{x}_c = (x_1^\alpha, \ldots, x_n^\beta, z_1^a, \ldots, z_n^b)^T$, $\boldsymbol{x}_r = (x_1^\alpha, \ldots, x_n^\beta, z_1^a, \ldots, z_{n-1}^b)^T$ and

$$\tilde{M}_c = \begin{pmatrix} \tilde{M}_{11} & \tilde{M}_{12} \\ \tilde{M}_{12}^T & \tilde{M}_{22} \end{pmatrix}. \quad (3.5.3)$$

The transformation which takes the coordinates $\boldsymbol{x}_c = (x_1^\alpha, \ldots, x_n^\beta, z_1^a, \ldots, z_n^b)$ to the coordinates $\boldsymbol{x}' = (x_1^\alpha, \ldots, x_n^\beta, y_1^c, \ldots, y_n^d)$ is given by the matrix

$$B = \begin{bmatrix} I_{mn\times mn} & 0 \\ 0 & B_{22} \end{bmatrix} \quad (3.5.4)$$

where B_{22} is the inverse of the transformation which takes $(y_1^c, \ldots, y_n^d)$ to the coordinates $(z_1^a, \ldots, z_n^b)$ given by

$$\begin{bmatrix} I_{r\times r} & -I_{r\times r} & 0 & \ldots & 0 \\ I_{r\times r} & 0 & -I_{r\times r} & \ldots & 0 \\ \vdots & \vdots & \vdots & \ldots & \vdots \\ I_{r\times r} & 0 & \ldots & 0 & -I_{r\times r} \\ I_{r\times r} & I_{r\times r} & \ldots & I_{r\times r} & I_{r\times r} \end{bmatrix} \quad (3.5.5)$$

Therefore,

$$B_{22} = \frac{1}{n}\begin{bmatrix} I_{r\times r} & I_{r\times r} & \ldots & I_{r\times r} \\ (1-n)I_{r\times r} & I_{r\times r} & \ldots & I_{r\times r} \\ \vdots & \vdots & \ldots & \vdots \\ I_{r\times r} & \ldots & (1-n)I_{r\times r} & I_{r\times r} \end{bmatrix} \quad (3.5.6)$$

and $I_{l\times l}$ denotes a $l \times l$ identity matrix and B_{22} is an $rn \times rn$ matrix. The expression for $\tilde{M}_c$ in terms of M_c from (3.4.4) is

$$\tilde{M}_c = B^T M_c B. \tag{3.5.7}$$

We can compute the block elements in $\tilde{M}_c$ to be

$$\tilde{M}_{11} = M_{11}, \tag{3.5.8}$$

$$\tilde{M}_{12} = \frac{1}{n}\begin{pmatrix} \tilde{g}^1_{\alpha a} & \tilde{g}^1_{\alpha a} & \dots & \tilde{g}^1_{\alpha a} & \tilde{g}^1_{\alpha a} \\ (1-n)\tilde{g}^2_{\alpha a} & \tilde{g}^2_{\alpha a} & \dots & \tilde{g}^2_{\alpha a} & \tilde{g}^2_{\alpha a} \\ & & \ddots & & \\ \tilde{g}^{n-1}_{\alpha a} & \tilde{g}^{n-1}_{\alpha a} & \dots & \tilde{g}^{n-1}_{\alpha a} & \tilde{g}^{n-1}_{\alpha a} \\ \tilde{g}^n_{\alpha a} & \tilde{g}^n_{\alpha a} & \dots & (1-n)\tilde{g}^n_{\alpha a} & \tilde{g}^n_{\alpha a} \end{pmatrix}, \tag{3.5.9}$$

$$\tilde{M}_{22} = \frac{1}{n^2} B_{22}^T M_{22} B_{22} \tag{3.5.10}$$

where M_{11} and M_{22} are as defined in (3.4.4). From (3.5.6) and (3.4.4), we can calculate the lowermost diagonal $r \times r$ block of $\tilde{M}_{22}$ to be

$$\tilde{g}_{ab} = \frac{1}{n^2}\sum_{i=1}^{n}(\tilde{g}^i_{ab}). \tag{3.5.11}$$

Thus, we can define $\bar{M}_{22} = \tilde{g}_{ab}$ and $\bar{M}_{11}$ and $\bar{M}_{12}$ in terms of the other blocks of $\tilde{M}_c$ such that

$$\begin{pmatrix} \bar{M}_{11} & \bar{M}_{12} \\ \bar{M}_{12}^T & \bar{M}_{22} \end{pmatrix} = \tilde{M}_c.$$

Then, we can rewrite (3.5.2) as

$$\tilde{L}_c = \frac{1}{2}\begin{pmatrix} \dot{\boldsymbol{x}}_r^T & \dot{\mathbf{z}}_n^T \end{pmatrix}\begin{pmatrix} \bar{M}_{11} & \bar{M}_{12} \\ \bar{M}_{12}^T & \bar{M}_{22} \end{pmatrix}\begin{pmatrix} \dot{\boldsymbol{x}}_r \\ \dot{\mathbf{z}}_n \end{pmatrix} - V'_\epsilon(\boldsymbol{x}_r)$$

where $\mathbf{z}_n = (z_n^a)^T$ and $\boldsymbol{x}_r = (x_1^\alpha, \dots, x_n^\beta, z_1^a, \dots, z_{n-1}^b)^T$.

As remarked before, in these coordinates z_n^a corresponds to the Abelian symmetry variable. We are interested in the relative equilibria given by

$$\begin{aligned}&(x_1^\alpha, \ldots, x_n^\gamma, z_1^a, \ldots, z_{n-1}^c, \dot{x}_1^\alpha, \ldots, \dot{x}_n^\gamma, \dot{z}_1^a, \ldots, \dot{z}_{n-1}^c, \dot{z}_n^d)\\ &= (0, \ldots, 0, 0, \ldots, 0, 0, \ldots, 0, 0, \ldots, 0, \zeta^d)\\ &=: \mathbf{v}_{RE}\end{aligned} \tag{3.5.12}$$

where ζ^d corresponds to (n times) the constant velocity of the center of mass of the network. For systems with an Abelian symmetry group, the Routh reduction is very useful for stability analysis of the relative equilibrium [33]. We will now define a quantity called the Amended Potential, which will be needed to prove stability of equilibrium given by (3.5.12).

Definition 3.5.1 (Amended Potential [33]) *The* amended potential *for the Lagrangian system with Lagrangian (3.5.2) is defined by*

$$V_\mu(\boldsymbol{x}_r) = V'_\epsilon(\boldsymbol{x}_r) + \frac{1}{2}\tilde{g}^{cd}\mu_c\mu_d$$

where V'_ϵ is given by (3.4.6) and $\tilde{g}_{ab}$ is given by (3.5.11). Let J_a be the momentum conjugate to z_n^a. Then μ_a is J_a evaluated at the relative equilibrium corresponding to $\dot{z}_n^a = \zeta^a$, i.e.,

$$J_a = \frac{\partial \tilde{L}_c}{\partial \dot{z}_n^a} = (\bar{M}_{12}^T \dot{\boldsymbol{x}}_r + \bar{M}_{22}\dot{\mathbf{z}}_n)_a, \qquad \mu_a = \left.\frac{\partial \tilde{L}_c}{\partial \dot{z}_n^a}\right|_{\boldsymbol{x}_r=0, \dot{z}_n^a=\zeta^a} = \tilde{g}_{ab}\zeta^a. \tag{3.5.13}$$

By the Routh criteria [33], the relative equilibrium is stable if the second variation of

$$E_\mu := \frac{1}{2}\dot{\boldsymbol{x}}_r^T(\bar{M}_{11} - \bar{M}_{12}\bar{M}_{22}^{-1}\bar{M}_{12}^T)\dot{\boldsymbol{x}}_r + V_\mu(\boldsymbol{x}_r) \tag{3.5.14}$$

evaluated at the origin is definite. Also, if $R^\mu(\boldsymbol{x}_r, \dot{\boldsymbol{x}}_r)$ is defined as

$$R^\mu := \frac{1}{2}\dot{\boldsymbol{x}}_r^T(\bar{M}_{11} - \bar{M}_{12}\bar{M}_{22}^{-1}\bar{M}_{12}^T)\dot{\boldsymbol{x}}_r - V_\mu(\boldsymbol{x}_r), \tag{3.5.15}$$

then the reduced Euler-Lagrange equations can be written as[2]

$$ER^{\mu}(x_r^{\alpha}) = 0.$$

Refer to [33] for more details on Routh reduction. The Routhian R^{μ} plays the role of a Lagrangian for the reduced system in variables $(\boldsymbol{x}_r, \dot{\boldsymbol{x}}_r)$. Since $\tilde{g}^i_{ab}$ is a constant for each $i \in \{1, 2, \ldots, n\}$, the second term in the amended potential V_{μ} does not contribute to the second variation. Therefore, the relative equilibrium with momentum μ_a is stable if the matrix $(\bar{M}_{11} - \bar{M}_{12}\bar{M}_{22}^{-1}\bar{M}_{12}^T)$ evaluated at the origin is negative definite, since the potential V'_{ϵ} is already maximum at the equilibrium. We now prove that this matrix is negative definite using the following results from linear algebra.

Lemma 3.5.2 *Consider the negative definite symmetric matrix*

$$T = \left(\begin{array}{c|c} T_{11} & T_{12} \\ \hline T_{12}^T & T_{22} \end{array}\right) \tag{3.5.16}$$

where (3.5.16) is any partition of the matrix T. Then T_{11} and T_{22} are also negative definite.

Proof. This follows by evaluating the definite matrix T on the vectors $(x, 0)$ and $(0, y)$, respectively. ∎

Lemma 3.5.3 *If T given by (3.5.16) is negative definite, then $T_{11} - T_{12}T_{22}^{-1}T_{12}^T$ is also negative definite.*

Proof. Let $(T'_{22})^2 = -T_{22}$. Then,

$$\begin{aligned}(x, y)^T T (x, y) &= x^T T_{11} x + 2y^T T_{12}^T x + y^T T_{22} y \\ &= x^T (T_{11} - T_{12}T_{22}^{-1}T_{12}^T)x - (T'_{22}y - T'^{-1}_{22}T_{12}^T x)^T (T'_{22}y - T'^{-1}_{22}T_{12}^T x).\end{aligned} \tag{3.5.17}$$

[2]For general Lagrangian systems, there are "gyroscopic force" terms on the right hand side of the reduced Euler-Lagrange equations. For SMC systems, these terms vanish.

For any x, one can choose $y = -T_{22}^{-1}T_{12}^{T}x$ so that the second term on the right hand side of (3.5.17) is made zero. Hence, it follows that $T_{11} - T_{12}T_{22}^{-1}T_{12}^{T} < 0$ since the left hand side is less than zero for all nonzero vectors (x, y). ∎

Theorem 3.5.4 (SSRE) *Consider a network of n SMC systems that each satisfy Assumption* **AS1**. *Suppose for each system that the origin is an equilibrium and that the original potential energy is maximum at the origin. Consider the kinetic energy shaping defined in §3.4 and potential energy coupling defined above with connected graph so that the closed-loop dynamics derive from the Lagrangian $\tilde{L}_c$ given by (3.5.2) and the potential energy $V + \tilde{V}_\epsilon$ is maximized at the relative equilibrium (3.5.12). The corresponding control law for the i^{th} mechanical system is*

$$\begin{aligned} u_{a,i} = u_{a,i}^{\text{cons}} = &- \kappa_i \left\{ g^i_{\beta a,\gamma} - g^i_{\delta a} A_i^{\delta\alpha} \left[g^i_{\alpha\beta,\gamma} - \frac{1}{2} g^i_{\beta\gamma,\alpha} - (1+\kappa_i) g^i_{\alpha d} g_i^{da} g^i_{\beta a,\gamma} \right] \right\} \dot{x}_i^\beta \dot{x}_i^\gamma \\ &+ \kappa_i g^i_{\delta a} A_i^{\delta\alpha} \frac{\partial V_i}{\partial x_i^\alpha} + \frac{\partial V_i}{\partial \theta_i^a} - \frac{1}{\rho_i} \left(1 + \kappa_i g^i_{\delta a} A_i^{\delta\alpha} g^i_{\alpha d} g_i^{db}\right) \frac{\partial (V + \tilde{V}_\epsilon)}{\partial \theta_i^a} \end{aligned} \tag{3.5.18}$$

where

$$A^i_{\alpha\beta} = g^i_{\alpha\beta} - (1+\kappa_i) g^i_{\alpha d} g_i^{da} g^i_{\beta a}, \quad \rho_i < 0$$

and

$$\kappa_i + 1 > \max \left\{ \lambda | \det \left(g^i_{\alpha\beta} - \lambda g^i_{\alpha a} g_i^{ab} g^i_{b\beta} \right) |_{x_i^\alpha = 0} = 0 \right\}.$$

Then, the relative equilibrium (3.5.12) is a Stable Synchronized Relative Equilibrium (SSRE) for any ζ^d.

Proof. By Lemmas 3.5.2 and 3.5.3, $(\bar{M}_{11} - \bar{M}_{12}\bar{M}_{22}^{-1}\bar{M}_{12}^{T})$ evaluated at the origin is negative definite. Thus, the second variation of E_μ evaluated at the origin is definite. Hence, the relative equilibrium (3.5.12) is stable for the total network system independent of momentum value μ_a. ∎

The control law (3.5.18) has the same form as in (3.3.5) except for the potential coupling term given by $V + \tilde{V}_\epsilon$ in (3.5.18). The conditions on ρ_i and κ_i are

required to make the mass matrix of the closed-loop Lagrangian negative definite at the equilibrium point [8].

3.6 Asymptotic Stability of Constant Momentum Solution

We now investigate ASSM coordination for a network of n SMC systems which have been stabilized using the control law prescribed in (3.5.18). To achieve ASSM, we need to add appropriate dissipation control terms to (3.5.18). We demonstrate how to design such a dissipation in this section. We prove ASSM in the case when there is no dissipation in the z_n^a direction. This means that the corresponding conjugate momentum J_a is preserved along the flow, i.e., the system evolves on the constant momentum surface which depends upon the initial conditions as illustrated in Figure 3.6.1. On this surface, E_μ as defined in (3.5.14) can be chosen as a Lyapunov

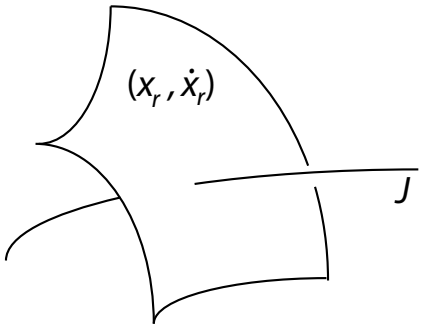

Figure 3.6.1: E_μ is a Lyapunov function on constant momentum surface $J_a = \mu_a$. Such a surface is illustrated here as a level set of J_a.

function to prove stability. The system without dissipation in the z_n^a direction evolves on the surface shown where E_μ is a conserved quantity. We show that by choosing dissipation as given by (3.6.7), the solution is ASSM. The main idea is to use the Energy-Momentum function as a Lyapunov function on the constant momentum surface and then use a LaSalle argument after adding dissipation to prove that the solutions tend to an ASSM solution.

Let the control input for the ith mechanical system be

$$u_{a,i} = u_{a,i}^{\text{cons}} + \frac{1}{\rho_i} u_{a,i}^{\text{diss}} \tag{3.6.1}$$

where $u_{a,i}^{\text{cons}}$ is the "conservative" control term given by (3.5.18) and $u_{a,i}^{\text{diss}}$ is the dissipative control term to be designed. The Euler-Lagrange equations in the original coordinates for the ith uncontrolled systems are

$$EL_i(x_i^\alpha) = 0 \;\; ; \;\; EL_i(\theta_i^a) = u_{a,i}^{\text{cons}} + \frac{1}{\rho_i} u_{a,i}^{\text{diss}}$$

where L_i is given by (3.4.1). In the (x_i^α, y_i^a) coordinates, the closed loop Euler-Lagrange equations are

$$E\tilde{L}_c(x_i^\alpha) = 0 \;\; ; \;\; E\tilde{L}_c(y_i^a) = u_{a,i}^{\text{diss}}$$

and these equations, in the new coordinates given by (3.5.1), transform to

$$E\tilde{L}_c(x_i^\alpha) = 0 \;\; ; \;\; E\tilde{L}_c(z_i^a) = \frac{1}{n} \tilde{u}_{a,i}^{\text{diss}} \tag{3.6.2}$$

where $\tilde{L}_c$ is given by (3.5.2) and

$$\tilde{u}_{a,i}^{\text{diss}} = \sum_{j=1, j\neq i+1}^{n} u_{a,j}^{\text{diss}} - (n-1) u_{a,i+1}^{\text{diss}}, \quad i = 1, \ldots, n-1$$

$$\tilde{u}_{a,n}^{\text{diss}} = \sum_{j=1}^{n} u_{a,j}^{\text{diss}}.$$

Case I: $\tilde{u}_{a,n}^{\text{diss}} = 0$.

Let $\tilde{E}_c$ be the energy function for the Lagrangian $\tilde{L}_c$. Given momentum value μ_a, let $\xi^b = \tilde{g}^{ab}\mu_a$. Then, the function $\tilde{E}_c^\xi$ defined by

$$\tilde{E}_c^\xi = \tilde{E}_c - J_a \xi^a$$

has the property that its restriction to the level set $J_a = \mu_a = \tilde{g}_{ab}\xi^b$ of the momentum gives E_μ. We can use this fact to calculate the time derivative of E_μ as follows. From (3.6.2), we get

$$\frac{d}{dt}\tilde{E}_c = \frac{1}{n} \sum_{i=1}^{n} (\dot{z}_i^a \tilde{u}_{a,i}^{\text{diss}}). \tag{3.6.3}$$

Using (3.6.3) and the fact that $\frac{d}{dt}J_a = \frac{1}{n}\tilde{u}^{\text{diss}}_{a,n}$, we get

$$\frac{d}{dt}\tilde{E}^{\xi}_{c} = \frac{1}{n}\sum_{i=1}^{n}(\dot{z}^a_i \tilde{u}^{\text{diss}}_{a,i}) - (\frac{1}{n}\tilde{u}^{\text{diss}}_{a,n}\xi^a). \tag{3.6.4}$$

The expression for time derivative of E_μ is obtained by restricting $\frac{d}{dt}\tilde{E}^{\xi}_{c}$ to the set $J_a = \mu_a$. This and (3.5.13) gives us

$$\begin{aligned}
\frac{d}{dt}E_\mu &= \frac{1}{n}\sum_{i=1}^{n-1}(\dot{z}^a_i \tilde{u}^{\text{diss}}_{a,i}) + \frac{1}{n}\tilde{u}^{\text{diss}}_{a,n}(\dot{z}^a_n|_{J_b=\mu_b} - \xi^a) \\
&= \frac{1}{n}\sum_{i=1}^{n-1}(\dot{z}^a_i \tilde{u}^{\text{diss}}_{a,i}) + \frac{1}{n}\tilde{u}^{\text{diss}}_{a,n}(\tilde{g}^{ab}(\mu_b - (\bar{M}^T_{12}\dot{\boldsymbol{x}}_r)_b) - \xi^a) \\
&= \frac{1}{n}\sum_{i=1}^{n-1}(\dot{z}^a_i \tilde{u}^{\text{diss}}_{a,i}) + \frac{1}{n}\tilde{u}^{\text{diss}}_{a,n}(-\tilde{g}^{ab}(\bar{M}^T_{12}\dot{\boldsymbol{x}}_r)_b).
\end{aligned}$$

Here, $\bar{M}^T_{12}\dot{\boldsymbol{x}}_r$ is a covariant vector just like a momentum. Hence, its component is denoted by a subscript. Since $u^{\text{diss}}_{a,n}$ is chosen to be zero, we get

$$\frac{d}{dt}E_\mu = \frac{1}{n}\sum_{i=1}^{n-1}(\dot{z}^a_i \tilde{u}^{\text{diss}}_{a,i}). \tag{3.6.5}$$

Expressing $\tilde{u}^{\text{diss}}_{a,i}$ in terms of $u^{\text{diss}}_{a,i}$, we can write the expression for $\dot{E}_\mu$ as

$$n\frac{d}{dt}E_\mu = u^{\text{diss}}_{a,1}(\sum_{j=1}^{n-1}\dot{z}^a_j) + \sum_{j=2}^{n-1}u^{\text{diss}}_{a,j}\left(-(n-1)\dot{z}^a_{j-1} + \sum_{k=1,k\neq j-1}^{n-1}\dot{z}^a_k\right) \tag{3.6.6}$$

and choose

$$\begin{aligned}
u^{\text{diss}}_{a,1} &= d_{ab}\left(\sum_{j=1}^{n-1}\dot{z}^b_j\right) \\
u^{\text{diss}}_{a,j} &= d_{ab}\left(-(n-1)\dot{z}^b_{j-1} + \sum_{k=1,k\neq j-1}^{n-1}\dot{z}^b_k\right) \\
& j = 2,\ldots,n-1,
\end{aligned} \tag{3.6.7}$$

where d_{ab} is a positive definite control gain matrix, possibly dependent on x^α_i, $i = 1,\ldots,n$, and z^a_i, $j = 1,\ldots,n-1$. With the dissipative control term (3.6.7), $\frac{d}{dt}E_\mu \geq 0$.

Note that this dissipation requires a complete communication topology as illustrated in Figure 3.6.2 for a network of 4 vehicles, i.e., ASSM requires more communication links between the vehicles as opposed to SSRE.

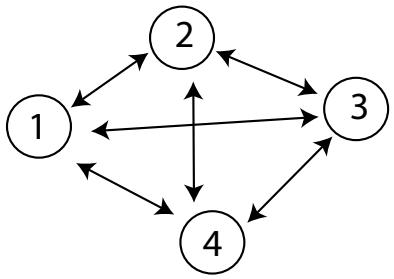

Figure 3.6.2: Completely connected communication graph for four vehicles.

Until now, we have shown that the system stays on a constant momentum surface and the dynamics are such that the time derivative of the Lyapunov function is non-negative. Using the LaSalle Invariance Principle [28], we will now characterize the solutions to which the system converges. For $c < 0$, the set given by $\Omega_c = \{(\boldsymbol{x}_r, \dot{\boldsymbol{x}}_r) | E_\mu \geq c\}$ is a compact and positive invariant set with integral curves starting in Ω_c staying in Ω_c for all $t \geq 0$. Define the LaSalle surface

$$\mathcal{E} = \left\{ (\boldsymbol{x}_r, \dot{\boldsymbol{x}}_r) \,\middle|\, \frac{d}{dt} E_\mu = 0 \right\} .$$

On this surface, $u_{a,j}^{\text{diss}} = 0$, $i = 1, \ldots, n$ which implies that $\dot{z}_i^a = 0$ for $i = 1, \ldots, n-1$. Let $\mathcal{M}$ be the largest invariant set contained in $\mathcal{E}$. By the LaSalle Invariance Principle, solutions that start in Ω_c approach $\mathcal{M}$. The relative equilibrium (3.5.12) in particular is contained in $\mathcal{M}$.

We now proceed to analyse in more detail the structure of solutions on the LaSalle surface $\mathcal{E}$. Using the condition $\dot{z}_i^a = 0$ for $i = 1, \ldots, n-1$, we get $\dot{y}_i^a = \dot{y}_j^a$ for all $i, j \in \{1, \ldots, n\}$. This gives $y_i^a - y_j^a =$ constant. Since we have chosen $\tilde{V}_\epsilon$ to be a quadratic function of the terms $y_i^a - y_j^a$, we get

$$\frac{\partial \tilde{V}_\epsilon}{\partial y_i^a} = \text{constant} =: \Delta_a^i.$$

The equations of motion for the y_i^a restricted to $\mathcal{E}$ are $EL_c'(y_i^a) = 0$, where L_c' is given by (3.4.3). Equivalently,

$$\ddot{y}_i^a + \frac{d}{dt}\left(\tilde{g}_i^{ab} g_{\alpha b}^i \dot{x}_i^\alpha\right) = -\tilde{g}_i^{ab} \frac{\partial \tilde{V}_\epsilon}{\partial y_i^b} = -\tilde{g}_i^{ab} \Delta_b^i \,. \tag{3.6.8}$$

Consider the function l_i^a defined by

$$l_i^a(x_i^\alpha) = \frac{1}{(\kappa_i + \dfrac{\rho_i - 1}{\rho_i})} h_i^a(x_i^\alpha)$$

where h_i^a is as defined in (3.4.5). Then we have,

$$\frac{\partial l_i^a}{\partial x_i^\alpha} = \tilde{g}_i^{ac} g_{\alpha c}^i \,. \tag{3.6.9}$$

We can assume, by shrinking Ω_c if necessary, that (3.6.9) holds in Ω_c.

Let K_c be the projection of Ω_c onto the coordinates $(\boldsymbol{x}_n, \dot{\boldsymbol{x}}_n)$ where $\boldsymbol{x}_n = (x_1^\alpha, \ldots, x_n^\alpha)$. Then, since l_i^a is continuous and K_c is compact, there exist constants m_i and n_i such that

$$m_i \leq ||l_i(x_i)|| \leq n_i \tag{3.6.10}$$

for all x_i^α such that $\boldsymbol{x}_n \in \Omega_c$. Using (3.6.8), (3.6.9) and the condition $\dot{y}_i^a = \dot{y}_j^a$ on $\mathcal{E}$, we get

$$\frac{d}{dt}(l_i^a - l_j^a) = \tilde{g}_j^{ab} \Delta_b^j - \tilde{g}_i^{ab} \Delta_b^i \,. \tag{3.6.11}$$

Therefore, on $\mathcal{E}$

$$l_i^a - l_j^a = \frac{1}{2}(\tilde{g}_j^{ab} \Delta_b^j - \tilde{g}_i^{ab} \Delta_b^i) t^2 + \nu_1^a t + \nu_2^a \tag{3.6.12}$$

for some constant vectors ν_1^a and ν_2^a. The only way (3.6.10) can also be satisfied is if $\tilde{g}_j^{ab} \Delta_b^j - \tilde{g}_i^{ab} \Delta_b^i = 0$ and $\nu_1^a = 0$.

To simplify our calculations, we assume the n individual mechanical systems to be identical. In this case, $\tilde{g}_j^{ab} = \tilde{g}_j^{ab}$ for any $i, j \in \{1, \ldots, n\}$. This gives, $\Delta_a^i = \Delta_a^j$ for any $i, j \in \{1, \ldots, n\}$ and so for a connected network with potential V_ϵ' having a

maximum at $x_i^\alpha = 0$ and $y_i^a = y_j^a$ for all $i \neq j$, we get that $y_i^a = y_j^a$ on $\mathcal{E}$ for all $i, j \in \{1, \ldots, n\}$.

Using the definition (3.6.9) and the assumption that the individual systems are identical, the fact that $\dot{l}_i^a - \dot{l}_j^a = 0$ on $\mathcal{E}$ yields

$$g_{\alpha b}^i \dot{x}_i^\alpha = g_{\alpha b}^j \dot{x}_j^\alpha \,, \tag{3.6.13}$$

where $g_{\alpha b}^k = g_{\alpha b}(x_k^\alpha)$, for all $k = 1, \ldots, n$. Therefore, on the LaSalle surface $\mathcal{E}$, we see that solutions are of the form $(\boldsymbol{x}_n(t), \dot{\boldsymbol{x}}_n(t), y_1^a(t), \ldots, y_n^b(t), \dot{y}_1^c(t), \ldots, \dot{y}_n^d(t))$ where $y_i^a(t) = y_j^a(t)$ for any $i, j \in \{1, \ldots, n\}$, $J_a = \mu_a$ and condition (3.6.13) holds. Since $z_n^a = \sum_{i=1}^n y_i^a$ and the individual systems are identical, we have

$$\begin{aligned} J_a = \frac{\partial \tilde{L}_c}{\partial \dot{z}_n^a} &= \sum_{i=1}^n (g_{\alpha a}^i \dot{x}_i^\alpha + \tilde{g}_{ab} \dot{y}_i^b) \\ &= \tilde{g}_{ab} \sum_{i=1}^n (\tilde{g}^{bc} g_{\alpha c}^i \dot{x}_i^\alpha + \dot{y}_i^b) \\ &= n \tilde{g}_{ab} (\tilde{g}^{bc} g_{\alpha c}^i \dot{x}_i^\alpha + \dot{y}_i^b) \end{aligned}$$

for any $i \in \{1, \ldots, n\}$, where we have used the facts that $\dot{y}_i^a = \dot{y}_j^a$ and (3.6.13) holds on $\mathcal{E}$. Therefore, for each i we get

$$\dot{y}_i^a = \frac{1}{n} \tilde{g}^{ab} \mu_b - \tilde{g}^{ab} g_{\alpha b}^i \dot{x}_i^\alpha \,. \tag{3.6.14}$$

Substituting (3.6.14) into the closed-loop equations for the Lagrangian L_c' (3.4.3), we get the following equations for the x_i^α variables,

$$\frac{d}{dt} \frac{\partial L^\mu}{\partial \dot{x}_i^\alpha} = \frac{\partial L^\mu}{\partial x_i^\alpha} \tag{3.6.15}$$

where

$$\begin{aligned} L^\mu &= \sum_{i=1}^n \left(\frac{1}{2} (\tilde{g}_{\alpha\beta}^i - \tilde{g}^{ab} g_{\alpha a}^i g_{\beta b}^i) \dot{x}_i^\alpha \dot{x}_i^\beta - V_{1i}(x_i^\alpha) \right) \\ &= \sum_{i=1}^n \left(\frac{1}{2} (g_{\alpha\beta}^i - (\kappa + 1) g^{ab} g_{\alpha a}^i g_{\beta b}^i) \dot{x}_i^\alpha \dot{x}_i^\beta - V_{1i}(x_i^\alpha) \right) , \end{aligned} \tag{3.6.16}$$

and V_{1i} is defined by assumption **AS1**. Here, $\kappa_i = \kappa$ for all $i = 1, \ldots, n$.

Note that L^μ is a sum of terms, each of which depends only upon the i^{th} vehicle variables, i.e., on the LaSalle surface, the dynamics of i^{th} and j^{th} vehicle completely decouple. Here L^μ is the Routhian R^μ for a mechanical system with Abelian symmetry variables without a linear term in velocity and without the amended part of the potential. For a general Lagrangian system, refer to [33] for an explicit expression for the Routhian. In our case, the Routhian does not have the linear term in velocity because, as mentioned in §3.3, for SMC systems, this term does not contribute to the dynamics of the reduced system. The y_i^a dynamics given by (3.6.14) can be thought of as a reconstruction of dynamics in the symmetry variables, obtained after solving the reduced dynamics in the x_i^α variables.

We now make the following assumption for our systems.

> **AS2.** *Consider two solutions $(x^\alpha(t), y^a(t))$ and $(\tilde{x}^\beta(t), \tilde{y}^b(t))$ of the Euler-Lagrange equations corresponding to the Lagrangian L_c given by* (3.3.9). *If $y^a(t) = \tilde{y}^a(t)$ and $g_{\alpha a}(x^\beta(t))\dot{x}^\beta(t) = g_{\alpha a}(\tilde{x}^\beta(t))\dot{\tilde{x}}^\beta(t)$ then $x^\alpha(t) = \tilde{x}^\alpha(t)$.*

Using (3.6.13) and the fact that $y_i^a = y_j^a$ on the LaSalle surface, we get from **AS2** that $x_i^\alpha = x_j^\alpha$ and $\theta_i^a = \theta_j^a$ for all $i, j \in \{1, \ldots, n\}$. So we get that the dissipation control law given by (3.6.7) yields asymptotic convergence to synchronized motion on a constant momentum surface (ASSM).

Theorem 3.6.1 (ASSM) *Consider a network of n identical SMC systems that each satisfy* **AS1** *and* **AS2**. *Suppose for each individual system that the origin is an equilibrium and that the original potential energy is maximum at the origin. Consider the kinetic energy shaping defined in §3.4 and potential energy coupling $\tilde{V}_\epsilon$ defined in §3.5 where the terms in $\tilde{V}_\epsilon$ are quadratic in $y_i^a - y_j^a$ and the corresponding interconnection graph is connected. The closed-loop dynamics (3.6.2) derive from the Lagrangian $\tilde{L}_c$ given by (3.5.2) and the potential energy V_ϵ' is maximized at the relative equilibrium (3.5.12). The control input takes the form (3.6.1) where $u_{a,i}^{\text{cons}}$ is given by (3.5.18) and $\rho_i = \rho$, $\kappa_i = \kappa$. The dissipative control term given by equation (3.6.7) asymptotically*

stabilizes the solution in which all the vehicles have synchronized dynamics such that $\theta_i^a = \theta_j^a$ *and* $x_i^\alpha = x_j^\alpha$ *for all* i *and* j*, and each has the same constant momentum in the* θ_i^a *direction. The system stays on the constant momentum surface determined by the initial conditions.* ∎

Recall that in **Case I** above, we set $\tilde{u}_{a,n}^{\text{diss}} = 0$. Now consider **Case II** in which we choose $\tilde{u}_{a,n}^{\text{diss}} = -\lambda(J_a - \mu_a)$. Let $u_{a,i}$ for $i = 1, \ldots, n-1$ as in **Case I**. Then $J_a = (J_a(0) - \mu_a)\exp(-\lambda t) + \mu_a$ and we can rewrite the reduced system in $(\boldsymbol{x}_r, \dot{\boldsymbol{x}}_r)$ coordinates as follows:

$$ER^\mu(\boldsymbol{x}_r) = \begin{pmatrix} 0 \\ \frac{1}{n}\tilde{\mathbf{u}}^{\text{diss}} \end{pmatrix} + \lambda \bar{M}_{12}\bar{M}^{22}(\mathbf{J}(0) - \mu)\exp(-\lambda t). \tag{3.6.17}$$

Here, $\tilde{\mathbf{u}}^{\text{diss}} = (\tilde{u}_{a,1}^{\text{diss}}, \ldots, \tilde{u}_{a,n-1}^{\text{diss}})$ is an $r(n-1)$-dimensional vector, $\mathbf{J}$ and μ are r-dimensional vectors with components J_a and μ_b, respectively. When $\lambda = 0$, we get **Case I**. When $\lambda \neq 0$, the momentum J_a is no longer a conserved quantity. This case needs to be analyzed more carefully since we are pumping energy into the system now to drive it to a particular momentum value. Equation (3.6.17) can be considered to be a parameter dependent differential equation with the parameter being λ. When $\lambda = 0$, we already know the solution from **Case I**. From the continuity of dependence of solutions upon parameters, we get that when $0 < \lambda < \delta$, the solution stays within an $\epsilon-$tube of the solution in **Case I** for time $t \in [0, t_1]$ for some t_1 if the initial conditions are in a δ neighbourhood. Our simulation for pendulum/cart systems suggests that this holds true for the infinite time interval. This can also be seen as a time scaling problem. The fast time scale stabilizes the individual vehicle and synchronizes the network. The slow time scale moves the whole network to a prescribed momentum surface.

3.7 Asymptotic Stabilization of Relative Equilibria

In the previous section, we showed how to choose dissipation to achieve nontrivial, synchronized dynamics given by $\theta_i^a = \theta_j^a$ and $x_i^\alpha = x_j^\alpha$ for all $i, j = 1, \ldots, n$. The dissipation was chosen such that the network evolved staying on a constant momentum surface depending upon the initial condition. Stabilization was proved using E_μ as a Lyapunov function on the reduced space. We also discussed the case (**Case II**) in which we seek to drive the system to a prescribed momentum surface. We will illustrate these dynamics for a planar pendulum-on-a-cart network in §3.8.

In this section, we show how to achieve ASSRE motion for a network of SMC vehicles. We demonstate ASSRE for the relative equilibria given by (3.5.12). This is done using a different choice of Lyapunov function from what is used in §3.6.

Consider the following function:

$$E_{RE} = \frac{1}{2}(\dot{\boldsymbol{x}}_c - \mathbf{v}_{RE})^T \tilde{M}_c (\dot{\boldsymbol{x}}_c - \mathbf{v}_{RE}) + V'_\epsilon - \frac{1}{2}\boldsymbol{\zeta}^T \bar{M}_{22} \boldsymbol{\zeta} \tag{3.7.1}$$

where $\mathbf{v}_{RE}$ is defined by (3.5.12). E_{RE} is a Lyapunov function in directions transverse to the group orbit of the relative equilibrium, i.e., $E_{RE} < 0$ in a neighbourhood of the Euler-Lagrange solution given by $(\boldsymbol{x}_r, \mathbf{z}_n, \dot{\boldsymbol{x}}_r, \dot{\mathbf{z}}_n) = (0, \boldsymbol{\zeta} t, 0, \boldsymbol{\zeta})$ as shown in Figure 3.7.1 and $E_{RE} = 0$ at this solution. In this figure, $E_{RE} < 0$ on each section corresponding to a particular value of $\mathbf{z}_n$.

If we are to use E_{RE} as a Lyapunov function, we need to know its time derivative. For this, we need the following theorem. See [13] for the steps involved in proving this theorem.

Theorem 3.7.1 *[13] Consider the Lagrangian system with Lagrangian $\tilde{L}_c$ given by* (3.5.2) *and equations of motion given by*

$$E\tilde{L}_c(x_i^\alpha) = u_\alpha^i \;\; ; \quad E\tilde{L}_c(z_i^a) = u_a^i.$$

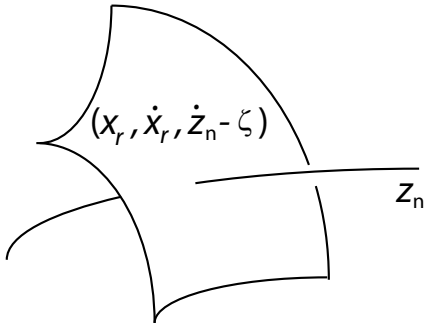

Figure 3.7.1: $E_{RE} < 0$ in neighbourhood of group orbit.

For this system, the time derivative of E_{RE} *defined by* (3.7.1) *is given by*

$$\frac{d}{dt}E_{RE} = (\dot{\boldsymbol{x}}_c - \mathbf{v}_{RE}) \cdot \begin{pmatrix} u_\alpha^i \\ u_a^i \end{pmatrix}$$

In our case, there is no dissipation in the x_i^α direction. Therefore, $u_\alpha^i = 0$. Using Theorem 3.7.1, the time derivative of E_{RE} along the flow given by (3.6.2) can be computed to be

$$\frac{d}{dt}E_{RE} = \frac{1}{n}(\dot{\boldsymbol{x}}_c - \mathbf{v}_{RE}) \cdot \begin{pmatrix} 0 \\ \tilde{\mathbf{u}}^{\text{diss}}. \end{pmatrix}$$

Choose

$$\tilde{u}_{a,i}^{\text{diss}} = \begin{cases} n\sigma_i \dot{z}_i^a & \text{for } i = 1, \ldots, n-1 \\ n\sigma_n(\dot{z}_n^a - \zeta^a) & \text{for } i = n \end{cases} \tag{3.7.2}$$

where control parameters σ_i are positive constants. Then,

$$\frac{d}{dt}E_{RE} = \sum_{j=1}^{n-1} \sigma_i(\dot{z}_j^a)^2 + \sigma_n(\dot{z}_n^b - \zeta^b)^2 \ \geq \ 0.$$

Let $\Omega_c^{RE} = \{(\boldsymbol{x}_r, \dot{\boldsymbol{x}}_r, \dot{z}_n^a) | E_{RE} \geq c\}$ for $c < 0$. Ω_c^{RE} is a compact set, i.e., E_{RE} is a proper Lyapunov function. Assume that the system given by (3.6.2) satisfies the following assumption.

AS3. *The system* (3.6.2) *is linearly controllable at each point in a neighbourhood of the relative equilibrium solution manifold.*

We now use the following result from nonlinear control theory which is stated as Lemma 2.1 in [13] and the remark after that.

Theorem 3.7.2 *[13] Let M be a smooth n-dimensional manifold and consider the control system on M with coordinates x*

$$\dot{x} = f(x) + \sum_{i=1}^{n} g_i(x) u_i \tag{3.7.3}$$

where f, g_i are smooth vector fields and $u_i(t)$ are bounded measurable functions. Let Φ be a smooth function such that $\Phi(x) = 0$ for $x \in S$ where S is a smooth, 1-dimensional submanifold of M. Let B_S be a neighbourhood of S in M and Φ be such that $\Phi(x) > 0$ whenever $x \in B_S - S$. Let Φ be a first integral of f and u_i be chosen to be $u_i = -\dfrac{\partial \Phi}{\partial \boldsymbol{x}} \cdot g_i$. If the system (3.7.3) is linearly controllable at each point in B_S and $\delta^2 \Phi(x) > 0$ for each $x \in S$, then the submanifold S is exponentially stable, i.e., $\Phi(x(t)) \leq c\Phi(x(0)) \exp^{-\lambda t}$ for some positive c and λ.

Using Theorem 3.7.2, we conclude that the system (3.6.2) with dissipative control terms given by (3.7.2) goes exponentially to the set

$$\mathcal{E}_{RE} = \{(\boldsymbol{x}_r, \dot{\boldsymbol{x}}_r, \dot{z}_n^a) \,|E_{RE} = 0\}\,.$$

On this set, the solution is given by (3.5.12). Thus, we have shown that the solutions of the controlled system will exponentially converge to $(x_i^\alpha, \theta_i^a, \dot{x}_i^\beta, \dot{\theta}_i^b) = (0, \dfrac{1}{n}\zeta^a t + \gamma^a, 0, \dfrac{1}{n}\zeta^b)$, with γ^a constant.

Theorem 3.7.3 (ASSRE) *Consider a network of n (not necessarily identical) individual SMC systems that each satisfy Assumption* **AS1**. *Suppose for each individual system that the origin is an equilibrium and that the original potential energy is maximum at the origin. Consider the kinetic energy shaping defined in §3.4 and potential energy coupling $\tilde{V}_\epsilon$ defined in §3.5 where the terms in $\tilde{V}_\epsilon$ are quadratic in $y_i^a - y_j^a$ and the corresponding interconnection graph is connected. The closed-loop dynamics (3.6.2) derive from the Lagrangian $\tilde{L}_c$ given by (3.5.2) and the potential energy V_ϵ'*

is maximized at the relative equilibrium (3.5.12). The control input takes the form (3.6.1) where $u_{a,i}^{\text{cons}}$ *is given by (3.5.18) and* $\rho_i = \rho$*. If the dynamics given by 3.6.2 satisfy* **AS3***, then the dissipative control term given by equation (3.7.2) exponentially stabilizes the relative equilibrium given by* (3.5.12) *in which* $x_i^\alpha = \dot{x}_i^\alpha = 0$ *for all* $i = 1, \ldots, n$ *and* $\theta_i^a = \theta_j^a$ *and* $\dot{\theta}_i^a = \dot{\theta}_j^a = \frac{1}{n}\zeta^a$ *for all* i *and* j*.*

3.8 Coordination of Multiple Inverted Pendulum on Cart Systems

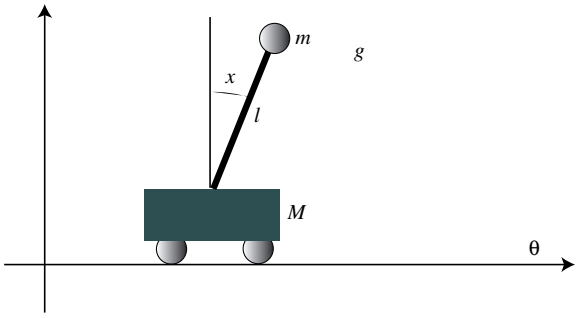

Figure 3.8.1: The planar pendulum on a cart.

As an illustration, we now consider the coordination of n identical planar inverted pendulum/cart systems. This section is taken verbatim from [38]. For the i^{th} system, the pendulum angle relative to the vertical is x_i and the position of the cart is θ_i. Let the Lagrangian for each system shown in Figure 3.8.1 be

$$L_i = \frac{1}{2}\alpha\dot{x}_i^2 + \beta\cos(x_i)\dot{x}_i\dot{\theta}_i + \frac{1}{2}\gamma\dot{\theta}_i^2 + D\cos(x_i)\ ; \quad i = 1, \ldots, n$$

where l, m, M are the pendulum length, pendulum bob mass and cart mass respectively. g is the acceleration due to gravity. The quantities α, β, γ and D are expressed in terms of l, m, M, g as follows:

$$\alpha = ml^2, \quad \beta = ml, \quad \gamma = m + M, \quad D = -mgl.$$

The equations of motion for the i^{th} system are

$$\begin{aligned} EL_i(x) &= 0 \\ EL_i(\theta) &= u_i \end{aligned}$$

where u_i is the control force applied to the i^{th} cart.

One can see that θ_i is a symmetry variable. Further, it can be easily verified that each pendulum/cart system satisfies the simplified matching conditions [8, 10]. The n inverted planar pendulum/cart systems lie on n parallel tracks corresponding to the θ_i directions. The coordination problem is to prescribe control forces u_i, $i = 1, \ldots, n$, that asymptotically stabilize the solution where each pendulum is in the vertical upright position (in the case of ASSRE) or moving synchronously (in the case of ASSM) and the carts are moving at the same position along their respective tracks with the same common velocity. The relative equilibrium $\mathbf{v}_{RE}$ (3.5.12) corresponds to $x_i = \dot{x}_i = 0$ for all i, $\theta_i = \theta_j$ for all $i \neq j$ and $\dot{\theta}_i = \frac{1}{n}\zeta$ for some constant scalar velocity ζ.

Following (3.5.2), the closed-loop Lagrangian for the total system in the coordinates $\boldsymbol{x}_c = (x_1, \ldots, x_n, z_1, \ldots, z_n) = (x_1, x_2, y_1 - y_2, \ldots, y_1 - y_n, y_1 + \cdots + y_n)$ where $y_i = \theta_i + p \sin x_i$ and $p = \kappa + 1 - \dfrac{1}{\rho}$ is

$$\tilde{L}_c = \frac{1}{2}\dot{\boldsymbol{x}}^T \tilde{M}_c \dot{\boldsymbol{x}} - V'_\epsilon(x_1, \ldots, x_n, z_1, \ldots, z_{n-1}). \tag{3.8.1}$$

where $\tilde{M}_c$ is as in (3.5.7) and M_c is as in (3.4.4),

$$\tilde{g}^i_{\alpha\beta} = \alpha - (\kappa + 1 - \frac{1}{\rho})\frac{\beta^2}{\gamma}\cos^2(x_i), \qquad \tilde{g}^i_{\alpha a} = \beta\cos(x_i)$$

$$\tilde{g}^i_{ab} = \rho\gamma, \qquad V'_\epsilon = -D\sum_{i=1}^{n-1}\left(\cos(x_i) - \frac{1}{2}\epsilon\frac{\gamma^2}{\beta^2}z_i^2\right) - D\cos(x_n)$$

with $\epsilon > 0$. The control law (3.6.1) for the i^{th} system is

$$u_i = \frac{\kappa\beta\left(\sin x_i\,(\alpha\dot{x}_i^2 + \cos(x_i)D) - B_i\left(\dfrac{\partial V'_\epsilon}{\partial\theta_i} - u_i^{\text{diss}}\right)\right)}{\alpha - \frac{\beta^2}{\gamma}(1+\kappa)\cos^2(x_i)} \tag{3.8.2}$$

where $B_i = \frac{1}{\rho}\left(\alpha - \frac{\beta^2 \cos^2(x_i)}{\gamma}\right)$. Note that we have chosen $\rho_i = \rho$ and $\kappa_i = \kappa$. In the case $u_i^{\text{diss}} = 0$, by Theorem 3.5.4, we get stability of the relative equilibrium $\mathbf{v}_{RE}$ (SSRE) if we choose $\rho < 0$, $\epsilon > 0$ and κ such that $m_\kappa := \alpha - (\kappa+1)\frac{\beta^2}{\gamma} < 0$. The choice of u_i^{diss} depends upon what kind of asymptotic stability we want, i.e, convergence to a synchronized constant momentum solution or to a relative equilibrium.

3.8.1 Asymptotic stability on constant momentum surface (ASSM)

Following (3.6.7), we let u_1^{diss} be

$$u_1^{\text{diss}} = d_1 \left(\sum_{k=1}^{n-1} (\dot{z}_k) \right)$$

and u_i^{diss} for $i = 2, \ldots, n$ be

$$u_i^{\text{diss}} = d_i \left(-(n-1)\dot{z}_{i-1} + \sum_{k=1, k\neq i-1}^{n-1} \dot{z}_k \right)$$

where coefficients d_i are constant positive scalars.

We now analyze the dynamics on the LaSalle surface. On this surface, we have $\dot{y}_i = \dot{y}_j$ for all $i, j \in \{1, \ldots, n\}$ and $J = \mu$ where momentum μ is determined by the initial conditions. The expression for J is

$$J = \sum_{i=1}^{n} \left(\rho\gamma\dot{\theta}_i + (\beta + p\rho\gamma)\cos(x_i)\dot{x}_i \right).$$

From the calculations made in §3.6, we also get $y_i = y_j$ and $\cos(x_i)\dot{x}_i = \cos(x_j)\dot{x}_j$. The x_i dynamics are given by (3.6.15) with

$$L^\mu = \sum_{i=1}^{n} \left(\frac{1}{2}\left(\alpha - (\kappa+1)\frac{\beta^2}{\gamma}\cos^2(x_i)\right)\dot{x}_i^2 + D\cos(x_i) \right). \tag{3.8.3}$$

To verify **AS2** we need to check that if $\cos(x_i)\dot{x}_i = \cos(x_j)\dot{x}_j$ about the origin for a system corresponding to the Lagrangian L^μ, then $x_i = x_j$ identically. This condition

can also be written as $\sin(x_i) = \sin(x_j) + c$, where c is a constant. Note that if $x_i(t)$ is an Euler-Lagrange solution corresponding to L^μ for the i^{th} vehicle, then $-x_i(t)$ is also a solution. Since we have a stable pendulum oscillation about the upright position, $x_i(t)$ and therefore $|\sin(x_i(t))|$ oscillates with mean zero for all i. This can also be concluded from the fact that the solution curves are closed level curves in the $(x_i, \dot{x}_i)$ plane of L^μ given by (3.8.3) and L^μ is invariant under the sign change $(x_i, \dot{x}_i) \mapsto -(x_i, \dot{x}_i)$. Since $|\sin(x_i)|$ oscillates with zero mean for all i, the constant c must be zero. Hence, $x_i(t) = x_j(t)$ for all i, j identically and **AS2** is verified. Thus by Theorem 3.6.1 the pendulum network asymptotically goes to an ASSM.

From (3.8.3), it can be seen that on the LaSalle surface, the dynamics of x_i are decoupled from the dynamics of x_j for all $i \neq j$. For small x_i, the dynamics of each individual term in L^μ corresponds to the stable dynamics of a spring-mass system with a κ-dependent mass $-m_\kappa > 0$ and spring constant $-D > 0$. The mass $-m_\kappa$, which determines the oscillation frequency of the pendulum for each individual cart, can be controlled by choice of κ. For the nonlinear system also, constant energy curves are closed curves in $(x_i, \dot{x}_i)$ plane. Hence, we have a periodic orbit for the angle made by each pendulum with the vertical line with a $\kappa-$dependent frequency. On the LaSalle surface, $\rho\gamma\dot{\theta}_i + (\beta + p\rho\gamma)\cos(x_i)\dot{x}_i = \text{constant}$. Therefore, the velocity of the cart $\dot{\theta}_i$ oscillates about a constant velocity with the same frequency as the pendulum oscillation.

Figure 3.8.2 shows the results of a MATLAB simulation for the controlled network of $n = 3$ pendulum/cart systems using the following values for the system parameters. The pendulum/cart systems have identical pendulum bob masses, lengths and cart masses. The pendulum bob mass is chosen to be $m = 0.14$ kg, cart mass is $M = 0.44$ kg, pendulum length is $l = 0.215$ m. The control gains are $\rho = -0.27$, $\kappa = 40$, $d_i = d = 0.6$ and $\epsilon = 0.0005$. We compute $m_\kappa = -0.058$ kgm$^2 < 0$ as required for

stability. The initial conditions for the three systems shown are

$$\begin{pmatrix} x_1(0) & \dot{x}_1(0) & \theta_1(0) & \dot{\theta}_1(0) & x_2(0) & \dot{x}_2(0) & \theta_2(0) & \dot{\theta}_2(0) & x_3(0) & \dot{x}_3(0) & \theta_3(0) & \dot{\theta}_3(0) \end{pmatrix}$$
$$= \begin{pmatrix} 0.45 & 0.70 & 0.58 & 0.50 & 0.07 & 0.19 & 0.37 & 0.27 & 0.77 & 0.31 & 0.63 & 0.98 \end{pmatrix},$$

where the x_i are in rad, $\dot{x}_i$ in rad/sec, θ_i in m and $\dot{\theta}_i$ in m/s. Figure 3.8.2 shows plots of the pendulum angle, cart position and cart velocity as a function of time for all three of the coupled pendulum/cart systems. Convergence to an ASSM is evident. The frequency of oscillation of the pendula can be observed to be the same as the frequency of oscillation in the cart velocities. This frequency of oscillation can be computed as $\omega = \sqrt{D/m_\kappa}$ and the period of oscillation as $T = 2\pi/\omega = 2.8$ s which is precisely the period of the oscillations observed in Figure 3.8.2.

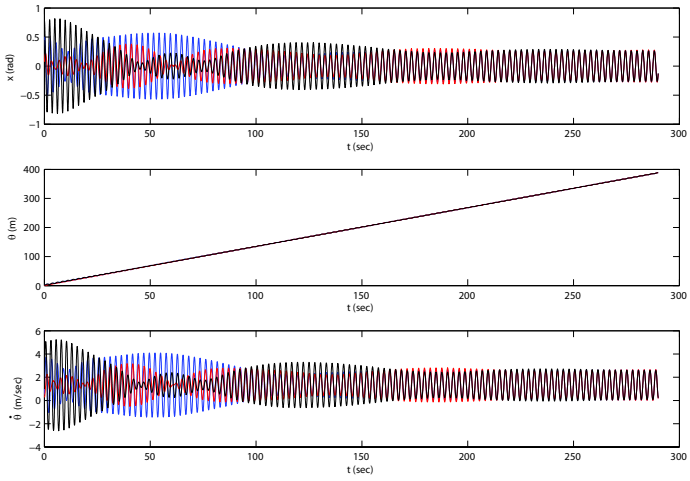

Figure 3.8.2: Simulation of a controlled network of pendulum/cart systems with dissipation designed for asymptotic stability of a synchronized motion on a constant momentum surface (ASSM). The pendulum angle, cart position and cart velocity are plotted as a function of time for each of three pendulum/cart systems in the network.

3.8.2 Asymptotic stability of relative equilibria (ASSRE)

In this case, we want to asymptotically stabilize the relative equilibrium $\mathbf{v}_{RE}$, i.e., $x_i = \dot{x}_i = 0$ for all i, $\theta_i = \theta_j$ for all $i \neq j$ and $\dot{\theta}_i = \frac{1}{n}\zeta$ for all i and any constant scalar velocity ζ. Recall that this corresponds to each pendulum angle at rest in the upright position and all carts aligned and moving together with the same constant velocity $\frac{1}{n}\zeta$. Following (3.7.2), we let

$$u_i^{\text{diss}} = nd_i\dot{z}_i$$

for $i = 1, \ldots, n-1$ and

$$u_n^{\text{diss}} = nd_n(\dot{z}_n - \zeta)$$

where the control parameters d_i are positive constants.

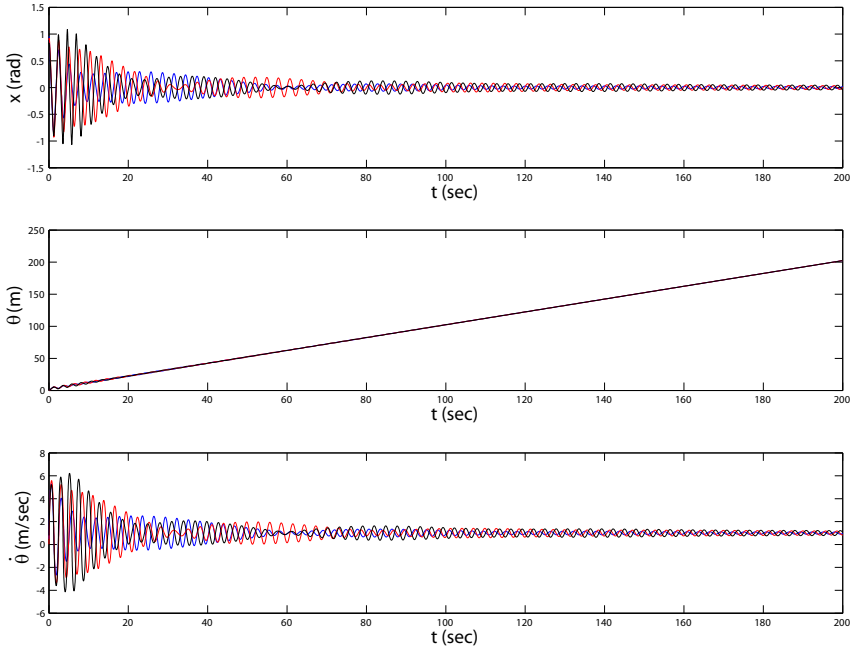

Figure 3.8.3: Simulation of a controlled network of pendulum/cart systems with dissipation designed for asymptotic stability of a relative equilibrium (ASSRE). The pendulum angle, cart position and cart velocity are plotted as a function of time for each of three pendulum/cart systems in the network.

Figure 3.8.3 shows the results of a MATLAB simulation for the controlled network of pendulum/cart systems with this dissipative control. We choose $\zeta = 3$ m/s and the remaining system and control parameters are as above in the ASSM case. The initial conditions for the three systems are

$$\begin{pmatrix} x_1(0) & \dot{x}_1(0) & \theta_1(0) & \dot{\theta}_1(0) & x_2(0) & \dot{x}_2(0) & \theta_2(0) & \dot{\theta}_2(0) & x_3(0) & \dot{x}_3(0) & \theta_3(0) & \dot{\theta}_3(0) \end{pmatrix}$$
$$= \begin{pmatrix} 0.95 & 0.23 & 0.61 & 0.49 & 0.89 & 0.76 & 0.46 & 0.02 & 0.82 & 0.44 & 0.62 & 0.79 \end{pmatrix},$$

with same units as before. Figure 3.8.3 shows convergence of all three systems to the relative equilibrium; the pendula are stabilized in the upright position, the cart positions become synchronized and the cart velocities converge to $\frac{\zeta}{3} = 1$ m/s.

Chapter 4

Reduced Equations of Motion for Networked Rigid Bodies

In this chapter, we derive the reduced Lagrangian equations of motion for a network of rigid bodies in $SO(3)$ and $SE(3)$. A similar problem is considered in [25], but in that paper, the authors do the reduction using the Poisson setting. In this section, we do Lagrangian reduction developed in [14]. Specifically, given a Lagrangian system on TQ with Lagrangian L and symmetry group G, the reduced Lagrangian l is a function on TQ/G. Using a principal connection α, the bundle TQ/G is identified with $T(Q/G) \oplus \tilde{\mathfrak{g}}$. Here, $\tilde{\mathfrak{g}}$ is a bundle with base Q/G [14] and fibre $\mathfrak{g}$. Using α, the variations are split into a vertical part and a horizontal part and the corresponding vertical and horizontal equations are derived. For more details on Lagrangian reduction, refer to [14].

The reduced dynamics derived in this chapter are used in Chapter 5 and 6 to study stabilization and coordinated control of a network of rigid bodies. For example, a network of rigid satellites has configuration space equal to n copies of $SO(3)$ and a network of underwater vehicles has configuration space equal to n copies of $SE(3)$. The symmetry in the dynamics of these systems comes from using coupling forces and moments that only depend upon relative orientations and/or relative positions of

the rigid bodies; the system dynamics are thus independent of the orientation and/or position of the whole network.

4.1 Reduced equations of motions for $SO(3)$ network.

Here, we show how to derive the equations of motion for n rigid bodies, each with configuration space $SO(3)$ defined by

$$SO(3) = \{R \in \mathbb{R}^{3\times 3} \mid \det(R) = 1, R^T R = \mathbb{I}_{3\times 3}\}$$

where $\mathbb{I}_{3\times 3}$ is the 3×3 identity matrix. These bodies are coupled with a potential depending upon their relative orientations. The configuration space is $SO(3)^n = SO(3) \times \ldots \times SO(3)$ and the phase space is $T(SO(3)^n)$ with coordinates

$$(R_1, \ldots, R_n, \dot{R}_1, \ldots, \dot{R}_n)$$

The coupling potential is chosen to be $V = \sigma \sum_{i=1}^{n-1} \mathrm{tr}(R_{i+1}^T R_i)$. Let for a vector u, $\hat{u}$ denote the operator such that $\hat{u}y = u \times y$ for any vector y. Then, the Lagrangian in terms of the angular velocity in body coordinates $\mathbf{\Omega}_i \in \mathbb{R}^3$ given by $\dot{R}_i = R_i \widehat{\mathbf{\Omega}_i}$ is

$$L = \frac{1}{2} \sum_{i=1}^{n} \left(\mathbf{\Omega}_i^T I_i \mathbf{\Omega}_i \right) - \sigma \sum_{i=1}^{n-1} \mathrm{tr}(R_{i+1}^T R_i) \tag{4.1.1}$$

L has $SO(3)$ as its symmetry group with the symmetry action given by

$$R \cdot (R_1, \ldots, R_n, R_1\widehat{\mathbf{\Omega}}_1, \ldots, R_n\widehat{\mathbf{\Omega}}_n) = (RR_1, \ldots, RR_n, RR_1\widehat{\mathbf{\Omega}}_1, \ldots, RR_n\widehat{\mathbf{\Omega}}_n). \tag{4.1.2}$$

Let $X_i = R_{i+1}^T R_i$, i.e., X_i is the difference in orientations represented by R_{i+1} and R_i. See Figure 4.1.1 for an illustration of the relative orientations in a system of three rigid bodies. Then $\dot{X}_i = X_i\widehat{\mathbf{\Omega}}_i - \widehat{\mathbf{\Omega}}_{i+1}X_i$ and $\dot{X}_i X_i^{-1} = X_i\widehat{\mathbf{\Omega}}_i X_i^{-1} - \widehat{\mathbf{\Omega}}_{i+1} = \widehat{X_i\mathbf{\Omega}_i} - \widehat{\mathbf{\Omega}}_{i+1}$. Let $\boldsymbol{w}_i = X_i\mathbf{\Omega}_i - \mathbf{\Omega}_{i+1}$ be the difference of angular velocities of i^{th} and $(i+1)^{\text{th}}$ body represented in the body frame of $i+1$.

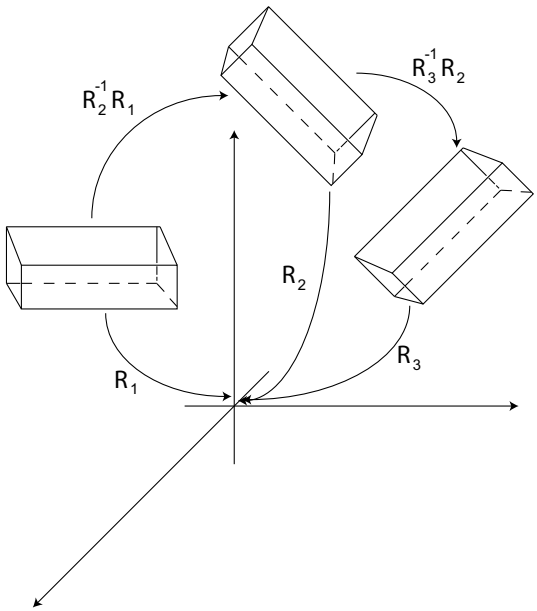

Figure 4.1.1: Illustration of relative orientation of body 1 with respect to body 2 and relative orientation of body 2 with respect to body 3.

We identify the reduced space as

$$\begin{aligned}&\left[R_1, R_2, \ldots, R_n, R_1\widehat{\boldsymbol{\Omega}}_1, R_2\widehat{\boldsymbol{\Omega}}_2, \ldots, R_n\widehat{\boldsymbol{\Omega}}_n\right]_{SO(3)}\\ &= (X_1, X_2, \ldots, X_{n-1}, \dot{X}_1X_1^{-1}, \dot{X}_2X_2^{-1}, \ldots, \dot{X}_{n-1}X_{n-1}^{-1}, \boldsymbol{\Omega}_1)\\ &= (X_1, X_2, \ldots, X_{n-1}, \boldsymbol{w}_1, \boldsymbol{w}_2, \ldots, \boldsymbol{w}_{n-1}, \boldsymbol{\Omega}_1)\end{aligned} \tag{4.1.3}$$

Here, we have used the notion of a principal connection on a principle bundle. In our case, the "value" of the principle connection is the angular velocity of the first rigid body in its body frame and belongs to the Lie algebra $so(3)$. In our case, $Q = SO(3)^n$, $G = SO(3)$, Q/G is $n-1$ copies of $SO(3)$ and $\mathfrak{g}$ is $so(3)$.

The Lagrangian L given by (4.1.1) should be thought of as a function of

$$(X, \boldsymbol{w}, \boldsymbol{\Omega}_1) = (X_1, \ldots, X_{n-1}, \boldsymbol{w}_1, \ldots, \boldsymbol{w}_{n-1}, \boldsymbol{\Omega}_1).$$

We denote by l the Lagrangian on the reduced space such that

$$l(X, \boldsymbol{w}, \boldsymbol{\Omega}_1) = \frac{1}{2}\sum_{i=1}^{n}\left(\boldsymbol{\Omega}_i^T I_i \boldsymbol{\Omega}_i\right) - V(X) \tag{4.1.4}$$

where $\boldsymbol{\Omega}_j$, $j = 1, \ldots, n$ can be expressed in terms of $\boldsymbol{\Omega}_1$ recursively as

$$\boldsymbol{\Omega}_j = X_{j-1}\boldsymbol{\Omega}_{j-1} - \boldsymbol{w}_{j-1}$$

and

$$V(X) = \sigma \sum_{i=1}^{n-1} \mathrm{tr} X_i$$

The equations of motion are derived using the variational formulation of mechanics. Using the identification given by (4.1.3), the variations are split into a vertical part and a horizontal part [14] given by

$$\delta_V(X, \boldsymbol{w}, \boldsymbol{\Omega}_1) = ((X, \boldsymbol{w}, \boldsymbol{\Omega}_1), (0, 0, \dot{\boldsymbol{\eta}} + \boldsymbol{\Omega}_1 \times \boldsymbol{\eta})) \tag{4.1.5}$$

$$\delta_H(X, \boldsymbol{w}, \boldsymbol{\Omega}_1) = \left((X, \boldsymbol{w}, \boldsymbol{\Omega}_1), (\widehat{\boldsymbol{\lambda}} X, \dot{\boldsymbol{\lambda}} - \boldsymbol{w} \times \boldsymbol{\lambda}, 0)\right) \tag{4.1.6}$$

where $\boldsymbol{\eta}(t_i) = 0, \boldsymbol{\lambda}_j(t_i) = 0$ for $i = 0, 1$ and $j = 1, \ldots, n-1$ and

$$\begin{aligned} \widehat{\boldsymbol{\lambda}} X &:= \left(\widehat{\boldsymbol{\lambda}}_1 X_1, \ldots, \widehat{\boldsymbol{\lambda}}_{n-1} X_{n-1}\right) \\ \dot{\boldsymbol{\lambda}} - \boldsymbol{w} \times \boldsymbol{\lambda} &:= \left(\dot{\boldsymbol{\lambda}}_1 - \boldsymbol{w}_1 \times \boldsymbol{\lambda}_1, \ldots, \dot{\boldsymbol{\lambda}}_{n-1} - \boldsymbol{w}_{n-1} \times \boldsymbol{\lambda}_{n-1}\right). \end{aligned}$$

Here, t_0, t_1 are the initial and final times respectively of the paths in the variations. We show the steps for calculating $\delta\boldsymbol{\Omega}_1$. The calculations for δX and $\delta \boldsymbol{w}$ are similar.

Let $\widehat{\boldsymbol{\eta}} = R_1^{-1}\delta R_1$, where δR_1 is the variation of a path R_1 in $SO(3)$ with fixed end points, i.e., $\delta R_1(t_0) = \delta R_1(t_1) = 0$. Since $\widehat{\boldsymbol{\Omega}}_1 = R_1^{-1}\dot{R}_1$, we have

$$\begin{aligned} \delta\widehat{\boldsymbol{\Omega}}_1 &= R_1^{-1}\delta\dot{R}_1 - R_1^{-1}\delta R_1 R_1^{-1}\dot{R}_1 \\ &= R_1^{-1}\delta\dot{R}_1 - R_1^{-1}\delta R_1 R_1^{-1}\dot{R}_1 + R_1^{-1}\dot{R}_1 R_1^{-1}\delta R_1 - R_1^{-1}\dot{R}_1 R_1^{-1}\delta R_1 \\ &= \dot{\widehat{\boldsymbol{\eta}}} + \left[\widehat{\boldsymbol{\Omega}}, \widehat{\boldsymbol{\eta}}\right] \end{aligned}$$

Therefore, $\delta\boldsymbol{\Omega}_1 = \dot{\boldsymbol{\eta}} + \boldsymbol{\Omega}_1 \times \boldsymbol{\eta}$.

The vertical variations correspond to variations in the group direction. In our case, these correspond to variations in $\boldsymbol{\Omega}_1$. The horizontal variations correspond to variations in the reduced space, which in our case is the $(X, \boldsymbol{w})$ space. An arbitrary variation in the full configuration space can be split into a vertical part and

a horizontal part once a connection is chosen. This splitting gives rise to a vertical equation and a horizontal equation of motion respectively. The vertical equation is the momentum conservation equation and is derived as follows using the fact

$$\delta_V \boldsymbol{\Omega}_i = X_i \delta_V \boldsymbol{\Omega}_{i-1} = X_i X_{i-1} \delta_V \boldsymbol{\Omega}_{i-2} = \ldots = R_i^T R_1 \delta_V \boldsymbol{\Omega}_1.$$

We compute

$$\begin{aligned}
\delta_V \int_{t_0}^{t_1} l(X, \boldsymbol{w}, \boldsymbol{\Omega}_1) dt &= \delta_V \int_{t_0}^{t_1} \left(\frac{1}{2} \sum_{i=1}^{n} \boldsymbol{\Omega}_i^T I_i \boldsymbol{\Omega}_i - V(X) \right) dt \\
&= \int_{t_0}^{t_1} \left(\sum_{i=1}^{n} \boldsymbol{\Omega}_i^T I_i \delta_V \boldsymbol{\Omega}_i \right) dt \\
&= \int_{t_0}^{t_1} \left(\sum_{i=1}^{n} \boldsymbol{\Omega}_i^T I_i R_i^T R_1 \right) \delta_V \boldsymbol{\Omega}_1 dt \\
&= \int_{t_0}^{t_1} \boldsymbol{a}^T (\dot{\boldsymbol{\eta}} + \boldsymbol{\Omega}_1 \times \boldsymbol{\eta}) dt \\
&= \int_{t_0}^{t_1} (-\dot{\boldsymbol{a}}^T + (\boldsymbol{a} \times \boldsymbol{\Omega}_1)^T) \boldsymbol{\eta}(t) dt
\end{aligned}$$

where we have used $\delta_V \boldsymbol{\Omega}_1 = \dot{\boldsymbol{\eta}} + \boldsymbol{\Omega}_1 \times \boldsymbol{\eta}$, $\boldsymbol{\eta}(t_0) = \boldsymbol{\eta}(t_1) = 0$ and integration by parts in the last step. Here,

$$\boldsymbol{a} = \left(\sum_{i=1}^{n} \boldsymbol{\Omega}_i^T I_i R_i^T R_1 \right)^T = I_1 \boldsymbol{\Omega}_1 + R_1^T R_2 I_2 \boldsymbol{\Omega}_2 + \ldots + R_1^T R_n I_n \boldsymbol{\Omega}_n, \tag{4.1.7}$$

the total angular momemtum as seen in body-1 frame, and $\boldsymbol{\eta}(t)$ is arbitrary. Hence, setting $\delta_V \int_{t_0}^{t_1} l = 0$ we get

$$\dot{\boldsymbol{a}} = \boldsymbol{a} \times \boldsymbol{\Omega}_1. \tag{4.1.8}$$

This is the equation for conservation of total angular momentum in inertial space as seen in body 1 frame.

Now, we calculate the horizontal equation of motion corresponding to the horizontal variation. To do this, we first prove the following useful lemma.

Lemma 4.1.1 *Let $\boldsymbol{b} \in \mathbb{R}^3$ and $R \in SO(3)$ where $\{\boldsymbol{c}_1, \boldsymbol{c}_2, \boldsymbol{c}_3\}$ are the column vectors of R. Then, $\mathrm{tr}(R\hat{\boldsymbol{b}}) = \boldsymbol{b} \cdot \boldsymbol{v}$ where, $\boldsymbol{v} = \boldsymbol{c}_1 \times \boldsymbol{e}_1 + \boldsymbol{c}_2 \times \boldsymbol{e}_2 + \boldsymbol{c}_3 \times \boldsymbol{e}_3$ is the eigenvector of R corresponding to eigenvalue 1 when $R \neq I$.*

Proof We have

$$\begin{aligned}
\mathrm{tr}(R\hat{\boldsymbol{b}}) &= \mathrm{tr}(\hat{\boldsymbol{b}}R) \\
&= \mathrm{tr}(\hat{\boldsymbol{b}}[\boldsymbol{c}_1\ \boldsymbol{c}_2\ \boldsymbol{c}_3]) \\
&= \mathrm{tr}([\boldsymbol{b}\times\boldsymbol{c}_1\ \ \boldsymbol{b}\times\boldsymbol{c}_2\ \ \boldsymbol{b}\times\boldsymbol{c}_3]) \\
&= \boldsymbol{e}_1\cdot(\boldsymbol{b}\times\boldsymbol{c}_1)+\boldsymbol{e}_2\cdot(\boldsymbol{b}\times\boldsymbol{c}_2)+\boldsymbol{e}_3\cdot(\boldsymbol{b}\times\boldsymbol{c}_3) \\
&= \boldsymbol{b}\cdot(\boldsymbol{c}_1\times\boldsymbol{e}_1+\boldsymbol{c}_2\times\boldsymbol{e}_2+\boldsymbol{c}_3\times\boldsymbol{e}_3)\,.
\end{aligned}$$

Now let $\boldsymbol{v}=\boldsymbol{c}_1\times\boldsymbol{e}_1+\boldsymbol{c}_2\times\boldsymbol{e}_2+\boldsymbol{c}_3\times\boldsymbol{e}_3$. Then,

$$\begin{aligned}
\boldsymbol{b}\cdot(R\boldsymbol{v}) &= (R^T\boldsymbol{b})\cdot\boldsymbol{v} \\
&= \mathrm{tr}(\widehat{RR^T\boldsymbol{b}}) \\
&= \mathrm{tr}(RR^T\hat{\boldsymbol{b}}R) \\
&= \mathrm{tr}(\hat{\boldsymbol{b}}R)\ =\ \mathrm{tr}(R\hat{\boldsymbol{b}})\ =\ \boldsymbol{b}\cdot\boldsymbol{v}\,.
\end{aligned}$$

Since $\boldsymbol{b}$ is arbitrary, $R\boldsymbol{v}=\boldsymbol{v}$, i.e., $\boldsymbol{v}$ is the eigenvector of R corresponding to eigenvalue 1. ∎

Next we calculate the horizontal variation of $V(X)$. Using Lemma 4.1.1 and the fact that trace is a linear operator, we get

$$\begin{aligned}
\delta_H V(X) &= \delta_H\sigma\,\mathrm{tr}\Big(\sum_{i=1}^{n-1}X_i\Big) \\
&= \sigma\sum_{i=1}^{n-1}\mathrm{tr}(\delta_H X_i) \\
&= \sigma\sum_{i=1}^{n-1}\mathrm{tr}(\hat{\boldsymbol{\lambda}}_i X_i) \\
&= \sigma\sum_{i=1}^{n-1}(\boldsymbol{u}_i^{ps})^T\boldsymbol{\lambda}_i \qquad (4.1.9)
\end{aligned}$$

where $\boldsymbol{u}_i^{ps}=(\boldsymbol{\Delta}_i\times\boldsymbol{e}_1+\boldsymbol{\Sigma}_i\times\boldsymbol{e}_2+\boldsymbol{\Gamma}_i\times\boldsymbol{e}_3)$ and $\boldsymbol{\Delta}_i,\boldsymbol{\Sigma}_i,\boldsymbol{\Gamma}_i$ are the column vectors of $X_i=R_{i+1}^{-1}R_i$. Hence, from (4.1.1), we get that u_i^{ps} is the eigenvector of X_i corresponding to eigenvalue 1.

Next, we calculate $\delta_H \mathbf{\Omega}_i$ for $i > 1$ using (4.1.6). We have $\mathbf{\Omega}_{i+1} = x_i \mathbf{\Omega}_i - \boldsymbol{w}_i$, therefore we get

$$\begin{aligned} \delta_H \mathbf{\Omega}_{i+1} &= -\delta_H \boldsymbol{w}_i + (\delta_H X_i)\mathbf{\Omega}_i + X_i \delta_H \mathbf{\Omega}_i \\ &= -\delta_H \boldsymbol{w}_i + \widehat{\boldsymbol{\lambda}}_i \mathbf{\Omega}_i + X_i \delta_H \mathbf{\Omega}_i \end{aligned}$$

Using this recursively, $\delta_H \mathbf{\Omega}_i = 0$ from (4.1.6) and the identity $Y(\boldsymbol{z}_1 \times \boldsymbol{z}_2) = (Y\boldsymbol{z}_1) \times (Y\boldsymbol{z}_2)$ for vectors $\boldsymbol{z}_1, \boldsymbol{z}_2$ and rotation matrix Y, we get

$$\begin{aligned} \delta_H \mathbf{\Omega}_{i+1} &= -\dot{\boldsymbol{\lambda}}_i + \boldsymbol{w}_i \times \boldsymbol{\lambda}_i + \boldsymbol{\lambda}_i \times (x_i \mathbf{\Omega}_i) + x_i \delta_H \mathbf{\Omega}_i \\ &= -\dot{\boldsymbol{\lambda}}_i + \boldsymbol{w}_i \times \boldsymbol{\lambda}_i + \boldsymbol{\lambda}_i \times (x_i \mathbf{\Omega}_i) - x_i \dot{\boldsymbol{\lambda}}_{i-1} + x_i \boldsymbol{w}_{i-1} \times x_i \boldsymbol{\lambda}_{i-1} + \\ &\quad x_i \boldsymbol{\lambda}_{i-1} \times (x_i x_{i-1} \mathbf{\Omega}_{i-1}) + x_i x_{i-1} \delta_H \mathbf{\Omega}_{i-1} \\ &= \vdots \\ &= x_{i+1}^{-1} \sum_{j=1}^{i} x_{i+1} x_i \cdots x_{j+1} \left(-\dot{\boldsymbol{\lambda}}_j + \boldsymbol{w}_j \times \boldsymbol{\lambda}_j + \boldsymbol{\lambda}_j \times (x_j \mathbf{\Omega}_j) \right) \\ &= x_{i+1}^{-1} \sum_{j=1}^{i} R_{i+2}^T R_{j+1} \left(-\dot{\boldsymbol{\lambda}}_j + \boldsymbol{w}_j \times \boldsymbol{\lambda}_j + \boldsymbol{\lambda}_j \times (x_j \mathbf{\Omega}_j) \right) \\ &= \sum_{j=1}^{i} R_{i+1}^T R_{j+1} \left(-\dot{\boldsymbol{\lambda}}_j + \boldsymbol{w}_j \times \boldsymbol{\lambda}_j + \boldsymbol{\lambda}_j \times (x_j \mathbf{\Omega}_j) \right). \end{aligned} \tag{4.1.10}$$

Now,

$$\begin{aligned}
\int_{t_0}^{t_1} \sum_{i=2}^{n} \boldsymbol{\Omega}_i^T I_i \delta_H \boldsymbol{\Omega}_i &= \int_{t_0}^{t_1} \sum_{i=2}^{n} \boldsymbol{\Omega}_i^T I_i \sum_{j=1}^{i-1} R_i^T R_{j+1} \left(-\dot{\boldsymbol{\lambda}}_j + \boldsymbol{w}_j \times \boldsymbol{\lambda}_j + \boldsymbol{\lambda}_j \times (x_j \boldsymbol{\Omega}_j) \right) dt \\
&= \int_{t_0}^{t_1} \sum_{i=2}^{n} \sum_{j=1}^{i-1} \left(R_{j+1}^T R_i I_i \boldsymbol{\Omega}_i \right)^T \left(-\dot{\boldsymbol{\lambda}}_j + \boldsymbol{w}_j \times \boldsymbol{\lambda}_j + \boldsymbol{\lambda}_j \times (x_j \boldsymbol{\Omega}_j) \right) dt \\
&= \int_{t_0}^{t_1} \sum_{i=2}^{n} \sum_{j=1}^{i-1} \Big(\frac{d}{dt} \left(R_{j+1}^T R_i I_i \boldsymbol{\Omega}_i \right)^T \boldsymbol{\lambda}_j \\
&\quad + \left(R_{j+1}^T R_i I_i \boldsymbol{\Omega}_i \right)^T \left(\boldsymbol{w}_j \times \boldsymbol{\lambda}_j + \boldsymbol{\lambda}_j \times (x_j \boldsymbol{\Omega}_j) \right) \Big) dt \\
&= \int_{t_0}^{t_1} \sum_{i=2}^{n} \sum_{j=1}^{i-1} \boldsymbol{\lambda}_j^T \Big(\frac{d}{dt} \left(R_{j+1}^T R_i I_i \boldsymbol{\Omega}_i \right) \\
&\quad + \left(R_{j+1}^T R_i I_i \boldsymbol{\Omega}_i \right) \times (\boldsymbol{w}_j - x_j \boldsymbol{\Omega}_j) \Big) dt \\
&= \int_{t_0}^{t_1} \sum_{j=1}^{n-1} \boldsymbol{\lambda}_j^T \sum_{i=j+1}^{n} \Big(\frac{d}{dt} \left(R_{j+1}^T R_i I_i \boldsymbol{\Omega}_i \right) \\
&\quad + \left(R_{j+1}^T R_i I_i \boldsymbol{\Omega}_i \right) \times (\boldsymbol{w}_j - x_j \boldsymbol{\Omega}_j) \Big) dt
\end{aligned} \tag{4.1.11}$$

where we have used integration by parts and the fact that $\boldsymbol{\lambda}(t)$ vanishes at t_0, t_1. Since by (4.1.4)

$$\begin{aligned}
\delta_H \int_{t_0}^{t_1} l(\boldsymbol{x}, \boldsymbol{w}, \boldsymbol{\Omega}_1) dt &= \delta_H \int_{t_0}^{t_1} \frac{1}{2} \left(\sum_{i=1}^{n} \boldsymbol{\Omega}_i^T I_i \boldsymbol{\Omega}_i - 2V(X) \right) dt \\
&= \int_{t_0}^{t_1} (\sum_{i=2}^{n} \boldsymbol{\Omega}_i^T I_i \delta_H \boldsymbol{\Omega}_i - \delta_H V(X)) dt
\end{aligned}$$

we get from (4.1.9), (4.1.10) and (4.1.11)

$$\begin{aligned}
\delta_H \int_{t_0}^{t_1} l(\boldsymbol{x}, \boldsymbol{w}, \boldsymbol{\Omega}_1) dt &= \int_{t_0}^{t_1} \sum_{j=1}^{n-1} \boldsymbol{\lambda}_j^T \sum_{i=j+1}^{n} \Big(\frac{d}{dt} \left(R_{j+1}^T R_i I_i \boldsymbol{\Omega}_i \right) \\
&\quad + \left(R_{j+1}^T R_i I_i \boldsymbol{\Omega}_i \right) \times (\boldsymbol{w}_j - x_j \boldsymbol{\Omega}_j) - \sigma \boldsymbol{u}_j^{ps} \Big) dt.
\end{aligned}$$

We set $\delta_H \int_{t_0}^{t_1} l = 0$ and note that this holds for arbitrary $\boldsymbol{\lambda}_j(t)$. Again, using the fact

that $\boldsymbol{\Omega}_{i+1} = x_i\boldsymbol{\Omega}_i - \boldsymbol{w}_i$ we get the horizontal equations to be for $j = 1, \ldots, n-1$

$$\frac{d}{dt}\left(\sum_{i=j+1}^{n} R_{j+1}^T R_i I_i \boldsymbol{\Omega}_i\right) = \left(\sum_{i=j+1}^{n} R_{j+1}^T R_i I_i \boldsymbol{\Omega}_i\right) \times (\boldsymbol{\Omega}_{j+1}) + \sigma \boldsymbol{u}_j^{ps}. \tag{4.1.12}$$

Since j goes from 1 to $n-1$, we have $n-1$ horizontal vector equations. For $j = n-1$, (4.1.12) is

$$I_n \frac{d}{dt}\boldsymbol{\Omega}_n = (I_n\boldsymbol{\Omega}_n) \times (\boldsymbol{\Omega}_n) + \sigma \boldsymbol{u}_{n-1}^{ps}. \tag{4.1.13}$$

Let $\boldsymbol{u}_n^{ps} = 0$. We now show that if

$$I_j \frac{d}{dt}\boldsymbol{\Omega}_j = (I_j\boldsymbol{\Omega}_j) \times (\boldsymbol{\Omega}_j) + \sigma(\boldsymbol{u}_{j-1}^{ps} - \boldsymbol{u}_j^{ps}) \tag{4.1.14}$$

for $j = n, n-1, \ldots, k+1$ where $k > 1$, then (4.1.14) is true for $j = k$. Let

$$\boldsymbol{a}_j = \left(\sum_{i=j+1}^{n} R_{j+1}^T R_i I_i \boldsymbol{\Omega}_i\right) = I_j\boldsymbol{\Omega}_j + R_{j+1}^{-1}\left(\sum_{i=j+2}^{n} R_i I_i \boldsymbol{\Omega}_i\right). \tag{4.1.15}$$

Then we have

$$\frac{d\boldsymbol{a}_j}{dt} = I_j\dot{\boldsymbol{\Omega}}_j - \widehat{\boldsymbol{\Omega}}_{j+1}R_{j+1}^{-1}\left(\sum_{i=j+2}^{n} R_i I_i \boldsymbol{\Omega}_i\right) + R_{j+1}^{-1}\sum_{i=j+2}^{n}\left(R_i\widehat{\boldsymbol{\Omega}}(I_i\boldsymbol{\Omega}_i) + R_i I_i\dot{\boldsymbol{\Omega}}_i\right). \tag{4.1.16}$$

Using (4.1.12) and (4.1.16), we get

$$I_j\dot{\boldsymbol{\Omega}}_j + R_{j+1}^{-1}\sum_{i=j+2}^{n} R_i\left(\widehat{\boldsymbol{\Omega}}(I_i\boldsymbol{\Omega}_i) + I_i\dot{\boldsymbol{\Omega}}_i\right) = (I_j\boldsymbol{\Omega}_j) \times \boldsymbol{\Omega}_j + \sigma\boldsymbol{u}_j^{ps}. \tag{4.1.17}$$

Now we use the assumption that for $j = n, n-1, \ldots, k+1$, (4.1.14) is satisfied. This gives

$$I_j\dot{\boldsymbol{\Omega}}_j + R_{j+1}^{-1}\sum_{i=j+2}^{n} R_i\left(\sigma(\boldsymbol{u}_{i-1}^{ps} - \boldsymbol{u}_i^{ps})\right) = (I_j\boldsymbol{\Omega}_j) \times \boldsymbol{\Omega}_j + \sigma\boldsymbol{u}_j^{ps}. \tag{4.1.18}$$

Now use the fact that u_i^{ps} is the eigenvector of $R_{i+1}^{-1}R_i$, i.e., $R_{i+1}u_i^{ps} = R_i u_i^{ps}$. This implies that all the terms inside the summation in (4.1.18) cancel except for $R_{j+2}u_{j+1}^{ps}$. We now get

$$I_j\dot{\boldsymbol{\Omega}}_j + R_{j+1}^{-1}R_{j+2}\sigma\boldsymbol{u}_{j+1}^{ps} = (I_j\boldsymbol{\Omega}_j) \times \boldsymbol{\Omega}_j + \sigma\boldsymbol{u}_j^{ps}. \tag{4.1.19}$$

Again, using $R_{j+1}^{-1}R_{j+2}u_{j+1}^{ps} = u_{j+1}^{ps}$, we get

$$I_j\dot{\mathbf{\Omega}}_j = (I_j\mathbf{\Omega}_j) \times \mathbf{\Omega}_j + \sigma(\boldsymbol{u}_j^{ps} - \boldsymbol{u}_{j+1}^{ps}). \tag{4.1.20}$$

(4.1.20) is satisfied for $j = 2, \ldots, n$. Using (4.1.20) in the expression for $\boldsymbol{a}$ in (4.1.8), we get the dynamical equations to be

$$\begin{aligned}
I_1\dot{\mathbf{\Omega}}_1 &= (I_1\mathbf{\Omega}_1) \times \mathbf{\Omega}_1 - \sigma\boldsymbol{u}_1^{ps} \\
I_2\dot{\mathbf{\Omega}}_2 &= (I_2\mathbf{\Omega}_2) \times \mathbf{\Omega}_2 + \sigma(\boldsymbol{u}_1^{ps} - \boldsymbol{u}_2^{ps}) \\
\vdots &= \vdots \\
I_{n-1}\dot{\mathbf{\Omega}}_{n-1} &= (I_{n-1}\mathbf{\Omega}_{n-1}) \times \mathbf{\Omega}_{n-1} + \sigma(\boldsymbol{u}_{n-2}^{ps} - \boldsymbol{u}_{n-1}^{ps}) \\
I_n\dot{\mathbf{\Omega}}_n &= (I_n\mathbf{\Omega}_n) \times \mathbf{\Omega}_n + \sigma\boldsymbol{u}_{n-1}^{c}
\end{aligned} \tag{4.1.21}$$

The following set of vector equations for $i = 1, \ldots, n-1$ along with (4.1.21) gives the complete reduced equations of motion in $(TSO(3))^n/SO(3)$. These equations correspond to the dynamics of the relative orientations and follow from the following expression for $\dot{X}_i$:

$$\begin{aligned}
\dot{X}_i &= \dot{(}R_{i+1}^{-1}R_i) \\
&= R_{i+1}^{-1}\dot{R}_i - R_{i+1}^{-1}\dot{R}_{i+1}R_{i+1}^{-1}R_i \\
&= R_{i+1}^{-1}R_iR_i^{-1}\dot{R}_i - R_{i+1}^{-1}\dot{R}_{i+1}R_{i+1}^{-1}R_i \\
&= R_{i+1}^{-1}R_i\widehat{\mathbf{\Omega}}_i - \widehat{\mathbf{\Omega}}_{i+1}R_{i+1}^{-1}R_i \\
&= X_i\widehat{\mathbf{\Omega}}_i - \widehat{\mathbf{\Omega}}_{i+1}X_i
\end{aligned}$$

Since $\mathbf{\Delta}_i, \mathbf{\Sigma}_i, \mathbf{\Gamma}_i$ are the column vectors of X_i, we have

$$\frac{d}{dt}\begin{bmatrix} \mathbf{\Delta}_i & \mathbf{\Sigma}_i & \mathbf{\Gamma}_i \end{bmatrix} = \begin{bmatrix} \mathbf{\Delta}_i & \mathbf{\Sigma}_i & \mathbf{\Gamma}_i \end{bmatrix}\widehat{\mathbf{\Omega}}_i - \widehat{\mathbf{\Omega}}_{i+1}\begin{bmatrix} \mathbf{\Delta}_i & \mathbf{\Sigma}_i & \mathbf{\Gamma}_i \end{bmatrix}. \tag{4.1.22}$$

4.2 Reduced equations of motions for $SE(3)$ network.

In this section, we show how to derive the equations of motion for n rigid bodies, each with configuration space $SE(3)$ coupled with a potential that depends upon their relative orientations and relative positions. The configuration space is $SE(3)^n = SE(3) \times \ldots \times SE(3)$ and the phase space is $T(SE(3)^n)$ with coordinates

$$(R_1, \ldots, R_n, \dot{R}_1, \ldots, \dot{R}_n, \boldsymbol{b}_1, \ldots, \boldsymbol{b}_n, \dot{\boldsymbol{b}}_1, \ldots, \dot{\boldsymbol{b}}_n)$$

The coupling potential is chosen to be

$$V = \sum_{i=1}^{n-1} \left(\sigma_1 \mathrm{tr}(R_{i+1}^T R_i) + \sigma_2 \|\boldsymbol{b}_i - \boldsymbol{b}_{i+1}\|^2 \right), \tag{4.2.1}$$

with $\sigma_1, \sigma_2 \in \mathbb{R}$. The Lagrangian in terms of the angular velocity in body coordinates $\boldsymbol{\Omega}_i$ given by $\dot{R}_i = R_i \widehat{\boldsymbol{\Omega}_i}$ and linear velocity in body coordinates given by $\boldsymbol{v}_i = R_i^{-1} \dot{\boldsymbol{b}}_i$ is:

$$L = \sum_{i=1}^{n} \frac{1}{2} \left(\boldsymbol{\Omega}_i^T I_i \boldsymbol{\Omega}_i + \boldsymbol{v}_i^T M_i \boldsymbol{v}_i \right) - \sigma_1 \mathrm{tr}(\sum_{i=1}^{n-1} R_{i+1}^T R_i) - \sigma_2 \sum_{i=1}^{n-1} \|\boldsymbol{b}_i - \boldsymbol{b}_{i+1}\|^2 \tag{4.2.2}$$

L has $SE(3)$ as its symmetry group with the symmetry action given by

$$\begin{aligned} &(\bar{R}, \bar{\boldsymbol{b}}) \cdot (R_1, \ldots, R_n, \dot{R}_1, \ldots, \dot{R}_n, \boldsymbol{b}_1, \ldots, \boldsymbol{b}_n, \dot{\boldsymbol{b}}_1, \ldots, \dot{\boldsymbol{b}}_n) \\ &= (\bar{R}R_1, \ldots, \bar{R}R_n, \bar{R}\dot{R}_1, \ldots, \bar{R}\dot{R}_n, \bar{R}\boldsymbol{b}_1 + \bar{\boldsymbol{b}}, \ldots, \bar{R}\boldsymbol{b}_n + \bar{\boldsymbol{b}}, \bar{R}\dot{\boldsymbol{b}}_1, \ldots, \bar{R}\dot{\boldsymbol{b}}_n) \end{aligned}$$

Let $\boldsymbol{y}_i = \boldsymbol{b}_{i+1} - \boldsymbol{b}_i$ and $X_i = R_{i+1}^{-1} R_i$ as defined in §4.1. We identify the reduced space as

$$\begin{aligned} &\left[R_1, R_2, \ldots, R_n, \boldsymbol{b}_1, \ldots, \boldsymbol{b}_n, R_1\widehat{\boldsymbol{\Omega}}_1, R_2\widehat{\boldsymbol{\Omega}}_2, \ldots, R_n\hat{\boldsymbol{\Omega}}_n, \dot{\boldsymbol{b}}_1, \ldots, \dot{\boldsymbol{b}}_n \right]_{SE(3)} \\ &= (X_1, \ldots, X_{n-1}, \boldsymbol{y}_1, \ldots, \boldsymbol{y}_{n-1}, \dot{X}_1 X_1^{-1}, \ldots, \dot{X}_{n-1} X_{n-1}^{-1}, \dot{\boldsymbol{y}}_1, \ldots, \dot{\boldsymbol{y}}_{n-1}, \boldsymbol{\Omega}_1, \boldsymbol{v}_1) \\ &= (X_1, \ldots, X_{n-1}, \boldsymbol{y}_1, \ldots, \boldsymbol{y}_{n-1}, \boldsymbol{w}_1, \ldots, \boldsymbol{w}_{n-1}, \dot{\boldsymbol{y}}_1, \ldots, \ldots \boldsymbol{y}_{n-1}, \boldsymbol{\Omega}_1, \boldsymbol{v}_1) \\ &= (X, \boldsymbol{y}, \boldsymbol{w}, \dot{\boldsymbol{y}}, \boldsymbol{\Omega}_1, \boldsymbol{v}_1) \end{aligned} \tag{4.2.3}$$

The horizontal and vertical variations corresponding to the identification made in (4.2.3) are

$$\delta_V(X, \boldsymbol{y}, \hat{\boldsymbol{w}}, , \dot{\boldsymbol{y}}, \boldsymbol{\Omega}_1, \boldsymbol{v}_1) = \Big((X, \boldsymbol{y}, \hat{\boldsymbol{w}}, , \dot{\boldsymbol{y}}, \boldsymbol{\Omega}_1, \boldsymbol{v}_1), (0, 0, 0, 0, \dot{\boldsymbol{\eta}}_1 + \boldsymbol{\Omega}_1 \times \boldsymbol{\eta}_1, \dot{\boldsymbol{\eta}}_2 + \boldsymbol{\Omega}_1 \times \boldsymbol{\eta}_2 + \boldsymbol{v}_1 \times \boldsymbol{\eta}_1)\Big) \quad (4.2.4)$$

$$\delta_H(X, \boldsymbol{y}, \hat{\boldsymbol{w}}, \dot{\boldsymbol{y}}, \boldsymbol{\Omega}_1, \boldsymbol{v}_1) = \Big((X, \boldsymbol{y}, \hat{\boldsymbol{w}}, \dot{\boldsymbol{y}}, \boldsymbol{\Omega}_1, \boldsymbol{v}_1), (\widehat{\boldsymbol{\lambda}} X, \delta \boldsymbol{y}, \dot{\boldsymbol{\lambda}} - \boldsymbol{w} \times \boldsymbol{\lambda}, \delta \dot{\boldsymbol{y}}, 0, 0)\Big) \quad (4.2.5)$$

where $\boldsymbol{\eta}_1(t_i) = 0, \boldsymbol{\eta}_2(t_i) = 0, \boldsymbol{\lambda}_j(t_i) = 0$ for $i = 0, 1$ and $j = 1, \ldots, n-1$ and

$$\begin{aligned} \widehat{\boldsymbol{\lambda}} X &:= \left(\widehat{\boldsymbol{\lambda}}_1 X_1, \ldots, \widehat{\boldsymbol{\lambda}}_{n-1} X_{n-1}\right) \\ \dot{\boldsymbol{\lambda}} - \boldsymbol{w} \times \boldsymbol{\lambda} &:= \left(\dot{\boldsymbol{\lambda}}_1 - \boldsymbol{w}_1 \times \boldsymbol{\lambda}_1, \ldots, \dot{\boldsymbol{\lambda}}_{n-1} - \boldsymbol{w}_{n-1} \times \boldsymbol{\lambda}_{n-1}\right). \end{aligned}$$

Here, t_0, t_1 are the initial and final times respectively of the paths in the variations. As in §4.1, setting the variations given in (4.2.4) and (4.2.5), we can find the corresponding vertical and horizontal equations of motion. Without going through the calculations, we state the final equations of motion below:

$$\begin{aligned} I_i \dot{\boldsymbol{\Omega}}_i &= (I_i \boldsymbol{\Omega}_i) \times \boldsymbol{\Omega}_i + (M_i \boldsymbol{v}_i) \times \boldsymbol{v}_i + \sigma_1 (\boldsymbol{u}^{ps}_{\tau, i-1} - \boldsymbol{u}^{ps}_{\tau i}) \\ M_i \dot{\boldsymbol{v}}_i &= (M_i \boldsymbol{v}_i) \times \boldsymbol{\Omega}_i + \sigma_2 \boldsymbol{u}^{ps}_{fi} \end{aligned}$$

where

$$\boldsymbol{u}^{ps}_{\tau i} = (\boldsymbol{\Delta}_i \times \boldsymbol{e}_1 + \boldsymbol{\Sigma}_i \times \boldsymbol{e}_2 + \boldsymbol{\Gamma}_i \times \boldsymbol{e}_3). \quad (4.2.6)$$

$\boldsymbol{\Delta}_i, \boldsymbol{\Sigma}_i, \boldsymbol{\Gamma}_i$ are the column vectors of $R_{i+1}^{-1} R_i$, $\boldsymbol{u}^{ps}_{\tau 0} = \boldsymbol{u}^{ps}_{\tau n} = 0$ and $\boldsymbol{u}^{ps}_{fi} = -R_i^{-1}(2\boldsymbol{b}_i - \boldsymbol{b}_{i+1} - \boldsymbol{b}_{i-1})$ for $i = 2, \ldots, n-1$, $\boldsymbol{u}^{ps}_{f1} = -R_i^{-1}(\boldsymbol{b}_1 - \boldsymbol{b}_2)$ and $\boldsymbol{u}^{ps}_{fn} = -R_i^{-1}(\boldsymbol{b}_n - \boldsymbol{b}_{n-1})$.

Chapter 5

Stable Synchronization of Networked Rigid Bodies

In this chapter we present a stabilizing and coordinating control law for a network of rigid bodies with unstable dynamics. The bodies are models for satellites in free space following the rigid body Euler equations or models for underwater vehicles following the Kirchoff's equations of motion. In the former case, the configuration space for each individual in the network is the Lie group $SO(3)$ and in the latter case, it is the Lie group $SE(3)$. The control law we derive is used to synchronize the dynamics across a network (using coupling potentials) of such bodies and also to stabilize each individual body (using kinetic shaping). The closed-loop system is again a Lagrangian system with $SO(3)$ or $SE(3)$ symmetry. This setting permits us to use energy methods to prove closed-loop stability.

We first design techniques to stabilize the relative equilibria for a single body and then go on to couple a group of such bodies and prove stability for the whole system. In Chapter 3, we studied coordinated control of networked systems belonging to the SMC class of mechanical systems with unstable dynamics. We proved stabilized, coordinated motion of a network of such systems and illustrated our results with a network of controlled carts each balancing an inverted pendulum. It was assumed

that each of the systems has a symmetry group that is Abelian and that there is no gyroscopic coupling between the symmetry and nonsymmetry configuration variables. The actuation was in the symmetry direction of the system. We continue with our theme of stabilization and synchronization and prove results for the case when the symmetry group is either of the non Abelian groups $SO(3)$ and $SE(3)$. We consider the $SO(3)$ case in §5.1 and move on to the $SE(3)$ case in §5.2.

5.1 Stable Synchronization of $SO(3)$ vehicles

The free rigid body in space has configuration space the Lie group $SO(3)$ and state space $TSO(3)$ where a particular element $(R, \boldsymbol{\omega}) \in TSO(3)$ denotes the orientation of the rigid body in inertial space and the angular velocity of the rigid body in inertial space. The angular velocity of the body in the body frame is denoted by $\boldsymbol{\Omega}$. In the language of Lie groups, $\boldsymbol{\omega}$ is the right translate of the element $\dot{R} \in T_R SO(3)$ to the tangent space at the identity $T_I SO(3)$ denoted by $so(3)$ and $\boldsymbol{\Omega}$ is the left translate of $\dot{R}$ to $so(3)$, i.e.,

$$\dot{R} = \hat{\boldsymbol{\omega}} R, \quad \dot{R} = R\hat{\boldsymbol{\Omega}}. \tag{5.1.1}$$

Here, for a vector $\boldsymbol{a}$, the notation $\hat{\boldsymbol{a}}$ denotes a matrix such that $\hat{\boldsymbol{a}}\boldsymbol{x} = \boldsymbol{a} \times \boldsymbol{x}$ for any vector $\boldsymbol{x}$.

Our goal is to couple n such rigid bodies using potentials designed to align their orientations in inertial space and make all of them point in a particular direction. An application example would be a network of rigid communicating satellites equipped with telescopes for interferometry purposes.

In this work, we consider the more challenging problem of coordinating the network so that the rigid bodies are not only synchronized in orientations but each one is also rotating about its individual (unstable) middle axis. We do this without destroying the Hamiltonian structure of the system as opposed to the treatment in [46]. As mentioned in the chapter introduction, this setting gives us the readily available

conserved Hamiltonian function for stability analysis.

In §5.1.1, we show how to achieve stability of the relative equilibrium of individual system corresponding to rotation about middle axis using kinetic shaping. The control law effectively swaps the middle axis and the short axis, thereby making the open-loop unstable axis a closed-loop, stable axis.

In §5.1.2, we couple n such systems using artificial potential for synchronization purposes. The coupling potential depends only upon the relative orientations and is extremized when the orientations are aligned. An analogous case for point particles would be to artificially couple them using controls coming from a potential that depends upon the relative spacing of the particles. Since the closed-loop system is Lagrangian, stability for a particular relative equilibrium of the system is proved using the Energy-Momentum method. This relative equilibrium corresponds to the case when the bodies are aligned and each one is rotating about its short axis.

In §5.1.3, we prove closed-loop stability of the network for the case when the bodies are aligned and each one is rotating about its middle axis. This is achieved by combining kinetic shaping in §5.1.1 and potential coupling in §5.1.2.

Aymptotic stability for the network is handled in Chapter 6.

5.1.1 Spin Stabilization of $SO(3)$ Vehicle about its Unstable Axis

Consider a rigid body with moments of inertia given by I_1, I_2, I_3 such that $I_1 > I_2 > I_3$. I_1, I_2, I_3 are called the short, middle and long axis, respectively. Refer to [34] to see a discussion of the various relative equilibria for this system and their stability. It is shown that the steady spin about the short axis is stable and about the middle axis is unstable.

Here, in the spirit of [9], we derive a kinetic shaping control law to stabilize the steady spin about the middle axis. In [9], the authors use an external control torque about the long axis and show stability of the steady spin about the middle axis.

In doing so, they also change the Hamiltonian structure of the system. In [9], the equations of motion with a single external torque about the long axis are as follows:

$$\begin{aligned} I_1\dot{\Omega}_1 &= (I_2 - I_3)\Omega_2\Omega_3 \\ I_2\dot{\Omega}_2 &= (I_3 - I_1)\Omega_3\Omega_1 \\ I_3\dot{\Omega}_3 &= (I_1 - I_2)\Omega_1\Omega_2 + u \end{aligned}$$

where $u = -\epsilon(I_1 - I_2)\Omega_1\Omega_2$ and $\epsilon > 1$. In the same paper, it is shown that the closed-loop system, though Hamiltonian, no longer evolves on $SO(3)$, but on $SO(2,1)$ defined as

$$SO(2,1) = \{P \in (\mathbb{R})^{3\times 3} \mid \det(P) = 1, P^T\mathbb{I}_{2,1}P = \mathbb{I}_{2,1}\},$$

where $\mathbb{I}_{2,1}$ is a diagonal matrix with entries $\{1, 1, -1\}$. In our work, the control laws are carefully chosen so that the closed-loop system also evolves on $SO(3)$. This is crucial in our setting since we use coupling potentials in §5.1.2 depending upon the relative orientations and these potentials are functions on $SO(3)$. Hence, it is important that the closed-loop system also evolve on $SO(3)$. This constraint is achieved by using control torques about at least two of the rigid body principle axes.

Let the angular velocity of the rigid body in the body frame be $\mathbf{\Omega} = (\Omega_1, \Omega_2, \Omega_3)$. The Lagrangian for the rigid body in terms of body angular velocity coordinates is $L = \frac{1}{2}(I_1\Omega_1^2 + I_2\Omega_2^2 + I_3\Omega_3^2)$ and the Euler equations of motion with control terms u_2^{ks} and u_3^{ks} about the 2 and 3 axes are

$$\begin{aligned} I_1\dot{\Omega}_1 &= (I_2 - I_3)\Omega_2\Omega_3 \\ I_2\dot{\Omega}_2 &= (I_3 - I_1)\Omega_3\Omega_1 + u_2^{ks} \\ I_3\dot{\Omega}_3 &= (I_1 - I_2)\Omega_1\Omega_2 + u_3^{ks}\,. \end{aligned} \tag{5.1.2}$$

We want to stabilize the otherwise unstable middle axis rotation $\bar{\mathbf{\Omega}} = (0, \bar{\Omega}, 0)$ for constant $\bar{\Omega}$. Our motivation here is to choose controls such that the closed-loop equation is Lagrangian with Lagrangian given by $L_c = \frac{1}{2}(I_1\Omega_1^2 + \rho_2 I_2\Omega_2^2 + \rho_3 I_3\Omega_3^2)$. We will choose the real constants ρ_2 and ρ_3 such that $\rho_2 I_2 > \rho_3 I_3 > I_1$. This way,

the middle axis of the system without controls is effectively made the short axis of the closed-loop system.

Consider the following choice of controls:

$$u_2^{ks} = \left(I_1(1 - \frac{1}{\rho_2}) + I_3(\frac{\rho_3}{\rho_2} - 1) \right) \Omega_3\Omega_1 \tag{5.1.3}$$

$$u_3^{ks} = \left(I_1(\frac{1}{\rho_3} - 1) + I_2(1 - \frac{\rho_2}{\rho_3}) \right) \Omega_1\Omega_2 \tag{5.1.4}$$

where the constants ρ_2, ρ_3 are chosen in the following manner:

$$\rho_3 > \frac{I_1}{I_3} > 1 \tag{5.1.5}$$

$$\rho_2 = (\rho_3 - 1)\frac{I_3}{I_2} + 1. \tag{5.1.6}$$

This gives us $\rho_3 I_3 > I_1$ and

$$I_2 - I_3 = \rho_2 I_2 - \rho_3 I_3 > 0. \tag{5.1.7}$$

The closed-loop system can be verified to be

$$\begin{aligned} I_1\dot{\Omega}_1 &= (\rho_2 I_2 - \rho_3 I_3)\Omega_2\Omega_3 \\ \rho_2 I_2\dot{\Omega}_2 &= (\rho_3 I_3 - I_1)\Omega_3\Omega_1 \\ \rho_3 I_3\dot{\Omega}_3 &= (I_1 - \rho_2 I_2)\Omega_1\Omega_2 \,. \end{aligned} \tag{5.1.8}$$

This corresponds to a Lagrangian system with the Lagrangian L_c given by

$$L_c = \frac{1}{2}\left(I_1\Omega_1^2 + \rho_2 I_2\Omega_2^2 + \rho_3 I_3\Omega_3^2 \right). \tag{5.1.9}$$

Also, from (5.1.7) and (5.1.5), it follows that $\rho_2 I_2 > \rho_3 I_3 > I_1$. Therefore, for the closed-loop system, the short axis is what corresponded to the middle axis in the open-loop system. Thus, we have effectively stabilized the steady middle axis rotation for the rigid body and we have the following theorem.

Theorem 5.1.1 *Consider a rigid body with equations of motion given by* (5.1.2). *If the controls are chosen to be those given by* (5.1.3) *and* (5.1.4), *then the closed loop*

equations are derived from the Lagrangian (5.1.9). *The control law stabilizes the rigid body rotating about its intermediate axis. The scalar constants* ρ_2 *and* ρ_3 *are given by* (5.1.6) *and* (5.1.5).

Note that the axes about which we apply controls in (5.1.2) are not unique. The kinetic shaping will work if we choose any two of the three axes of the rigid body. We chose the second and third axis in this section only for illustrative purposes. Also, we can make the original long axis effectively look like a short axis in the closed loop system using kinetic shaping. This could turn out to be useful, for example, when we want to make the Hamiltonian a minimum for rotation about the long axis.

The controls u_2^{ks} and u_3^{ks} in (5.1.2) do not break the symmetry of the system since they depend only on Ω and not on the orientation R directly. Hence, the closed-loop equations of motion make sense as reduced equations for a rigid body with $SO(3)$ symmetry.

We can at this point introduce dissipation to asymptotically stabilize the solution given by $\mathbf{\Omega}(t) = (0, \bar{\Omega}, 0)$ for some constant $\bar{\Omega}$. This will correspond to the case when the rigid body rotating about its unstable axis with a constant angular velocity is made asymptotically stable. But this does not achieve the goal we have set forth for ourselves. Our aim is also to make the rigid body orient in a particular direction in inertial space in addition to having it rotate stably about its middle axis. Since our controls at this stage still has the orientation symmetry in it, we can only achieve asymptotic stability in the reduced space. This does not translate to asymptotic stability in the inertial space. To do this, we will need to break the symmetry in the control law as we demonstrate in the next chapter.

5.1.2 Coordination of $SO(3)$ Network with Stable Dynamics

In this section, we show how to use an artificial coupling potential to achieve alignment of n rigid bodies in inertial space and at the same time each individual body rotates

about it short axis. In Chapter 4, we already saw the derivation of reduced equations of motion for the following choice of coupling potential:

$$V = \sigma \mathrm{tr}(\sum_{i=1}^{n-1} R_{i+1}^T R_i), \tag{5.1.10}$$

with $\sigma \in \mathbb{R}$. Note that if $R_i = R_{i+1}$ for $i = 1, \ldots, n-1$, the potential V is at a minimum if $\sigma < 0$. For the sake of completeness, we will show that this potential is at a minimum when $R_i = R_{i+1}$ for $\sigma < 0$ for the case of two bodies. The case for n bodies is an easy extension. The proof will proceed in two steps. First, we will show that δV is zero when $R_1 = R_2$ and then we will show that $\delta^2 V \geq 0$ when $R_1 = R_2$ and is equal to zero only when $\delta R_1 = \delta R_2$.

Step 1

$$\begin{aligned}
\delta V &= \sigma \delta \mathrm{tr}(R_2^{-1} R_1) \\
&= \sigma \mathrm{tr}(\delta(R_2^{-1} R_1)) \\
&= \sigma \mathrm{tr}(R_2^{-1}\delta R_1 - R_2^{-1}\delta R_2 R_2^{-1} R_1) \\
&= \sigma \mathrm{tr}(R_2^{-1}\widehat{\delta\boldsymbol{\theta}_1} R_1 - R_2^{-1}\widehat{\delta\boldsymbol{\theta}_2} R_1) \quad \text{where} \quad \widehat{\delta\boldsymbol{\theta}_i} = \delta R_i R_i^{-1} \\
&= \sigma \mathrm{tr}((\widehat{\delta\boldsymbol{\theta}_1} - \widehat{\delta\boldsymbol{\theta}_2}) R_1 R_2^{-1}).
\end{aligned}$$

Therefore, $\delta V|_{R_1 = R_2} = \sigma \mathrm{tr}(\widehat{\delta\boldsymbol{\theta}_1} - \widehat{\delta\boldsymbol{\theta}_2}) = 0$.

Step 2 Using a similar procedure, we can show that

$$\delta^2 V = \sigma \mathrm{tr}(R_2^{-1}\widehat{\delta\boldsymbol{\theta}_1}\widehat{\delta\boldsymbol{\theta}_1} R_1 + R_2^{-1}\widehat{\delta\boldsymbol{\theta}_2}\widehat{\delta\boldsymbol{\theta}_2} R_1 - 2R_2^{-1}\widehat{\delta\boldsymbol{\theta}_2}\widehat{\delta\boldsymbol{\theta}_1} R_1).$$

Therefore,

$$\delta^2 V|_{R_1 = R_2} = \sigma \mathrm{tr}(\widehat{\delta\boldsymbol{\theta}_1}\widehat{\delta\boldsymbol{\theta}_1} + \widehat{\delta\boldsymbol{\theta}_2}\widehat{\delta\boldsymbol{\theta}_2} - 2\widehat{\delta\boldsymbol{\theta}_2}\widehat{\delta\boldsymbol{\theta}_1}) = -2\sigma(\delta\boldsymbol{\theta}_1 - \delta\boldsymbol{\theta}_2)^T(\delta\boldsymbol{\theta}_1 - \delta\boldsymbol{\theta}_2). \tag{5.1.11}$$

Here, we have used the identity that $\mathrm{tr}(\hat{\boldsymbol{a}}\hat{\boldsymbol{b}}) = -\boldsymbol{a} \cdot \boldsymbol{b}$. For $\sigma < 0$, the expression (5.1.11) is always positive semi-definite and equal to zero only when $\delta\boldsymbol{\theta}_1 = \delta\boldsymbol{\theta}_2$, i.e., when $\delta R_1 = \delta R_2$. Hence, the potential V is a minimum when $R_1 = R_2$. ∎

We would also like to mention that a variation of this potential is also used as a Morse function to study the topology of $SO(3)$. See [35] for example.

As in Chapter 4, the Lagrangian for the network L_{net_c} is

$$L_{\text{net}_c} = L_{\text{net}} - V = \sum_{i=1}^{n} \frac{1}{2} \mathbf{\Omega}_i^T I_i \mathbf{\Omega}_i - \sigma \text{tr}(\sum_{i=1}^{n-1} R_{i+1}^T R_i).$$

The equation of motion for the i^{th} body is

$$I_i \dot{\mathbf{\Omega}}_i = (I_i \mathbf{\Omega}_i) \times \mathbf{\Omega}_i + \sigma(\boldsymbol{u}_{i-1}^{ps} - \boldsymbol{u}_i^{ps}) \tag{5.1.12}$$

where

$$\boldsymbol{u}_i^{ps} = (\mathbf{\Delta}_i \times \boldsymbol{e}_1 + \mathbf{\Sigma}_i \times \boldsymbol{e}_2 + \mathbf{\Gamma}_i \times \boldsymbol{e}_3)\,, \tag{5.1.13}$$

$\mathbf{\Delta}_i, \mathbf{\Sigma}_i, \mathbf{\Gamma}_i$ are the column vectors of $R_{i+1}^{-1} R_i$ and $\boldsymbol{u}_0^{ps} = \boldsymbol{u}_n^{ps} = 0$. Here, $\boldsymbol{e}_1 = (1,0,0)^T$, $\boldsymbol{e}_2 = (0,1,0)^T$ and $\boldsymbol{e}_3 = (0,0,1)^T$.

Remark 5.1.2 *1. Forces coming from a potential between two bodies are equal and opposite in inertial space according to Newton's third law. However, here we see that they are equal and opposite in the body frames as well. This is because the vector $\boldsymbol{u}_i^{ps}$ is the eigenvector of $R_{i+1}^T R_i$ as we shall show below in Lemma 4.1.1.*

2. If we consider a graph with vertices representing the bodies and edges the potential between them, then the potential we have chosen is "minimal", i.e., the graph is connected as illustrated in Figure 3.5.1.

We will show in this section that the relative equilibrium corresponding to

$$\begin{gathered} \mathbf{\Omega}_{ie} = (\bar{\Omega}, 0, 0) \\ \begin{bmatrix} \mathbf{\Delta}_{ie} & \mathbf{\Sigma}_{ie} & \mathbf{\Gamma}_{ie} \end{bmatrix} = \begin{bmatrix} \boldsymbol{e}_1 & \boldsymbol{e}_2 & \boldsymbol{e}_3 \end{bmatrix} \end{gathered} \tag{5.1.14}$$

where $i = 1, \ldots, n$ is stable. This solution corresponds to the case where each body is rotating about its short axis and the bodies are aligned, i.e., $R_1 = R_2 = \ldots = R_n$.

Let $\boldsymbol{\pi}_i = R_i I_i \boldsymbol{\Omega}_i$ be the angular momentum of the i^{th} body in inertial space. The momentum phase space is $T^*(SO(3)^n)$ and the momentum map is

$$\boldsymbol{J}(R_1, \ldots, R_n, \hat{\boldsymbol{\pi}}_1 R_1, \ldots, \hat{\boldsymbol{\pi}}_n R_n) = \sum_{i=1}^{n} \hat{\boldsymbol{\pi}}_i \,. \tag{5.1.15}$$

The Energy-Momentum Method [33]

The Energy-Momentum method is a technique for proving stability of relative equilibria. For simple mechanical systems, we have the following setting: A symplectic manifold $P = T^*Q$ with a symplectic action of a Lie group G on P, an equivariant momentum map $\boldsymbol{J} : P \to \mathfrak{g}^*$ and a $G-$invariant Hamiltonian $H : P \to \mathbb{R}$. If the Hamiltonian vector at the point $z_e \in P$ points in the direction of the group orbit through z_e, then the point is called a *relative equilibrium.* It can be shown [33] that z_e is a relative equilibrium if and only if there is a $\boldsymbol{\xi} \in \mathfrak{g}$ such that $z_e(t)$ is a critical point of the augmented Hamiltonian $H_{\boldsymbol{\xi}}(z) := H(z) - \langle \boldsymbol{J} - \boldsymbol{\mu}, \boldsymbol{\xi} \rangle$ where $\boldsymbol{\mu} = \boldsymbol{J}(z_e)$.

Definition 5.1.3 *Let $S \subset \ker D\boldsymbol{J}(z_e)$ and S be transverse to the $G_{\boldsymbol{\mu}}-$orbit within $\ker D\boldsymbol{J}(z_e)$, where $G_{\boldsymbol{\mu}} = \{g \in G \mid g \cdot \boldsymbol{\mu} = \boldsymbol{\mu}\}$.*

Theorem 5.1.4 The Energy-Momentum Theorem [33]. *If $\delta^2 H_\xi(z_e)$ is definite on the subspace S, then z_e is $G_{\boldsymbol{\mu}}-$orbitally stable in $\boldsymbol{J}^{-1}(\boldsymbol{\mu})$ and $G-$orbitally stable in P.*

Let us first explain the interpretation of the above theorem for the rigid body case. For the rigid body, the space P consists of its orientation and angular momentum, i.e., $(R, \boldsymbol{\pi})$ is an element of P where R denotes the orientation and $\boldsymbol{\pi}$ is the angular momentum of the body in inertial space. The space S is a subset of a constant momentum surface which is transverse to a $G_{\boldsymbol{\mu}}$-orbit within the constant momentum surface. For a rigid body, $G_{\boldsymbol{\mu}}$ orbit at a point corresponds to infinitesimal rotations about the $\boldsymbol{\mu}$ axis. For a rigid body, the conditions in the above theorem are satisfied for a relative equilibrium where the body is rotating about its short principle axis. The statement $SO(3)-$orbitally stable in P means that the rotation of the rigid body

about its short axis is stable, but there could be drift in its orientation in the inertial space. Even though the rotation about short axis is Lyapunov stable in reduced space, what we physically "see" in inertial space is that the rotation about short axis is Lyapunov stable but the overall orientation of the body could be drifting.

Even though the Energy-Momentum theorem only gives us stability of rigid body modulo drift in the group direction, for the rigid body, we can conclude a bit more stability, which is that the rotational drift is such that the axis of rotation stays "close" to the initial orientation. This is because of the compactness of the group $SO(3)$ [43]. This conclusion does not hold true in $SE(3)$ as observed in [32]. There can be drift in the non compact $\mathbb{R}^3$ direction in the $SE(3)$ case.

The augmented Hamiltonian in our problem setting is given by

$$H_{\boldsymbol{\xi}} = H - \langle \boldsymbol{J} - \boldsymbol{\mu}, \boldsymbol{\xi} \rangle \tag{5.1.16}$$

where H is the Hamiltonian corresponding to L_{net_c},

$$H = \frac{1}{2} \sum_{i=1}^{n} \left(\boldsymbol{\pi}_i^T R_i I_i^{-1} R_i^{-1} \boldsymbol{\pi}_i \right) + \sigma \text{tr}(\sum_{i=1}^{n-1} R_{i+1}^T R_i) \, .$$

Here, $\boldsymbol{\xi}$ is the common angular velocity of the rigid bodies at the equilibrium and $\boldsymbol{\mu}$ is the corresponding total angular momentum at the relative equilibrium. Let $I_{li}^{-1} = R_i I_i^{-1} R_i^{-1}$ where I_i is the constant moment of inertia matrix of body i in its own frame and I_{li} is the moment of inertia of the i^{th} body in the inertial (lab) frame. We will need Lemma 4.1.1 and the following lemma in our calculations.

Lemma 5.1.5 *For $R \in SO(3)$ and $\boldsymbol{a}, \boldsymbol{b} \in \mathbb{R}^3$, we have* $\text{tr}(R\hat{\boldsymbol{a}}\hat{\boldsymbol{b}}) = \boldsymbol{a}^T R \boldsymbol{b} - (\boldsymbol{a} \cdot \boldsymbol{b}) \text{tr}(R)$.

Proof Let $\{\boldsymbol{c}_1, \boldsymbol{c}_2, \boldsymbol{c}_3\}$ be the columns of R. Then,

$$\begin{aligned}
\mathrm{tr}(R\hat{\boldsymbol{a}}\hat{\boldsymbol{b}}) &= \mathrm{tr}(\hat{\boldsymbol{a}}\hat{\boldsymbol{b}}[\boldsymbol{c}_1\ \boldsymbol{c}_2\ \boldsymbol{c}_3]) \\
&= \mathrm{tr}(\boldsymbol{a}\times(\boldsymbol{b}\times\boldsymbol{c}_1)\ \ \boldsymbol{a}\times(\boldsymbol{b}\times\boldsymbol{c}_2)\ \ \boldsymbol{a}\times(\boldsymbol{b}\times\boldsymbol{c}_3)) \\
&= \mathrm{tr}(\begin{bmatrix} \boldsymbol{d}_1 & \boldsymbol{d}_2 & \boldsymbol{d}_3 \end{bmatrix}) \text{ where } \boldsymbol{d}_i = (\boldsymbol{a}\cdot\boldsymbol{c}_i)\boldsymbol{b} - (\boldsymbol{a}\cdot\boldsymbol{b})\boldsymbol{c}_i \\
&= \sum_{i=1}^{3}\Big((\boldsymbol{a}\cdot\boldsymbol{c}_i)(\boldsymbol{b}\cdot\boldsymbol{e}_i) - (\boldsymbol{a}\cdot\boldsymbol{b})(\boldsymbol{c}_i\cdot\boldsymbol{e}_i)\Big) \\
&= \boldsymbol{a}^T R\boldsymbol{b} - (\boldsymbol{a}\cdot\boldsymbol{b})\mathrm{tr}(R)
\end{aligned}$$

∎

Let $\widehat{\delta\boldsymbol{\theta}_i} = \delta R_i R_i^T$ be the right translate of the variation of δR to the identity and $\mathfrak{A}_i = (\boldsymbol{\Delta}_{i,i+1}\times\boldsymbol{e}_1 + \boldsymbol{\Sigma}_{i,i+1}\times\boldsymbol{e}_2 + \boldsymbol{\Gamma}_{i,i+1}\times\boldsymbol{e}_3)$ where $\boldsymbol{\Delta}_{i,i+1}, \boldsymbol{\Sigma}_{i,i+1}, \boldsymbol{\Gamma}_{i,i+1}$ are the column vectors of $R_i R_{i+1}^{-1}$. Then using Lemma 4.1.1, we get the following expression for the first variation of H_ξ:

$$\begin{aligned}
\delta H_{\boldsymbol{\xi}} &= \sum_{i=1}^{n}\left(\boldsymbol{\pi}_i^T R_i I_i^{-1}(\delta R_i^{-1}\boldsymbol{\pi}_i + R_i^{-1}\delta\boldsymbol{\pi}_i)\right) - \boldsymbol{\xi}\cdot(\sum_{i=1}^{n}\delta\boldsymbol{\pi}_i) \\
&\qquad +\sigma\mathrm{tr}\left(\sum_{i=1}^{n-1}\delta R_{i+1}^{-1}R_i + R_{i+1}^{-1}\delta R_i\right) \\
&= \sum_{i=1}^{n}\left(\boldsymbol{\pi}_i^T R_i I_i^{-1}(-R_i^{-1}\delta R_i R_i^{-1}\boldsymbol{\pi}_i + R_i^{-1}\delta\boldsymbol{\pi}_i)\right) - \boldsymbol{\xi}\cdot(\sum_{i=1}^{n}\delta\boldsymbol{\pi}_i) \\
&\quad +\sigma\mathrm{tr}\left(\sum_{i=1}^{n-1}(-R_{i+1}^{-1}\delta R_{i+1}R_{i+1}^{-1}R_i + R_{i+1}^{-1}\delta R_i)\right) \\
&= \sum_{i=1}^{n}\left(\boldsymbol{\pi}_i^T R_i I_{li}^{-1}(-\widehat{\delta\boldsymbol{\theta}_i}\boldsymbol{\pi}_i + \delta\boldsymbol{\pi}_i)\right) - \boldsymbol{\xi}\cdot(\sum_{i=1}^{n}\delta\boldsymbol{\pi}_i) \\
&\quad +\sigma\mathrm{tr}\left(\sum_{i=1}^{n-1}(-R_{i+1}^{-1}\widehat{\delta\boldsymbol{\theta}_{i+1}}R_i + R_{i+1}^{-1}\widehat{\delta\boldsymbol{\theta}_i}R_i)\right) \\
&= \sum_{i=1}^{n}\left(\boldsymbol{\pi}_i^T R_i I_{li}^{-1}(\delta\boldsymbol{\pi}_i - \delta\boldsymbol{\theta}_i\times\boldsymbol{\pi}_i)\right) - \boldsymbol{\xi}\cdot(\sum_{i=1}^{n}\delta\boldsymbol{\pi}_i) \\
&\quad +\sigma\mathrm{tr}\left(\sum_{i=1}^{n-1}(R_{i+1}^{-1}(\widehat{\delta\boldsymbol{\theta}_i} - \widehat{\delta\boldsymbol{\theta}_{i+1}})R_i)\right)
\end{aligned}$$

Therefore, we get

$$\delta H_{\boldsymbol{\xi}} = \sum_{i=1}^{n} \left(\boldsymbol{\pi}_i^T I_{li}^{-1} (\delta \boldsymbol{\pi}_i - \delta \boldsymbol{\theta}_i \times \boldsymbol{\pi}_i) \right) - \boldsymbol{\xi} \cdot (\sum_{i=1}^{n} \delta \boldsymbol{\pi}_i) + \sigma \sum_{i=1}^{n-1} (\delta \boldsymbol{\theta}_i - \delta \boldsymbol{\theta}_{i+1}) \cdot \mathfrak{A}_i \quad (5.1.17)$$

Therefore, for an equilibrium $\boldsymbol{\pi}_i = \boldsymbol{\pi}_{ie}, R_i = R_{ie}$,

$$\delta H_{\boldsymbol{\xi}}|_{eq} = \sum_{i=1}^{n} \left(\delta \boldsymbol{\pi}_i \cdot (I_{lei}^{-1} \boldsymbol{\pi}_{ie} - \boldsymbol{\xi}) + \delta \boldsymbol{\theta}_i \cdot ((I_{lei}^{-1} \boldsymbol{\pi}_{ie}) \times \boldsymbol{\pi}_{ie} + \sigma (\mathfrak{A}_{ie} - \mathfrak{A}_{(i-1)e})) \right) \quad (5.1.18)$$

where $\mathfrak{A}_{0e} = \mathfrak{A}_{ne} = 0$ and $I_{lei}^{-1} = I_{li}^{-1}|_{eq}$. Note that $\mathfrak{A}_{ie} = 0$ when $R_i = R_{i+1}$. Therefore, $\delta H_{\boldsymbol{\xi}}|_{eq} = 0$ when the following conditions hold,

$$\begin{aligned} I_{lei}^{-1} \boldsymbol{\pi}_{ie} = \boldsymbol{\xi} &= \lambda_i \boldsymbol{\pi}_{ie} \\ R_i &= R_j \quad \text{for } i \neq j \end{aligned} \quad (5.1.19)$$

where λ_i is an eigenvalue of I_{lei}^{-1}. An equilibrium given by (5.1.19) corresponds to a system in which all the bodies have the same orientation and each is rotating about the same principle axis at the same rate. Note that we can have a system where each body has the same rotation matrix, but different "physical orientations". This is related to the freedom in choosing the matrix K in [25]. This can happen when we represent the orientation matrices of the bodies in different inertial frames.

The second variation of $H_{\boldsymbol{\xi}}$ can be calcuated using the same procedure used to derive (5.1.17). We will also need Lemma 5.1.5 and the result is as follows:

$$\delta^2 H_{\boldsymbol{\xi}} = \sum_{i=1}^{n} \left(\delta^2 K_i \right) + \delta^2 V \quad (5.1.20)$$

where

$$\delta^2 K_i = \delta \boldsymbol{\pi}_i^T I_{li}^{-1} \delta \boldsymbol{\pi}_i + 2 \delta \boldsymbol{\pi}_i^T \left(I_{li}^{-1} \hat{\boldsymbol{\pi}}_i - \widehat{I_{li}^{-1} \boldsymbol{\pi}_i} \right) \delta \boldsymbol{\theta}_i + \delta \boldsymbol{\theta}_i^T \left(\widehat{I_{li}^{-1} \boldsymbol{\pi}_i} \hat{\boldsymbol{\pi}}_i - \hat{\boldsymbol{\pi}}_i I_{li}^{-1} \hat{\boldsymbol{\pi}}_i \right) \delta \boldsymbol{\theta}_i \quad (5.1.21)$$

$$\delta^2 V = \sigma \sum_{i=1}^{n-1} \left((\delta \boldsymbol{\theta}_i - \delta \boldsymbol{\theta}_{i+1})^T \left(R_i R_{i+1}^T - \mathrm{tr}(R_i R_{i+1}^T) \mathbb{I}_{3\times 3} \right) (\delta \boldsymbol{\theta}_i - \delta \boldsymbol{\theta}_{i+1}) \right). \quad (5.1.22)$$

Therefore, for identical bodies with body moment of inertia matrices $I_1 = I_2 = \ldots = I_n = I$, at the relative equilibrium given by (5.1.19), we have

$$\begin{aligned}
\delta^2 K_i|_{eq} &= \delta\boldsymbol{\pi}_i^T I_{le}^{-1}\delta\boldsymbol{\pi}_i + 2\delta\boldsymbol{\pi}_i^T\big(I_{le}^{-1} - \lambda\mathbb{I}_{3\times 3}\big)\hat{\boldsymbol{\pi}}_e\delta\boldsymbol{\theta}_i \\
&\quad -\delta\boldsymbol{\theta}_i^T\hat{\boldsymbol{\pi}}_e\big(I_{le}^{-1} - \lambda\mathbb{I}_{3\times 3}\big)\hat{\boldsymbol{\pi}}_e\delta\boldsymbol{\theta}_i \qquad (5.1.23)\\
\delta^2 V|_{eq} &= -2\sigma\sum_{i=1}^{n-1}\big((\delta\boldsymbol{\theta}_i - \delta\boldsymbol{\theta}_{i+1})^T(\delta\boldsymbol{\theta}_i - \delta\boldsymbol{\theta}_{i+1})\big)\,. \qquad (5.1.24)
\end{aligned}$$

We will show that the sum of the above two expressions is positive definite restricted to the subspace $S \subset \ker D\boldsymbol{J}$ such that S is transverse to the $G\boldsymbol{\mu}$-orbit within $\ker D\boldsymbol{J}$ for sufficiently negative σ. Since $S \subset \ker D\boldsymbol{J}$, we have $\sum_{i=1}^n \delta\boldsymbol{\pi}_i = 0$. Using this information, (5.1.23)-(5.1.24) can be written as

$$\begin{aligned}
\delta^2 H_{\boldsymbol{\xi}}|_{eq} = \sum_{k=1}^{n-1}\Bigg(\sum_{j=k}^{n-1}\Big(\delta\boldsymbol{\pi}_k^T\frac{I_{le}^{-1}}{n-k}\delta\boldsymbol{\pi}_k + 2\delta\boldsymbol{\pi}_k^T(I_{le}^{-1} - \lambda I)\hat{\boldsymbol{\pi}}_e(\delta\boldsymbol{\theta}_j - \delta\boldsymbol{\theta}_{j+1}) \\
- \frac{2\sigma}{j}(\delta\boldsymbol{\theta}_j - \delta\boldsymbol{\theta}_{j+1})^T(\delta\boldsymbol{\theta}_j - \delta\boldsymbol{\theta}_{j+1})\Big)\Bigg) \qquad (5.1.25)\\
+ \delta\boldsymbol{\pi}_n^T I_{le}^{-1}\delta\boldsymbol{\pi}_n - \sum_{j=1}^{n}\delta\boldsymbol{\theta}_j^T\hat{\boldsymbol{\pi}}_e\big(I_{le}^{-1} - \lambda I\big)\hat{\boldsymbol{\pi}}_e\delta\boldsymbol{\theta}_j
\end{aligned}$$

where we have substituted $\delta\boldsymbol{\pi}_n = -\sum_{j=1}^{n-1}\delta\boldsymbol{\pi}_j$ in the expression linear in $\delta\boldsymbol{\pi}_i$ in (5.1.23). Now suppose $\lambda_i = \dfrac{1}{(I_i)_1} = \dfrac{1}{(I)_1} = \lambda$ for $i = 1, \ldots, n$, i.e., each body is rotating about its short axis (the original equilibrium of interest (5.1.14)).

Lemma 5.1.6 *Suppose A, B are constant matrices with A symmetric positive definite. Let ν_1, ν_2, ν_3 be the eigenvalues of $B^T A^{-1} B$. If $k < -\max\{\nu_1, \nu_2, \nu_3\}$ then $\boldsymbol{x}^T A\boldsymbol{x} + 2\boldsymbol{x}^T B\boldsymbol{y} - k\boldsymbol{y}^T\boldsymbol{y} > 0$.*

Proof Since A is symmetric positive definite, we can find a symmetric A' such that

$A = A'A'$. Therefore,

$$\begin{aligned} \boldsymbol{x}^T A\boldsymbol{x} + 2\boldsymbol{x}^T B\boldsymbol{y} - k\boldsymbol{y}^T\boldsymbol{y} &= (A'\boldsymbol{x} + A'^{-1}B\boldsymbol{y})^T(A'\boldsymbol{x} + A'^{-1}B\boldsymbol{y}) \\ &\quad -(B\boldsymbol{y})^T A^{-1}B\boldsymbol{y} - k\boldsymbol{y}^T\boldsymbol{y} \\ &= (A'\boldsymbol{x} + A'^{-1}B\boldsymbol{y})^T(A'\boldsymbol{x} + A'^{-1}B\boldsymbol{y}) \\ &\quad +\boldsymbol{y}^T\left(-kI - B^T A^{-1}B\right)\boldsymbol{y} \end{aligned}$$

From the above expression we see that if $k < -\max\{\nu_1, \nu_2, \nu_3\}$, the only way the expression can be zero is when $\boldsymbol{x} = \boldsymbol{y} = 0$. Otherwise it is greater than zero. ∎

Using the above lemma, we get that if we choose $\sigma < -\dfrac{(n-1)^2}{2}\nu$ where ν is the maximum eigenvalue of $-\hat{\boldsymbol{\pi}}_e\left(I_{le}^{-1} - \lambda I\right) I_{le}\left(I_{le}^{-1} - \lambda I\right)\hat{\boldsymbol{\pi}}_e$, then the first expression in $\delta^2 H_{\boldsymbol{\xi}}|_{eq}$ is positive definite. The second term is positive definite and the third term is positive semi-definite since λ is the smallest eigenvalue of I_{le}^{-1}. The null space of $(I_{le}^{-1} - \lambda I)$ consists of vectors parallel to $\boldsymbol{\pi}_e$. But these vectors are excluded when we evaluate this on $\hat{\boldsymbol{\pi}}_e\delta\boldsymbol{\theta}_i$. Therefore, the only time $\delta^2 H_{\boldsymbol{\xi}}|_{eq} = 0$ is when $\delta\boldsymbol{\pi}_i = 0, \delta\boldsymbol{\theta}_i = \delta\boldsymbol{\theta}_{i+1}$ and $\delta\boldsymbol{\theta}_i \parallel \boldsymbol{\pi}_e$ for $i = 1, \ldots, n$. Now if each $\delta\boldsymbol{\theta}_i \parallel \boldsymbol{\pi}_e$, then this means that the infinitesimal rotation of each body is about the $\boldsymbol{\pi}_e$ axis. Therefore, using the fact that $\delta\boldsymbol{J} = 0$, these infinitesimal rotations correspond to the G_μ orbit within $\ker D\boldsymbol{J}$. Hence, Hence, $\delta^2 H_{\boldsymbol{\xi}}|_{eq}$ is definite when evaluated on the subspace S.

Theorem 5.1.7 *For the n rigid body problem, the relative equilibrium (5.1.14) is stabilized with the potential shabping control law given by* (5.1.13). *This equilibrium corresponds to all n rigid bodies having the same orientation with each one rotating about its short axis.*

5.1.3 Coordination of $SO(3)$ Network with Unstable Dynamics

In this section, we use kinetic shaping developed in §5.1.1 and potential coupling used in §5.1.2 to achieve stability of the relative equilibrium corresponding to the case when the rigid bodes are aligned and each one is rotation about its otherwise unstable middle axis.

Consider the following controlled dynamics for the ith body given by

$$I_i\dot{\mathbf{\Omega}}_i = (I_i\mathbf{\Omega}_i) \times \mathbf{\Omega}_i + \begin{pmatrix} -(u^{ps}_{i-1,1} - u^{ps}_{i1}) \\ -(u^{ps}_{i-1,2} - u^{ps}_{i2})/\rho_2 + u^{ks}_{i2} \\ -(u^{ps}_{i-1,3} - u^{ps}_{i3})/\rho_3 + u^{ks}_{i3} \end{pmatrix} \tag{5.1.26}$$

where $\boldsymbol{u}^{ps}_i$ is the potential shaping control term defined by (5.1.13). Also, u^{ps}_{il} denotes the l^{th} component of the vector $\boldsymbol{u}^{ps}_i$ and similarly for u^{ks}_{il}. The kinetic shaping control terms u^{ks}_{i2}, u^{ks}_{i3} are as given in (5.1.3) and (5.1.4) for the ith body. It can easily be checked that the closed-loop equations now have the form (5.2.28), but with the original middle axis now the short axis. Hence, we get the following corollary.

Corollary 5.1.8 *The relative equilibrium corresponding to n rigid bodies with the same orientation and each rotating about its unstable, middle axis, is stabilized for the controlled dynamics of (5.1.26).*

In this section, we have shown how to couple n rigid bodies in $SO(3)$ using potentials to stabilize the solution in which all of them are aligned with each other and at the same time rotating about their individual middle axis. We will show how to achieve asymptotic stability of this solution in the next chapter. In the next section, we will consider n rigid bodies in $SE(3)$ and show how to achieve a stable synchronization.

5.2 Stable Synchronization of $SE(3)$ vehicles

We now consider the case when the rigid bodies are immersed in a fluid with a potential flow. The bodies, in addition to having an orientation, can also translate and in this case, the configuration space is the Lie group $SE(3)$. An element in $SE(3)$ is denoted by $(R, \boldsymbol{b})$ with $R \in SO(3)$ and $\boldsymbol{b} \in \mathbb{R}^3$ with the group action being

$$(R, \boldsymbol{b}) \cdot (R_1, \boldsymbol{b}_1) = (RR_1, R\boldsymbol{b}_1 + \boldsymbol{b}). \tag{5.2.1}$$

Here, R represents the orientation of the body and $\boldsymbol{b}$ the displacement vector of the body from the origin of an inertial frame. For this action, the inverse of $(R, \boldsymbol{b})$ is $(R^{-1}, -R^{-1}\boldsymbol{b})$. A more illustrative notation is written in a matrix form in which the group action is represented by matrix multiplication as follows:

$$\begin{bmatrix} R & \boldsymbol{b} \\ 0 & 1 \end{bmatrix} \cdot \begin{bmatrix} R' & \boldsymbol{b}' \\ 0 & 1 \end{bmatrix} = \begin{bmatrix} RR' & R\boldsymbol{b}' + \boldsymbol{b} \\ 0 & 1 \end{bmatrix}. \tag{5.2.2}$$

The angular and linear velocities of the body in the inertial space are obtained by computing the right translate to the tangent space at identity of an element belonging to the tangent space of $SE(3)$ at a particular point $(R, \boldsymbol{b})$ as follows:

$$\begin{bmatrix} \dot{R} & \dot{\boldsymbol{b}} \\ 0 & 0 \end{bmatrix} \cdot \begin{bmatrix} R^{-1} & -R^{-1}\boldsymbol{b} \\ 0 & 1 \end{bmatrix} = \begin{bmatrix} \hat{\boldsymbol{\omega}} & \dot{\boldsymbol{b}} - \hat{\boldsymbol{\omega}}\boldsymbol{b} \\ 0 & 0 \end{bmatrix} \tag{5.2.3}$$

Here, $\boldsymbol{\omega}$ is the angular velocity of the body in inertial space and $\dot{\boldsymbol{b}} - \hat{\boldsymbol{\omega}}\boldsymbol{b}$ is its linear velocity in inertial space. The velocity components in the body frame are similarly obtained using the left translate. They are denoted by $\boldsymbol{\Omega}$ and $\boldsymbol{v}$ and calculated as follows:

$$\begin{bmatrix} R^{-1} & -R^{-1}\boldsymbol{b} \\ 0 & 1 \end{bmatrix} \cdot \begin{bmatrix} \dot{R} & \dot{\boldsymbol{b}} \\ 0 & 0 \end{bmatrix} = \begin{bmatrix} R^{-1}\dot{R} & R^{-1}\dot{\boldsymbol{b}} \\ 0 & 0 \end{bmatrix} = \begin{bmatrix} \hat{\boldsymbol{\Omega}} & \boldsymbol{v} \\ 0 & 0 \end{bmatrix}. \tag{5.2.4}$$

The rigid body $SE(3)$ dynamics have been studied in the literature [29, 30, 31, 32] and a number of other papers in the context of dynamics of underwater vehicle. In

[32], the authors show that the relative equilibrium for a rigid body rotating and translating along its short axis is Lyapunov stable modulo drift in the translational parameters. They obtain this result using the reduction by stages technique. This kind of stability is the best we can hope for and indeed in simulations, the authors observe such drift.

In our work, we would like to asymptotically stabilize this motion for individual as well as a synchronized network of such bodies and also get rid of the translational drifts. We will consider bodies whose centre of gravity and centre of buoyancy coincide. In [30], it is shown how the dynamics of such a body can be modelled as a Lie-Poisson system on $se(3)^*$. The kinetic energy of the body is given by

$$T = \frac{1}{2}\left(\boldsymbol{\Omega}^T I \boldsymbol{\Omega} + \boldsymbol{v}^T M \boldsymbol{v}\right). \tag{5.2.5}$$

Here, M is the sum of the mass matrix of the body and the added mass matrix associated with the fluid and I is the sum of the body inertia matrix plus the added inertia matrix associated with the potential flow model of the fluid. We will also assume that the body is a symmetric ellipsoid with uniformly distributed mass, which means M and I can both be chosen to be diagonal matrices. The equations of motion of the body in body coordinates are given by Kirchhoff's equations which are

$$I\dot{\boldsymbol{\Omega}} = (I\boldsymbol{\Omega}) \times \boldsymbol{\Omega} + (M\boldsymbol{v}) \times \boldsymbol{v} + \boldsymbol{u}_\tau \tag{5.2.6}$$

$$M\dot{\boldsymbol{v}} = (M\boldsymbol{v}) \times \boldsymbol{\Omega} + \boldsymbol{u}_f \tag{5.2.7}$$

where $\boldsymbol{u}_\tau$ is the control torque and $\boldsymbol{u}_f$ is the control force acting on the body in body coordinates. In the next section we will show how to stabilize the relative equilibrium solution in which the rigid body is rotating about and translating along its middle axis.

5.2.1 Translation and Spin Stabilization of $SE(3)$ vehicle about its Unstable Axis

In [30], it is shown that for an underwater vehicle with coincident centre of gravity and centre of buoyancy, the relative equilibrium in which the body is rotating about its short axis and translating along the short axis is stable. We will use kinetic shaping to stabilize the relative equilibrium in which the body is rotating about its middle axis and translating along the middle axis. To do this, we will choose controls which make the original middle axis effectively look like a short axis in the closed loop. It appears that for the $SE(3)$ case, we need full actuation forces in the $\mathbb{R}^3$ direction and two control torques in the $SO(3)$ direction. As in the $SO(3)$ in §5.1.1, the motivation is to choose controls such that the closed-loop equation is Lagrangian and the middle axis for both the mass matrix and the inertia matrix of the system without controls is effectively made the closed-loop short axis.

In the equations of motion given by (5.2.6) and (5.2.7), we choose the components of $\boldsymbol{u}_\tau$ and $\boldsymbol{u}_f$ as follows:

$$\begin{aligned}
u^{ks}_{\tau 1} &= 0 \\
u^{ks}_{\tau 2} &= \left(I_3(\frac{\rho_3}{\rho_2}-1)+I_1(1-\frac{1}{\rho_2})\right)\Omega_3\Omega_1+\left(M_3(\frac{\bar\rho_3}{\rho_2}-1)+M_1(1-\frac{1}{\rho_2})\right)v_3v_1 \\
u^{ks}_{\tau 3} &= \left(I_1(\frac{1}{\rho_3}-1)+I_2(1-\frac{\rho_2}{\rho_3})\right)\Omega_1\Omega_2+\left(M_1(\frac{1}{\rho_3}-1)+M_2(1-\frac{\bar\rho_2}{\rho_3})\right)v_1v_2 \\
u^{ks}_{f1} &= ((\bar\rho_2-1)M_2v_2\Omega_3+(1-\bar\rho_3)M_3v_3\Omega_2) \\
u^{ks}_{f2} &= \left((\frac{\bar\rho_3}{\bar\rho_2}-1)M_3v_3\Omega_1+(1-\frac{1}{\bar\rho_2})M_1v_1\Omega_3\right) \\
u^{ks}_{f3} &= \left((\frac{1}{\bar\rho_3}-1)M_1v_1\Omega_2+(1-\frac{\bar\rho_2}{\bar\rho_3})M_2v_2\Omega_1\right)
\end{aligned} \tag{5.2.8}$$

where ρ_2 and ρ_3 satisfy the equation

$$\rho_2 I_2 - \rho_3 I_3 = I_2 - I_3 \tag{5.2.9}$$

and $\bar\rho_2$ and $\bar\rho_3$ satisfy the equation

$$\bar\rho_2 M_2 - \bar\rho_3 M_3 = M_2 - M_3. \tag{5.2.10}$$

Here, the superscript ks denotes kinetic shaping. The closed-loop equations are

$$\begin{aligned} \bar{I}\dot{\boldsymbol{\Omega}} &= (\bar{I}\boldsymbol{\Omega}) \times \boldsymbol{\Omega} + (\bar{M}\boldsymbol{v}) \times \boldsymbol{v} \\ \bar{M}\dot{\boldsymbol{v}} &= (\bar{M}\boldsymbol{v}) \times \boldsymbol{\Omega} \end{aligned}$$

where $\bar{I}$ is a diagonal matrix with entries $I_1, \rho_2 I_2, \rho_3 I_3$ and $\bar{M}$ is a diagonal matrix with entries $M_1, \bar{\rho}_2 M_2, \bar{\rho}_3 M_3$. Therefore, the closed-loop equations correspond to a rigid body with Lagrangian

$$L_c = \frac{1}{2}\left(\boldsymbol{\Omega}^T \bar{I}\boldsymbol{\Omega} + \boldsymbol{v}^T \bar{M}\boldsymbol{v}\right). \tag{5.2.11}$$

Since $I_2 > I_3$ and $M_2 > M_3$, we get $\rho_2 I_2 > \rho_3 I_3$ and $\bar{\rho}_2 M_2 > \bar{\rho}_3 M_3$. If we now choose

$$\rho_3 > \frac{I_1}{I_3} \tag{5.2.12}$$

and

$$\bar{\rho}_3 > \frac{M_1}{M_3}, \tag{5.2.13}$$

then we get the following two inequalities

$$\begin{aligned} \rho_2 I_2 > \rho_3 I_3 > I_1 \\ \bar{\rho}_2 M_2 > \bar{\rho}_3 M_3 > M_1. \end{aligned}$$

The open-loop middle axis for both the mass matrix and inertia matrix is effectively made the closed-loop short axis using kinetic shaping. We have stabilized the relative equilibrium when the rigid body is rotating about its middle axis and translating about the middle axis.

Theorem 5.2.1 *The control law* $\boldsymbol{u}_\tau^{ks}$ *and* $\boldsymbol{u}_f^{ks}$ *whose components are given by the set of equations in* (5.2.8) *stabilizes the rigid body rotating about its middle axis and at the same time translating along its middle axis. The scalars* ρ_3 *and* $\bar{\rho}_3$ *are chosen using* (5.2.12) *and* (5.2.13) *respectively and the scalars* ρ_2 *and* $\bar{\rho}_2$ *are obtained by solving* (5.2.9) *and* (5.2.10) *respectively.*

Our final goal is to couple a network of n vehicles in $SE(3)$ using potentials and stabilize the solution when each of these is rotating and translating along its middle axis. We will first solve this problem for the case when each body is rotating about and translating along its short axis. Such a solution for an individual body is stable in the reduced space, but in the full phase space, there are drift in the non compact $\mathbb{R}^3$ direction as shown in [32]. Before coupling of the network of n vehicles, we first remove these drifts using additional potential terms in the control law as described in the next section.

5.2.2 Drift Removal for $SE(3)$ vehicle

Observe that the control equations given by (5.2.8) depend only upon the reduced variables $\boldsymbol{\Omega}$ and $\boldsymbol{v}$ and hence the closed-loop equations still have $SE(3)$ symmetry. The drift we observe in the $\mathbb{R}^3$ direction are what we "physically see" in the inertial space. These drifts cannot be removed by controls which still retain the $SE(3)$. Instead we introduce additional control terms coming from a potential which breaks the $SE(3)$ symmetry and reduces it to $S^1 \times \mathbb{R}$ symmetry corresponding to rotation about and translation along a particular axis in the inertial space.

The kinetic energy of the body in inertial coordinates is

$$T = \frac{1}{2}\left(\boldsymbol{\omega}^T\left(I_l - \hat{\boldsymbol{b}}M_l\hat{\boldsymbol{b}}\right)\boldsymbol{\omega} - 2\boldsymbol{u}^T M_l\hat{\boldsymbol{b}}\boldsymbol{\omega} + \boldsymbol{u}^T M_l\boldsymbol{u}\right) \tag{5.2.14}$$

where $I_l = RIR^{-1}$, $M_l = RMR^{-1}$ and $\boldsymbol{u} = \dot{\boldsymbol{b}} - \hat{\boldsymbol{\omega}}\boldsymbol{b}$. The expression for the conjugate momentum is

$$\boldsymbol{p_u} = M_l(\boldsymbol{u} - \hat{\boldsymbol{b}}\boldsymbol{\omega}) = M_l\dot{\boldsymbol{b}} \tag{5.2.15}$$

$$\boldsymbol{p_\omega} = I_l\boldsymbol{\omega} + \boldsymbol{b} \times (M_l(\boldsymbol{u} - \hat{\boldsymbol{b}}\boldsymbol{\omega})) = I_l\boldsymbol{\omega} + \boldsymbol{b} \times (M_l\dot{\boldsymbol{b}}). \tag{5.2.16}$$

Here, $\boldsymbol{p_u}$ is the linear momentum of the body and $\boldsymbol{p_\omega}$ is the angular momentum of the body about the origin. The Hamiltonian written in terms of momentum variables is

$$H = \frac{1}{2}\left(\boldsymbol{p_u}^T M_l^{-1}\boldsymbol{p_u} + (\boldsymbol{p_\omega} - \boldsymbol{b} \times \boldsymbol{p_u})^T I_l^{-1}(\boldsymbol{p_\omega} - \boldsymbol{b} \times \boldsymbol{p_u})\right). \tag{5.2.17}$$

To make calculations easier, we assume that the translational direction is the $\boldsymbol{e}_1$ axis. If the vector $\boldsymbol{b}$ has components (b_1, b_2, b_3), the potential we introduce is

$$V_d(R, \boldsymbol{b}) = \sigma_1 \boldsymbol{e}_1^T R \boldsymbol{e}_1 + \frac{\sigma_2}{2}(b_2^2 + b_3^2). \tag{5.2.18}$$

Here, σ_1 and σ_2 are real constants which we choose later. The symmetry group is now reduced to $S^1 \times \mathbb{R}$ with the product group structure, corresponding to rotation about the $\boldsymbol{e}_1$ axis and translation along the $\boldsymbol{e}_1$ axis. I.e.,

$$V_d(\bar{R}R, \bar{R}\boldsymbol{b} + \bar{\boldsymbol{b}}) = V_d(R, \boldsymbol{b})$$

whenever $\bar{R}\boldsymbol{e}_1 = \boldsymbol{e}_1$ and $\bar{\boldsymbol{b}} = k\boldsymbol{e}_1$ for some real number k. The momentum map corresponding to this symmetry group is the projection of linear and angular momentum in the $\boldsymbol{e}_1$ direction. Stability of the system modulo this symmetry group implies that the drift in the direction transverse to the translational direction $\boldsymbol{e}_1$ are removed.

Since $S^1 \times \mathbb{R}$ is an Abelian group, we only need to verify that the amended potential has a definite second variation at the relative equilibrium of interest in the direction transverse to the group orbit. This is because, for a mechanical system with an Abelian symmetry group, the potential term in the Routhian is the amended potential. Since the kinetic energy part is already positive definite and the energy corresponding to the Routhian is a conserved quantity, stability follows if we can show that the second variation of the amended potential is also positive definite in the reduced space. Since for an Abelian group G, $G_{\boldsymbol{\mu}} = G$, this is same as showing that the second variation of amended potential is positive definite on *any* complement to the group orbit direction.

The expression for the amended potential at a particular value of momentum $\boldsymbol{\mu} = \begin{pmatrix} \boldsymbol{p}_{\boldsymbol{\omega}} \\ \boldsymbol{p}_{\boldsymbol{u}} \end{pmatrix}$ is

$$V_{\boldsymbol{\mu}}(R, \boldsymbol{b}) = V_d(R, \boldsymbol{b}) + \frac{1}{2}\langle \boldsymbol{\mu}, I^{-1}_{(R,\boldsymbol{b})}\boldsymbol{\mu} \rangle \tag{5.2.19}$$

where $I^{-1}_{(R,\boldsymbol{b})}$ is the inverse of the locked inertia tensor at the given configuration.

The locked inertia tensor is given by

$$I(R, \boldsymbol{b}) = \begin{bmatrix} I_l & 0 \\ 0 & M_l \end{bmatrix}. \tag{5.2.20}$$

Therefore,

$$V_{\boldsymbol{\mu}}(R, \boldsymbol{b}) = \sigma_1 \boldsymbol{e}_1^T R \boldsymbol{e}_1 + \frac{\sigma_2}{2}(b_2^2 + b_3^2) + \frac{1}{2}\left(\boldsymbol{\mu}_1^T I_l^{-1} \boldsymbol{\mu}_1 + \boldsymbol{\mu}_2^T M_l^{-1} \boldsymbol{\mu}_2\right), \tag{5.2.21}$$

Here, $\boldsymbol{\mu}_1$ is the part of $\boldsymbol{\mu}$ corresponding to S^1 symmetry and $\boldsymbol{\mu}_2$ is the part of $\boldsymbol{\mu}$ corresponding to $\mathbb{R}$ symmetry, i.e, these are the projections of angular and linear momentum along the $\boldsymbol{e}_1$ axis respectively. They are $\boldsymbol{\mu}_1 = \mu_1 \boldsymbol{e}_1$ and $\boldsymbol{\mu}_2 = \mu_4 \boldsymbol{e}_1$. For a body rotating about its short axis and translating about its short axis aligned with the $\boldsymbol{e}_1$ axis, the second and third components of $\boldsymbol{\mu}_1$ and $\boldsymbol{\mu}_2$ are zero. If $\delta R = \widehat{\delta\boldsymbol{\theta}} R$, then

$$\begin{aligned} \delta^2 V_{\boldsymbol{\mu}} =& \sigma_1 \boldsymbol{e}_1^T \widehat{\delta\boldsymbol{\theta}} \widehat{\delta\boldsymbol{\theta}} R \boldsymbol{e}_1 + \sigma_2 \left((\delta b_2)^2 + (\delta b_3)^2\right) + \left(\delta\boldsymbol{\theta}^T \widehat{I_l^{-1}\boldsymbol{\mu}_1} \hat{\boldsymbol{\mu}}_1 \delta\boldsymbol{\theta} - \delta\boldsymbol{\theta}^T \hat{\boldsymbol{\mu}}_1 I_l^{-1} \hat{\boldsymbol{\mu}}_1 \delta\boldsymbol{\theta}\right) \\ &+ \left(\delta\boldsymbol{\theta}^T \widehat{M_l^{-1}\boldsymbol{\mu}_2} \hat{\boldsymbol{\mu}}_2 \delta\boldsymbol{\theta} - \delta\boldsymbol{\theta}^T \hat{\boldsymbol{\mu}}_2 M_l^{-1} \hat{\boldsymbol{\mu}}_2 \delta\boldsymbol{\theta}\right). \end{aligned} \tag{5.2.22}$$

At the relative equilibrium of interest, $R = R_e$ is a rotation about the $\boldsymbol{e}_1$ axis. Therefore, $R_e \boldsymbol{e}_1 = \boldsymbol{e}_1$. This also implies $R_e \boldsymbol{\mu}_1 = \boldsymbol{\mu}_1$ and $R_e \boldsymbol{\mu}_2 = \boldsymbol{\mu}_2$. We also have the following at the relative equilibrium:

$$\begin{aligned} I_l^{-1}\boldsymbol{\mu}_1 &= R_e I^{-1} R_e^{-1} \boldsymbol{\mu}_1 \\ &= R_e I^{-1} \boldsymbol{\mu}_1 \\ &= I_1^{-1} R_e \boldsymbol{\mu}_1 \\ &= I_1^{-1} \boldsymbol{\mu}_1 \end{aligned} \tag{5.2.23}$$

Hence, the second variation of the amended potential evaluated at the relative equilibrium configuration is

$$\begin{aligned} \delta^2 V_{\boldsymbol{\mu}}|_e =& -\sigma_1 (\widehat{\delta\boldsymbol{\theta}} \boldsymbol{e}_1)^T \widehat{\delta\boldsymbol{\theta}} \boldsymbol{e}_1 + 2\sigma_2 \left((\delta b_2)^2 + (\delta b_3)^2\right) + \\ &- \left((\hat{\boldsymbol{\mu}}_1 \delta\boldsymbol{\theta})^T R_e \left(I_1^{-1} \mathbb{I}_{3\times 3} - M^{-1}\right) R_e^{-1} \hat{\boldsymbol{\mu}}_1 \delta\boldsymbol{\theta}\right) \\ &- \left((\hat{\boldsymbol{\mu}}_2 \delta\boldsymbol{\theta})^T R_e \left(M_1^{-1} \mathbb{I}_{3\times 3} - I^{-1}\right) R_e^{-1} \hat{\boldsymbol{\mu}}_2 \delta\boldsymbol{\theta}\right). \end{aligned} \tag{5.2.24}$$

where M_1, M_2, M_3 and I_1, I_2, I_3 are the diagonal elements of M and I respectively. If $M_1 > M_2 > M_3$ and $I_1 > I_2 > I_3$, then $\delta^2 V_{\boldsymbol{\mu}}|_e$ can be made positive semi-definite by choosing $\sigma_1 < 0$ and $\sigma_2 > 0$. The null space consists of vectors in the translational direction δb_1 and in the rotational direction $\delta\boldsymbol{\theta}$ parallel to $\boldsymbol{e}_1$, i.e., the only way $\delta^2 V_{\boldsymbol{\mu}}|_e$ can be zero is when $\delta b_2 = \delta b_3 = 0$ and when $\delta\boldsymbol{\theta} \| \boldsymbol{e}_1$. This motion corresponds to rotation about the $\boldsymbol{e}_1$ axis and translation along the $\boldsymbol{e}_1$ axis which is the symmetry direction. Therefore, by the theory of stability using amended potential, the dynamics are stable and we have also managed to remove the drifts in the transverse translational direction.

The dynamics of the rigid body with the control input that removes drift can be obtained by calculating the first variation of V_d as follows:

$$\begin{aligned} \delta V_d &= \sigma_1 \boldsymbol{e}_1^T \delta R \boldsymbol{e}_1 + \sigma_2 (b_2 \delta b_2 + b_3 \delta b_3) \\ &= \sigma_1 \boldsymbol{e}_1^T \widehat{\delta\boldsymbol{\theta}} R \boldsymbol{e}_1 + \sigma_2 (b_2 \delta b_2 + b_3 \delta b_3) \\ &= \sigma_1 \delta\boldsymbol{\theta}^T (R\boldsymbol{e}_1 \times \boldsymbol{e}_1) + \sigma_2 (b_2 \delta b_2 + b_3 \delta b_3). \end{aligned} \tag{5.2.25}$$

Using (5.2.25), we get the expression for the rigid body dynamics with control terms as

$$\dot{\boldsymbol{p}}_{\boldsymbol{\omega}} = -\sigma_1 (R\boldsymbol{e}_1) \times \boldsymbol{e}_1 \tag{5.2.26}$$

$$\dot{\boldsymbol{p}}_{\boldsymbol{u}} = -\sigma_2 \begin{pmatrix} 0 \\ b_2 \\ b_3 \end{pmatrix}. \tag{5.2.27}$$

Theorem 5.2.2 *Consider a single rigid body in $SE(3)$ with equations of motion given by* (5.2.26) *and* (5.2.27). *The closed-loop equations are again a Lagrangian system on $SE(3)$ with potential given by* (5.2.18). *The closed-loop Lagrangian has $S^1 \times \mathbb{R}$ as the symmetry group and the corresponding relative equilibrium when the body is rotating about its short axis and translating along the short axis aligned with the $\boldsymbol{e}_1$ axis is stable.*

The rigid body motion is in fact stabilized when it is rotating about its short axis and translating along its short axis aligned along any direction in the inertial space. We chose this axis to be $\boldsymbol{e}_1$ in Theorem 5.2.2 only for illustration.

5.2.3 Coordination of $SE(3)$ Network with Stable Dynamics

We now consider the case of n rigid bodies with each having $SE(3)$ as its configuration space. As mentioned in Chapter 4, the phase space for the $n-$body system is n copies of $TSE(3)$ which we denote by $T(\underbrace{SE(3) \times \ldots \times SE(3)}_{n \text{ times}}) := T(SE(3)^n)$.

In Chapter 4, the reduced equations of motion are derived using the potential $V = \sum_{i=1}^{n-1} \left(\sigma_1 \text{tr}(R_{i+1}^T R_i) + \sigma_2 \|\boldsymbol{b}_i - \boldsymbol{b}_{i+1}\|^2\right)$, with $\sigma_1, \sigma_2 \in \mathbb{R}$. Note that if $R_i = R_{i+1}$ and $\boldsymbol{b}_i = \boldsymbol{b}_{i+1}$ for $i = 1, \ldots, n-1$, the potential V is at a minimum if $\sigma_1 < 0$ and $\sigma_2 > 0$. These σ_1 and σ_2 are the same constants as in the previous section in (5.2.18). The Lagrangian for the controlled network L_{net_c} is then

$$L_{\text{net}_c} = L_{\text{net}} - V = \sum_{i=1}^{n} \frac{1}{2}\left(\boldsymbol{\Omega}_i^T I_i \boldsymbol{\Omega}_i + \boldsymbol{v}_i^T M_i \boldsymbol{v}_i\right) - \sigma_1 \text{tr}(\sum_{i=1}^{n-1} R_{i+1}^T R_i) - \sigma_2 \sum_{i=1}^{n-1} \|\boldsymbol{b}_i - \boldsymbol{b}_{i+1}\|^2$$

The equations of motion for the controlled system corresponding to this Lagrangian L_{net_c} on the reduced space $T(SE(3)^n)/SE(3)$ corresponding to the i^{th} body are as derived in (4.2.6)

$$\begin{aligned} I_i \dot{\boldsymbol{\Omega}}_i &= (I_i \boldsymbol{\Omega}_i) \times \boldsymbol{\Omega}_i + (M_i \boldsymbol{v}_i) \times \boldsymbol{v}_i + \sigma_1 (\boldsymbol{u}_{\tau,i-1}^{ps} - \boldsymbol{u}_{\tau i}^{ps}) \\ M_i \dot{\boldsymbol{v}}_i &= (M_i \boldsymbol{v}_i) \times \boldsymbol{\Omega}_i + \sigma_2 \boldsymbol{u}_{fi}^{ps} \end{aligned}$$

where

$$\boldsymbol{u}_{\tau i}^{ps} = (\boldsymbol{\Delta}_i \times \boldsymbol{e}_1 + \boldsymbol{\Sigma}_i \times \boldsymbol{e}_2 + \boldsymbol{\Gamma}_i \times \boldsymbol{e}_3) \tag{5.2.28}$$

and $\boldsymbol{\Delta}_i, \boldsymbol{\Sigma}_i, \boldsymbol{\Gamma}_i$ are the column vectors of $R_{i+1}^{-1} R_i$, $\boldsymbol{u}_{\tau 0}^{ps} = \boldsymbol{u}_{\tau n}^{ps} = 0$ and $\boldsymbol{u}_{fi}^{ps} = -R_i^{-1}(2\boldsymbol{b}_i - \boldsymbol{b}_{i+1} - \boldsymbol{b}_{i-1})$ for $i = 2, \ldots, n-1$, $\boldsymbol{u}_{f1}^{ps} = -R_i^{-1}(\boldsymbol{b}_1 - \boldsymbol{b}_2)$ and $\boldsymbol{u}_{fn}^{ps} = -R_i^{-1}(\boldsymbol{b}_n - \boldsymbol{b}_{n-1})$.

We are interested in the relative equilibrium given by

$$\begin{aligned} \boldsymbol{\Omega}_{ie} &= (\bar{\Omega}, 0, 0) \\ \boldsymbol{v}_{ie} &= (\bar{v}, 0, 0) \\ \left[\begin{array}{ccc} \boldsymbol{\Delta}_{ie} & \boldsymbol{\Sigma}_{ie} & \boldsymbol{\Gamma}_{ie} \end{array} \right] &= \left[\begin{array}{ccc} \boldsymbol{e}_1 & \boldsymbol{e}_2 & \boldsymbol{e}_3 \end{array} \right] \\ \boldsymbol{b}_i &= \boldsymbol{b}_{i+1} \end{aligned} \tag{5.2.29}$$

where $i = 1, \ldots, n$. Here, we are looking for solutions where each body is rotating about its short axis and the bodies are aligned, i.e., $R_1 = R_2 = \ldots = R_n$, their positions are also aligned, i.e., $\boldsymbol{b}_i = \boldsymbol{b}_{i+1}$ for all i and all the bodies are translating along the same vector. That this is indeed a relative equilibrium can be easily checked. We now study stability properties of the above system.

Let $\boldsymbol{p}_{\boldsymbol{\omega}i}$ be the angular momentum of the i^{th} body in inertial space and $\boldsymbol{p}_{\boldsymbol{u}i}$ be its linear momentum in inertial space. The phase space is $T^*(SE(3)^n)$ and the momentum map is

$$\boldsymbol{J} = \sum_{i=1}^{n} \begin{pmatrix} \boldsymbol{p}_{\boldsymbol{\omega}i} \\ \boldsymbol{p}_{\boldsymbol{u}i} \end{pmatrix} \tag{5.2.30}$$

Let $M_{li} = RM_iR^{-1}$ and $I_{li} = RI_iR^{-1}$. Therefore, H can be written as

$$\begin{aligned} H = \quad & \frac{1}{2} \sum_{i=1}^{n} \left(\boldsymbol{p}_{\boldsymbol{u}i}{}^T M_{li}^{-1} \boldsymbol{p}_{\boldsymbol{u}i} + (\boldsymbol{p}_{\boldsymbol{\omega}i} - \boldsymbol{b}_i \times \boldsymbol{p}_{\boldsymbol{u}i})^T I_{li}^{-1} (\boldsymbol{p}_{\boldsymbol{\omega}i} - \boldsymbol{b}_i \times \boldsymbol{p}_{\boldsymbol{u}i}) \right) \\ & + \sigma_1 \mathrm{tr}(\sum_{i=1}^{n-1} R_{i+1}^T R_i) + \sigma_2 \sum_{i=1}^{n-1} \|\boldsymbol{b}_i - \boldsymbol{b}_{i+1}\|^2. \end{aligned} \tag{5.2.31}$$

Let us assume that the motion is along the $\boldsymbol{e}_1$ axis of the inertial frame. Since H given by (5.2.31) still has $SE(3)$ symmetry, the system will have drifts in the non compact direction. Just as for the single $SE(3)$ case, we now introduce additional potentials to reduce the symmetry to $S^1 \times \mathbb{R}$. This will not only remove drifts but will also allow us to use the amended potential and check for its definiteness in directions traverse to the group orbit to conclude stability. We introduce these

potentials carefully so that the relative equilibrium of interest is not destroyed. The final Hamiltonian looks as follows

$$\begin{aligned} H = \quad & \frac{1}{2}\sum_{i=1}^{n}\left(\boldsymbol{p_u}_i^T M_{li}^{-1}\boldsymbol{p_u}_i + (\boldsymbol{p_\omega}_i - \boldsymbol{b}_i \times \boldsymbol{p_u}_i)^T I_{li}^{-1}(\boldsymbol{p_\omega}_i - \boldsymbol{b}_i \times \boldsymbol{p_u}_i)\right) \\ & +\sigma_1 \mathrm{tr}(\sum_{i=1}^{n-1} R_{i+1}^T R_i) + \frac{\sigma_2}{2}\sum_{i=1}^{n-1}\|\boldsymbol{b}_i - \boldsymbol{b}_{i+1}\|^2 + \sigma_1(R_1\boldsymbol{e}_1)^T\boldsymbol{e}_1 + \frac{\sigma_2}{2}(b_{12}^2 + b_{13}^2) \end{aligned}$$

For this Hamiltonian, the potential

$$V = \sigma_1 \mathrm{tr}(\sum_{i=1}^{n-1} R_{i+1}^T R_i) + \frac{\sigma_2}{2}\sum_{i=1}^{n-1}\|\boldsymbol{b}_i - \boldsymbol{b}_{i+1}\|^2 + \sigma_1(R_1\boldsymbol{e}_1)^T\boldsymbol{e}_1 + \frac{\sigma_2}{2}(b_{12}^2 + b_{13}^2) \quad (5.2.32)$$

reduces the symmetry group to $S^1 \times \mathbb{R}$ with the product group structure, corresponding to rotation about the $\boldsymbol{e}_1$ axis and translation along the $\boldsymbol{e}_1$ axis. Note that the symmetry breaking here is done using the orientation and position R_1 and $\boldsymbol{b}_1$ of the first body. This is an arbitrary choice and was made for illustration purposes. Hence, the relative equilibrium given by (5.2.29) is not destroyed by introducing extra potentials. The corresponding momentum map is the total angular momentum about the $\boldsymbol{e}_1$ direction and the total linear momentum along the $\boldsymbol{e}_1$ axis and is given by

$$\tilde{\boldsymbol{J}} = \begin{pmatrix} J_1\boldsymbol{e}_1 \\ J_4\boldsymbol{e}_1 \end{pmatrix} \quad (5.2.33)$$

where $\boldsymbol{J}$ is given by (5.2.30).

To prove stability of the relative equilibrium (5.2.29), we need to verify that $\delta^2 V_{\boldsymbol{\mu}}$ is definite on the space transverse to the group orbit. At the relative equilibrium of interest, $R_1 = R_2 = \ldots = R_n = R_e$ and $\boldsymbol{b}_1 = \boldsymbol{b}_2 = \ldots = \boldsymbol{b}_n = b_e$ and R_e is rotation about the $\boldsymbol{e}_1$ axis and the second and third components of $\boldsymbol{b}_e$ are zero. The expression for the locked inertia tensor at this configuration is

$$I(R_1, \ldots, R_n, b_1, \ldots, b_n) = \begin{bmatrix} R_e(\sum_{i=1}^n I_i)R_e^{-1} & 0 \\ 0 & R_e(\sum_{i=1}^n M_i)R_e^{-1} \end{bmatrix}. \quad (5.2.34)$$

Now,

$$V_{\boldsymbol{\mu}} = \sigma_1 \mathrm{tr}(\sum_{i=1}^{n-1} R_{i+1}^T R_i) + \frac{\sigma_2}{2} \sum_{i=1}^{n-1} \|\boldsymbol{b}_i - \boldsymbol{b}_{i+1}\|^2 + \sigma_1 (R_1 \boldsymbol{e}_1)^T \boldsymbol{e}_1 + \frac{\sigma_2}{2}(b_{12}^2 + b_{13}^2) + \langle \boldsymbol{\mu}, I^{-1}\boldsymbol{\mu} \rangle \tag{5.2.35}$$

Let $M_\Sigma = \sum_{i=1}^n M_i$ and $I_\Sigma = \sum_{i=1}^n I_i$. The second variation of $V_{\boldsymbol{\mu}}$ evaluated at the relative equilibrium configuration is

$$\begin{aligned}
\delta^2 V_{\boldsymbol{\mu}}|_e = \quad & -\sigma_1 (\widehat{\delta\boldsymbol{\theta}_1}\boldsymbol{e}_1)^T \widehat{\delta\boldsymbol{\theta}_1}\boldsymbol{e}_1 + \sigma_2 \left((\delta b_{12})^2 + (\delta b_{13})^2\right) \\
& - \left((\hat{\boldsymbol{\mu}}_1 \delta\boldsymbol{\theta})^T R_e \left(I_{\Sigma 1}^{-1} I_{3\times 3} - I_\Sigma^{-1}\right) R_e^{-1} \hat{\boldsymbol{\mu}}_1 \delta\boldsymbol{\theta}\right) \\
& - \left((\hat{\boldsymbol{\mu}}_2 \delta\boldsymbol{\theta})^T R_e \left(M_{\Sigma 1}^{-1} I_{3\times 3} - M_\Sigma^{-1}\right) R_e^{-1} \hat{\boldsymbol{\mu}}_2 \delta\boldsymbol{\theta}\right) \\
& -2\sigma_1 \sum_{i=1}^{n-1} \left((\delta\boldsymbol{\theta}_i - \delta\boldsymbol{\theta}_{i+1})^T (\delta\boldsymbol{\theta}_i - \delta\boldsymbol{\theta}_{i+1})\right) + \sigma_2 \sum_{i=1}^{n-1} \|\delta\boldsymbol{b}_i - \delta\boldsymbol{b}_{i+1}\|^2
\end{aligned}$$

Here, $M_{\Sigma 1}$ is the $(1,1)$ entry of M_Σ and $I_{\Sigma 1}$ is the $(1,1)$ entry of I_Σ. If for each body, $M_{i1} > M_{i2} > M_{i3}$ and $I_{i1} > I_{i2} > I_{i3}$, then the above expression becomes positive semi-definite if $\sigma_1 < 0, \sigma_2 > 0$. $\delta^2 V_{\boldsymbol{\mu}}|_e = 0$ when evaluated only on the following vectors:

$$\begin{aligned}
\delta\boldsymbol{b}_i &= \delta\boldsymbol{b}_{i+1} \\
\delta\boldsymbol{\theta}_i &= \delta\boldsymbol{\theta}_{i+1} \\
\delta\boldsymbol{\theta}_1 &\parallel e_1 \\
\delta b_{12} = \delta b_{13} &= 0
\end{aligned}$$

These vectors belong to the group orbit space. Hence, $\delta^2 V_{\boldsymbol{\mu}}|_e > 0$ in directions transverse to the group orbit and we get that the system has a stable relative equilibrium. The final equations of motion with control terms are

$$I_i \dot{\boldsymbol{\Omega}}_i = (I_i \boldsymbol{\Omega}_i) \times \boldsymbol{\Omega}_i + (M_i \boldsymbol{v}_i) \times \boldsymbol{v}_i + \sigma_1 (\boldsymbol{u}_{\tau,i-1}^{ps} - \boldsymbol{u}_{\tau i}^{ps}) \tag{5.2.36}$$

$$M_i \dot{\boldsymbol{v}}_i = (M_i \boldsymbol{v}_i) \times \boldsymbol{\Omega}_i + \sigma_2 \boldsymbol{u}_{fi}^{ps} \tag{5.2.37}$$

where $\boldsymbol{u}_{\tau i}^{ps}$ for $i \neq 0, n$ is given by (5.2.28), $\boldsymbol{u}_{\tau 0}^{ps} = -((R_1 \boldsymbol{e}_1) \times \boldsymbol{e}_1)$, $\boldsymbol{u}_{\tau n}^{ps} = 0$,

$$\boldsymbol{u}_{f1}^{ps} = - \begin{pmatrix} 0 \\ b_{12} \\ b_{13} \end{pmatrix} - R_i^{-1}(\boldsymbol{b}_1 - \boldsymbol{b}_2), \tag{5.2.38}$$

$\boldsymbol{u}_{fi}^{ps} = -R_i^{-1}(2\boldsymbol{b}_i - \boldsymbol{b}_{i+1} - \boldsymbol{b}_{i-1})$ for $i = 2, \ldots, n-1$ and $\boldsymbol{u}_{fn}^{ps} = -R_i^{-1}(\boldsymbol{b}_n - \boldsymbol{b}_{n-1})$.

Theorem 5.2.3 *For the n rigid body problem with closed-loop equations given by* (5.2.36) *and* (5.2.37)*, the relative equilibrium (5.2.29) is stable. This equilibrium corresponds to all n rigid bodies having the same orientation and position vectors with each one rotating about its short axis and translating along the same axis aligned with the* $\boldsymbol{e}_1$ *axis in the inertial frame.*

Note that we chose the translation axis to be $\boldsymbol{e}_1$ in Theorem 5.2.3 only for illustration. Since V is defined intrinsically, the result is independent of the coordinate system and holds true for any axis we choose in the inertial space.

Suppose the potential V given by (5.2.32) is modified to

$$V = \sigma_1 \mathrm{tr}(\sum_{i=1}^{n-1} R_{i+1}^T R_i) + \frac{\sigma_2}{2} \sum_{i=1}^{n-1} \|\boldsymbol{b}_i - \boldsymbol{b}_{i+1} - \boldsymbol{d}_i\|^2 + \sigma_1 (R_1 \boldsymbol{e}_1)^T \boldsymbol{e}_1 + \frac{\sigma_2}{2}(b_{12}^2 + b_{13}^2) \tag{5.2.39}$$

where $\boldsymbol{d}_i$ is a constant vector for $i = 1, \ldots, n-1$. This will correspond to the case when we want the i^{th} and $(i+1)^{\text{th}}$ vehicle to maintain a constant relative spacing vector given by $\boldsymbol{d}_i$ and the 1^{st} vehicle rotates about and translates along the $\boldsymbol{e}_1$ axis. This is the relative velocity we stabilize. This does not imply that there wont be any collisions starting from an arbitrary initial state. For collision avoidance, we will need to introduce some more terms in the potential V which blow up when the interspacing distance drops below a certain value.

In the SMC setting in Chapter 3, the kinetic energy in the closed-loop system was made negative definite. Since the open-loop system had a potential which was maximum, the control gains were chosen to make the closed-loop kinetic energy also

maximum so that the closed-loop energy could be used as a Lyapunov function. In this chapter, the only term in the Lagrangian before adding controls was the kinetic energy. Hence, we choose to retain the positive definiteness of the kinetic energy and the control gains were chosen such that the new potential terms were positive semi-definite. Though the stability results are the same in these two approaches, when there is physical dissipation like friction in the system, the treatment is more subtle in the former case. Some of these issues are addressed in [47].

5.2.4 Coordination of $SE(3)$ Network with Unstable Dynamics

We now show how to stabilize the relative equilibrium corresponding to the bodies oriented alike with same position vector and each body rotating about and translating along its *unstable* middle axis. The idea is to use kinetic shaping from §5.2.1 to stabilize the unstable rotation and potential shaping from §5.2.3 to coordinate the orientations of the bodies.

Consider the controlled dynamics for the ith body given by

$$I_i\dot{\boldsymbol{\Omega}}_i = (I_i\boldsymbol{\Omega}_i)\times\boldsymbol{\Omega}_i + (M_i\boldsymbol{v}_i)\times\boldsymbol{v}_i + \begin{pmatrix} -(u^{ps}_{\tau i-1,1} - u^{ps}_{\tau i1}) \\ -(u^{ps}_{\tau i-1,2} - u^{ps}_{\tau i2})/\rho_2 + u^{ks}_{\tau i2} \\ -(u^{ps}_{\tau i-1,3} - u^{ps}_{\tau i3})/\rho_3 + u^{ks}_{\tau i3} \end{pmatrix} \quad (5.2.40)$$

$$M_i\dot{\boldsymbol{v}}_i = (M_i\boldsymbol{v}_i)\times\boldsymbol{\Omega}_i + \begin{pmatrix} -(u^{ps}_{fi-1,1} - u^{ps}_{fi1}) + u^{ks}_{fi1} \\ -(u^{ps}_{fi-1,2} - u^{ps}_{fi2})/\bar{\rho}_2 + u^{ks}_{fi2} \\ -(u^{ps}_{fi-1,3} - u^{ps}_{fi3})/\bar{\rho}_3 + u^{ks}_{fi3} \end{pmatrix} \quad (5.2.41)$$

where $\boldsymbol{u}^{ps}_{\tau i}$ and $\boldsymbol{u}^{ps}_{fi}$ are the potential shaping control terms given by (5.2.36) and (5.2.37). The kinetic shaping control terms $u^{ks}_{\tau i2}, u^{ks}_{\tau i3}, u^{ks}_{fi1}, u^{ks}_{fi2}, u^{ks}_{fi3}$ are as given in (5.2.8) for the ith body. It can easily be checked that the closed-loop equations now have the form (5.2.36) and (5.2.37), but with the original middle axis now the short

axis. Hence, we get the following corollary.

Corollary 5.2.4 *The relative equilibrium corresponding to n rigid bodies with the same orientation and position vector and each rotating about and translating along its unstable, middle axis, is stabilized for the controlled dynamics of (5.2.40) and (5.2.41).*

Chapter 6

Asymptotic Synchronization of Networked Rigid Bodies

In Chapter 5, we derived controls to stabilize the relative equilibrium of a network of rigid bodies in $SO(3)$ and $SE(3)$. For the $SO(3)$ network case, the stabilized solution is the case when the rigid bodies are aligned in orientation and each is rotating about its individual unstable middle axis. In the $SE(3)$ network case, the stabilized solution is the one in which the bodies have aligned orientations and positions and each one is rotating about and translating along its middle axis. In this section, we will add dissipation terms to the control law to make these synchronized solutions asymptotically stable. We show asymptotic stability of the synchronized $SO(3)$ network in §6.1 and asymptotic stability of $SE(3)$ network in §6.2.

6.1 Asymptotic Synchronization of Networked $SO(3)$ Bodies

Our goal in this section is to asymptotically stabilize the solution where the $SO(3)$ bodies are synchronized, pointing in a particular direction in inertial space and rotating about their short axis. The analogous case when the bodies are rotating about

their middle axis can be obtained by combining results in this section with kinetic shaping described in §5.1.1. We will assume that the direction about which the rigid bodies are rotating is the $\boldsymbol{e}_1$ axis. The potential we introduced in (5.1.10) to couple the network has $SO(3)$ symmetry. We will now add an additional term to reduce it to S^1. The final potential we use is:

$$V = \sigma \mathrm{tr}(\sum_{i=1}^{n-1} R_{i+1}^T R_i) + \sigma \boldsymbol{e}_1^T R_1 \boldsymbol{e}_1. \tag{6.1.1}$$

The only symmetry left after introducing this potential is rotation about the $\boldsymbol{e}_1$ axis. The equations of motion for the network are

$$I_i \dot{\boldsymbol{\Omega}}_i = (I_i \boldsymbol{\Omega}_i) \times \boldsymbol{\Omega}_i + \sigma(\boldsymbol{u}_{i-1}^{ps} - \boldsymbol{u}_i^{ps}) + \boldsymbol{u}_i^{\mathrm{diss}} \quad i = 1, \ldots, n \tag{6.1.2}$$

where

$$\boldsymbol{u}_i^{ps} = (\boldsymbol{\Delta}_i \times \boldsymbol{e}_1 + \boldsymbol{\Sigma}_i \times \boldsymbol{e}_2 + \boldsymbol{\Gamma}_i \times \boldsymbol{e}_3), \quad i = 1, \ldots, n-1, \tag{6.1.3}$$

$\boldsymbol{\Delta}_i, \boldsymbol{\Sigma}_i, \boldsymbol{\Gamma}_i$ are the column vectors of $R_{i+1}^{-1} R_i$ and $\boldsymbol{u}_0^{ps} = -\sigma R_1^{-1}((R_1 \boldsymbol{e}_1) \times \boldsymbol{e}_1)$, $\boldsymbol{u}_n^{ps} = 0$. The terms $\boldsymbol{u}_i^{\mathrm{diss}}$ are the disspation terms we will introduce for asymptotic stabilization. The relative equilibrium to be asymptotically stabilized is

$$\begin{aligned} R_i &= R_j = R_e, \quad i \neq j \\ R_e \boldsymbol{e}_1 &= \boldsymbol{e}_1 \\ \boldsymbol{\Omega}_i &= \boldsymbol{\omega}_i = k\boldsymbol{e}_1, \quad k \in \mathbb{R} \end{aligned} \tag{6.1.4}$$

Consider the following function

$$E_1 = \frac{1}{2} \sum_{i=1}^{n} \Big((\boldsymbol{\omega}_i - k\boldsymbol{e}_1)^T R_i I_i R_i^{-1} (\boldsymbol{\omega}_i - k\boldsymbol{e}_1) \Big) + V_{\boldsymbol{e}_1} \tag{6.1.5}$$

where

$$V_{\boldsymbol{e}_1} = \sigma \mathrm{tr}(\sum_{i=1}^{n-1} R_{i+1}^T R_i) + \sigma \boldsymbol{e}_1^T R_1 \boldsymbol{e}_1 - \frac{1}{2} \sum_{i=1}^{n} \boldsymbol{e}_1^T (R_i I_i R_i^{-1}) \boldsymbol{e}_1. \tag{6.1.6}$$

Here, $V_{\boldsymbol{e}_1}$ is the amended potential for the system corresponding to the relative equilibrium given by (6.1.4). The function E_1 has the same form as (3.7.1) with $k\boldsymbol{e}_1$

playing the role of v_{RE}. Hence, we can use Theorem 3.7.1 to calculate the time derivative of E_1 as

$$\frac{d}{dt}E_1 = \sum_{i=1}^{n}(\boldsymbol{\omega} - k\boldsymbol{e}_1)\cdot(R_i\boldsymbol{u}_i^{\text{diss}}) \tag{6.1.7}$$

The time derivative of E_1 can also be calculated directly and is illustrated in Appendix A. If we choose

$$\boldsymbol{u}_i^{\text{diss}} = -\kappa R_i^{-1}(\boldsymbol{\omega}_i - k\boldsymbol{e}_1), \quad \kappa > 0 \tag{6.1.8}$$

then $\dot{E}_1 \leq 0$. Since the system is fully actuated, it is also linearly controllable at each point. To use Theorem 3.7.2, we need to show that E_1 is a Lyapunov function for the relative equilibrium solution manifold given by (6.1.4). Since the kinetic energy part of E_1 is already positive semi-definite, we need to show that $\delta^2 V_{\boldsymbol{e}_1} \geq 0$ and is equal to zero only when the conditions in (6.1.4) are met. Using the same calculations as done in the first two paragraphs of §5.1.2, we find that when the conditions in (6.1.4) are met,

$$\begin{aligned}\delta^2 V_{\boldsymbol{e}_1} &= -2\sigma\sum_{i=1}^{n-1}(\delta\boldsymbol{\theta}_{i+1} - \delta\boldsymbol{\theta}_i)^T(\delta\boldsymbol{\theta}_{i+1} - \delta\boldsymbol{\theta}_i) - \sigma(\delta\boldsymbol{\theta}_1 \times \boldsymbol{e}_1)^T(\delta\boldsymbol{\theta}_1 \times \boldsymbol{e}_1) \\ &\quad + \sum_{i=1}^{n}(\delta\boldsymbol{\theta}_i \times \boldsymbol{e}_1)^T(I_{i,1}\mathbb{I}_{3\times 3} - I_{li})(\delta\boldsymbol{\theta}_i \times \boldsymbol{e}_1),\end{aligned}$$

where $I_{i,1}$ is the moment of inertia corresponding to the short axis of i^{th}-body. When $\sigma < 0$, $\delta^2 V_{\boldsymbol{e}_1} \geq 0$ and is equal to zero only when (6.1.4) is satisfied. Hence, E_1 is minimum when the conditions in (6.1.4) are satisfied, i.e., it is a Lyapunov function for the relative equilibrium solution manifold. We can now use Theorem 3.7.2 to conclude that the solution goes to the set $E_1 = 0$. On this set,

$$\begin{aligned}\boldsymbol{\omega}_i &= k\boldsymbol{e}_1 \\ R_i &= R_j = R_e \\ R_e\boldsymbol{e}_1 &= \boldsymbol{e}_1.\end{aligned}$$

This corresponds to the synchronized motion where the rigid bodies are aligned with each other, each one is rotating about the $\boldsymbol{e}_1$ axis in the inertial frame. Since $R_e\boldsymbol{e}_1 =$

$\boldsymbol{e}_1$, we get

$$\Omega_i = R_e^{-1}\boldsymbol{\omega}_i = kR_e^{-1}\boldsymbol{e}_1 = k\boldsymbol{e}_1$$

Therefore, we get that the rotation is about the short axis, which in turn is aligned with the $\boldsymbol{e}_1$ axis in inertial space. Hence, we get that the solution asymptotically goes to the one given by (6.1.4) and we have the following theorem.

Theorem 6.1.1 *The rigid body $SO(3)$ network with equations of motion given by* (6.1.2) *and dissipation chosen as in* (6.1.8) *has exponentially stable relative equilibria given by* (6.1.4).

Figures 6.1.1 and 6.1.2 illustrate the results of a MATLAB simulation for the controlled network of three identical $SO(3)$ systems. The inertia matrix parameters are $I_1 = 8\text{kg} - \text{m}^2$, $I_2 = 4\text{kg} - \text{m}^2$, $I_3 = 1\text{kg} - \text{m}^2$. The relative equilibrium velocity is chosen to be $\boldsymbol{\omega}_i = \boldsymbol{e}_1 rad/sec$. The rotation part is parametrized using quaternions given by

$$\boldsymbol{q}_i = \begin{bmatrix} \cos(\theta_i/2) & \sin(\theta_i/2)\bar{\boldsymbol{q}}_i \end{bmatrix}$$

where $\bar{\boldsymbol{q}}_i$ denotes the axis of rotation and θ_i denotes the angle of rotation for the i^{th} body. The control gains are $\sigma = 2, \kappa = 2$. The initial conditions are

$$\boldsymbol{q}_1(0) = \begin{pmatrix} 0.88 \\ 0.25 \\ 0.40 \\ 0.05 \end{pmatrix}, \boldsymbol{q}_2(0) = \begin{pmatrix} 0.93 \\ 0.19 \\ 0.24 \\ 0.18 \end{pmatrix}, \boldsymbol{q}_3(0) = \begin{pmatrix} 0.10 \\ 0.01 \\ 0.00 \\ 0.00 \end{pmatrix},$$

$$\dot{\boldsymbol{q}}_1(0) = \begin{pmatrix} -0.41 \\ -0.13 \\ 0.86 \\ 0.79 \end{pmatrix}, \dot{\boldsymbol{q}}_2(0) = \begin{pmatrix} 0.41 \\ -0.49 \\ -0.56 \\ -0.84 \end{pmatrix}, \dot{\boldsymbol{q}}_3(0) = \begin{pmatrix} 0.01 \\ -0.80 \\ -0.67 \\ -0.67 \end{pmatrix}.$$

Figure 6.1.1 shows plots of $\boldsymbol{\Omega}_i$ as a function of time and Figure 6.1.2 shows the attitude in terms of quartenions $\boldsymbol{q}_i$ as a function of time. Note that in the steady state,

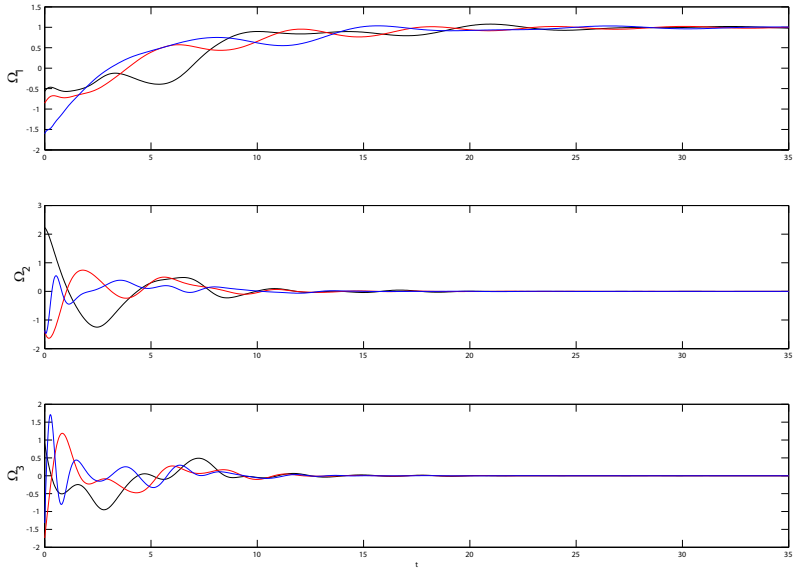

Figure 6.1.1: The angular velocities $\mathbf{\Omega}_i$ (rad/s) three $SO(3)$ vehicles as a function of time.

the last two components of the quaternions are zero which indicates that the bodies are rotating about the $\boldsymbol{e}_1$ axis. Also, since the first component of $\boldsymbol{q}_i$ is $\cos(\theta_i/2)$, the time period in Figure 6.1.2 is twice the time period of the body, which is 4π seconds.

6.2 Asymptotic Synchronization of Networked $SE(3)$ Bodies

For the $SE(3)$ network case, our goal is first to asymptotically stabilize the solution where the bodies are synchronized, rotating about and translating along a particular direction in inertial space, also aligned with their short axis. The analogous case when each of the bodies is rotating about its middle axis can be obtained by combining techniques in this section with kinetic shaping described in §5.1.1. We will assume that the direction of rotation and translation is the $\boldsymbol{e}_1$ axis.

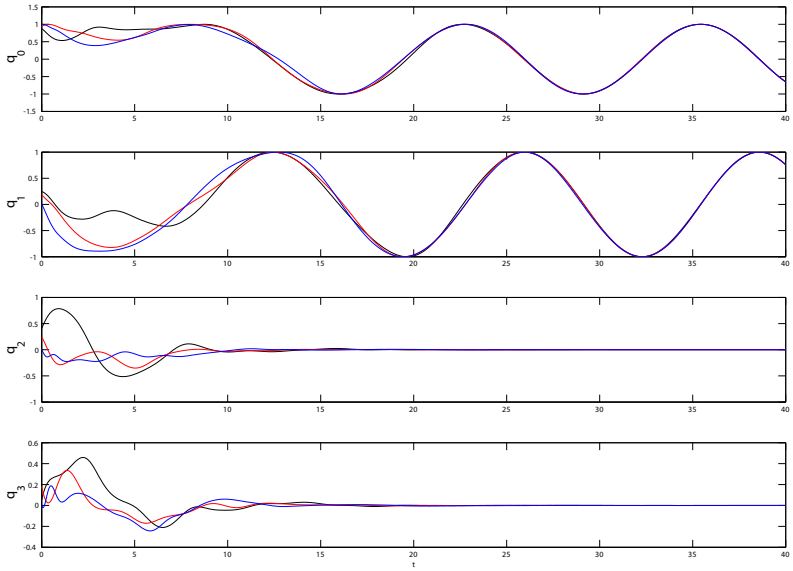

Figure 6.1.2: The attitudes $\boldsymbol{q}_i$ (rad) for three $SO(3)$ vehicles as a function of time.

The equations of motion with dissipation terms are

$$I_i\dot{\boldsymbol{\Omega}}_i = (I_i\boldsymbol{\Omega}_i)\times\boldsymbol{\Omega}_i + (M_i\boldsymbol{v}_i)\times\boldsymbol{v}_i + \sigma_1(\boldsymbol{u}^{ps}_{\tau,i-1} - \boldsymbol{u}^{ps}_{\tau i}) + \boldsymbol{u}^{\text{diss}}_{\tau i} \tag{6.2.1}$$

$$M_i\dot{\boldsymbol{v}}_i = (M_i\boldsymbol{v}_i)\times\boldsymbol{\Omega}_i + \sigma_2\boldsymbol{u}^{ps}_{fi} + \boldsymbol{u}^{\text{diss}}_{fi} \tag{6.2.2}$$

where $\boldsymbol{u}^{ps}_{\tau i}$ for $i \neq 0, n$ is given by (5.2.28), $\boldsymbol{u}^{ps}_{\tau 0} = -R_1^{-1}((R_1\boldsymbol{e}_1)\times\boldsymbol{e}_1)$, $\boldsymbol{u}^{ps}_{\tau n} = 0$,

$$\boldsymbol{u}^{ps}_{f1} = -R_1^{-1}\begin{pmatrix} 0 \\ b_{12} \\ b_{13} \end{pmatrix} - R_1^{-1}(\boldsymbol{b}_1 - \boldsymbol{b}_2), \tag{6.2.3}$$

$\boldsymbol{u}^{ps}_{fi} = -R_i^{-1}(2\boldsymbol{b}_i - \boldsymbol{b}_{i+1} - \boldsymbol{b}_{i-1})$ for $i = 2, \ldots, n-1$ and $\boldsymbol{u}^{ps}_{fn} = -R_n^{-1}(\boldsymbol{b}_n - \boldsymbol{b}_{n-1})$.

The relative equilibrium we want to asymptotically stabilize is:

$$\begin{aligned} R_i &= R_j = R_e, \quad i \neq j \\ \boldsymbol{b}_i &= \boldsymbol{b}_j, \quad i \neq j \\ R_e \boldsymbol{e}_1 &= \boldsymbol{e}_1 \\ \boldsymbol{b}_i &\parallel \boldsymbol{e}_1 \\ \boldsymbol{\Omega}_i &= \boldsymbol{\omega}_i = k_1 \boldsymbol{e}_1, \quad k_1 \in \mathbb{R} \\ \boldsymbol{v}_i &= \dot{\boldsymbol{b}}_i = k_2 \boldsymbol{e}_1, \quad k_2 \in \mathbb{R}. \end{aligned} \tag{6.2.4}$$

The following function will be used as a Lyapunov function for the relative equilibrium manifold:

$$\begin{aligned} E_2 = \quad & \frac{1}{2} \sum_{i=1}^{n} \Big((\boldsymbol{\omega}_i - k_1 \boldsymbol{e}_1)^T I_{li} (\boldsymbol{\omega}_i - k_1 \boldsymbol{e}_1) + (\dot{\boldsymbol{b}}_i - k_2 \boldsymbol{e}_1)^T M_{li}^{-1} (\dot{\boldsymbol{b}}_i - k_2 \boldsymbol{e}_1) \Big) \\ & + V_{\boldsymbol{\mu}} \end{aligned}$$

where $V_{\boldsymbol{\mu}}$ is given by (5.2.35). The function E_2 has the same form as (3.7.1) with v_{RE} being the vector obtained by concatenating $k_1 \boldsymbol{e}_1$ and $k_2 \boldsymbol{e}_1$. Hence, we can use Theorem 3.7.1 or a direcet calculation similar to the $SO(3)$ case which was worked out in Appendix A to calculate the time derivative of E_2 as

$$\frac{d}{dt} E_2 = \sum_{i=1}^{n} (\boldsymbol{\omega} - k_1 \boldsymbol{e}_1) \cdot (R_i \boldsymbol{u}_{\tau i}^{\text{diss}}) + \sum_{i=1}^{n} (\boldsymbol{v}_i - k_2 \boldsymbol{e}_1) \cdot (R_i \boldsymbol{u}_{fi}^{\text{diss}}). \tag{6.2.5}$$

If we choose

$$\boldsymbol{u}_{\tau i}^{\text{diss}} = -\kappa R_i^{-1} (\boldsymbol{\omega}_i - k_1 \boldsymbol{e}_1) \tag{6.2.6}$$

$$\boldsymbol{u}_{fi}^{\text{diss}} = -\kappa R_i^{-1} (\dot{\boldsymbol{b}}_i - k_2 \boldsymbol{e}_1) \tag{6.2.7}$$

where $\kappa > 0$, then $\dot{E}_2 \leq 0$. Since the system is fully actuated, it is also linearly controllable at each point. By construction, E_2 is minimun when conditions in (6.2.4) are satisfied. Hence, it is a Lyapunov function for the relative equilibrium manifold. We can now use Theorem 3.7.2 to conclude that the solution exponentially goes to

the set $E_2 = 0$. On this set, the only solution is

$$\begin{aligned} \boldsymbol{\omega}_i &= k_1 \boldsymbol{e}_1 \\ \dot{\boldsymbol{b}}_i &= k_2 \boldsymbol{e}_1 \\ R_i &= R_j = R_e \\ \boldsymbol{b}_i &= \boldsymbol{b}_j \\ R_e \boldsymbol{e}_1 &= \boldsymbol{e}_1 \\ \boldsymbol{b}_i &\parallel \boldsymbol{e}_1. \end{aligned}$$

This corresponds to the synchronized motion where the rigid bodies are aligned with each other, each one is rotating about the $\boldsymbol{e}_1$ axis and translating along the same axis. We also have $\boldsymbol{\Omega}_i = R_e^{-1}\boldsymbol{\omega}_i = k_1\boldsymbol{e}_1$ and $\boldsymbol{v}_i = R_e^{-1}\dot{\boldsymbol{b}}_i = k_2\boldsymbol{e}_1$. Therefore, the rotation and translation axis of each body is its short axis which is aligned with the $\boldsymbol{e}_1$ axis in the inertial frame. Hence, we get the following theorem.

Theorem 6.2.1 *The rigid body $SE(3)$ network with equations of motion given by* (6.2.1) *and* (6.2.2) *and dissipation chosen as in* (6.2.6) *and* (6.2.7) *has asymptotically stable synchronized relative equilibria solutions given by* (6.2.4).

Figures 6.2.1 and 6.2.2 illustrate the results of a MATLAB simulation for the controlled network of three identical $SE(3)$ systems. The inertia and mass matrix parameters are $I_1 = 6\text{kg} - \text{m}^2$, $I_2 = 4\text{kg} - \text{m}^2$, $I_3 = 2\text{kg} - \text{m}^2$, $M_1 = 8\text{kg}$, $M_2 = 5\text{kg}$ and $M_3 = 1\text{kg}$. The relative equilibrium velocities are chosen to be $\boldsymbol{\omega}_i = \boldsymbol{e}_1$ and

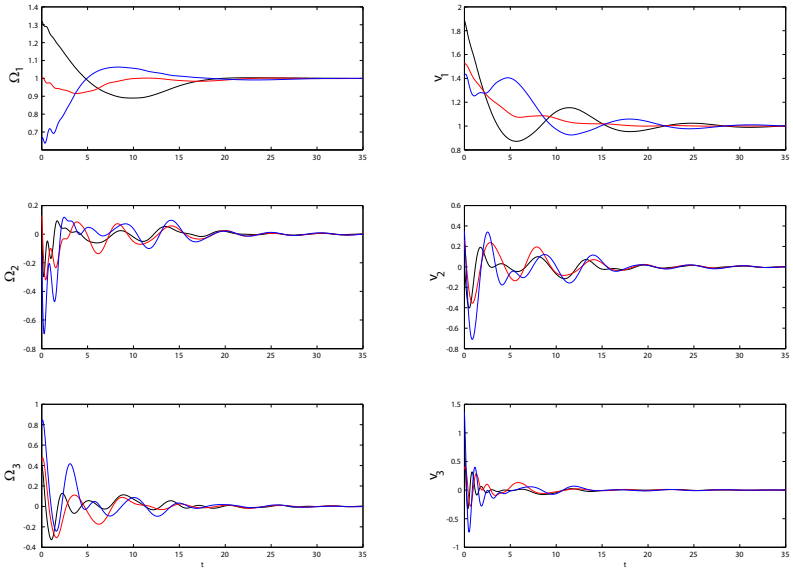

Figure 6.2.1: The angular velocities $\boldsymbol{\Omega}_i$ (rad/s) and linear velocities $\boldsymbol{v}_i$ (m/s) for three $SE(3)$ vehicles as a function of time.

$\dot{\boldsymbol{b}}_i = \boldsymbol{e}_1$. The initial conditions are:

$$\boldsymbol{q}_1(0) = \begin{pmatrix} 0.10 \\ 0.00 \\ 0.02 \\ 0.01 \end{pmatrix}, \boldsymbol{q}_2(0) = \begin{pmatrix} 0.10 \\ 0.09 \\ 0.04 \\ 0.02 \end{pmatrix}, \boldsymbol{q}_3(0) = \begin{pmatrix} 1.00 \\ 0.00 \\ 0.00 \\ 0.00 \end{pmatrix},$$

$$\dot{\boldsymbol{q}}_1(0) = \begin{pmatrix} -0.00 \\ 0.54 \\ 0.06 \\ 0.19 \end{pmatrix}, \dot{\boldsymbol{q}}_2(0) = \begin{pmatrix} -0.06 \\ 0.59 \\ 0.17 \\ 0.13 \end{pmatrix}, \dot{\boldsymbol{q}}_3(0) = \begin{pmatrix} -0.00 \\ 0.71 \\ 0.21 \\ 0.24 \end{pmatrix},$$

$$\boldsymbol{b}_1(0) = \begin{pmatrix} 0.06 \\ 0.11 \\ 0.81 \end{pmatrix}, \boldsymbol{b}_2(0) = \begin{pmatrix} 0.38 \\ 0.56 \\ 0.49 \end{pmatrix}, \boldsymbol{b}_3(0) = \begin{pmatrix} 0.81 \\ 0.26 \\ 0.21 \end{pmatrix},$$

$$\dot{\boldsymbol{b}}_1(0) = \begin{pmatrix} 1.46 \\ 0.91 \\ 0.90 \end{pmatrix}, \dot{\boldsymbol{b}}_2(0) = \begin{pmatrix} 1.16 \\ 0.65 \\ 0.73 \end{pmatrix}, \dot{\boldsymbol{b}}_3(0) = \begin{pmatrix} 1.93 \\ 0.39 \\ 0.06 \end{pmatrix},$$

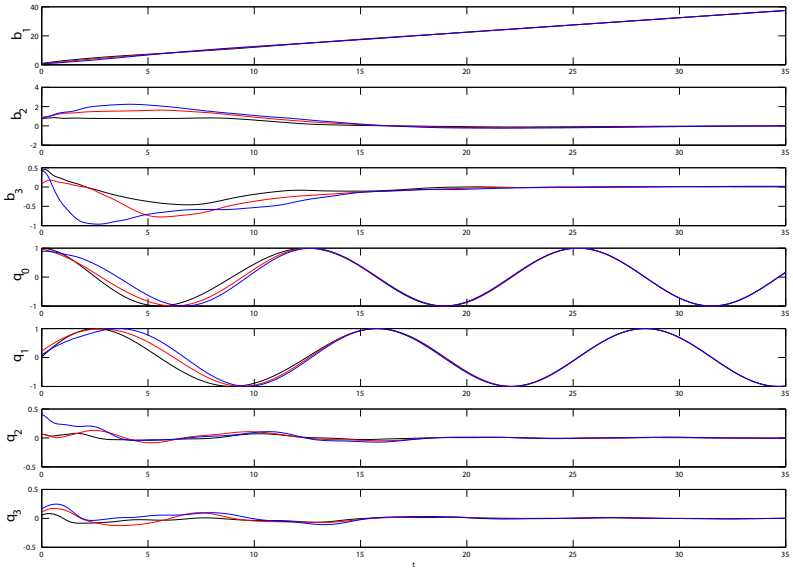

Figure 6.2.2: The attitudes $\boldsymbol{q}_i$ (rad) and position $\boldsymbol{b}_i$ (m) for three $SE(3)$ vehicles as a function of time.

and the control gains are $\sigma_1 = 1, \sigma_2 = 2, \kappa = 2$. Figure 6.2.1 shows plots of $\boldsymbol{\Omega}_i$ and $\boldsymbol{v}_i$ as a function of time and Figure 6.2.1 shows the attitude and position in terms of quartenions $\boldsymbol{q}_i$ and $\boldsymbol{b}_i$ respectively as a function of time.

Chapter 7

Conclusions and Future Work

In this chapter, we summarize the main contributions of this thesis work. We also briefly discuss some directions in which this work can be extended.

7.1 Summary

The primay contribution of this thesis is to foundations and provable strategies for coordination and control of a class of mechanical systems. These mechanical systems also have possibly unstable dynamics unlike point mass models. The natural Lagrangian structure of the individual mechanical system is used to derive an energy-based control law to achieve the task. This is done so that the controlled dynamics describe a multi-body, mechanical system. Because of underactuation, after adding a dissipative term to the control, not all the eigenvalues of the linearized controlled system lie in the strict left-half plane. Hence, the natural energy of the closed-loop system plays a crucial role in proving stability. In addition to studying stabilization of relative equilibria of coupled network of a class of mechanical systems, we have also shown how to achieve more general synchronized behaviour using energy-based methods. For example, these solutions turn out to be periodic solutions for a network of inverted pendulum/cart systems.

We will compare our coordination results with a technique based on LQR method in §7.1.1 and give a summary of the results from Chapter 3 through Chapter 6 in §7.1.2.

7.1.1 Comparison with LQR

We will now discuss how our method compares with the following procedure using LQR to stabilize individual system and then coordinating them using the state of one system as a setpoint for another system. We look at the specific example of n identical inverted pendulum/cart system and illustrate the differences in methods using simulation.

For the individual linearized inverted pendulum/cart system, the state of the i^{th} system is given by the column vector $(x_i \;\; \dot{x}_i \;\; \theta_i \;\; \dot{\theta}_i)^T$. The notation used here is the same as used in §3.8 where x_i and θ_i denote the angle made by pendulum with the vertical line and cart position of the i^{th} system respectively. The cart mass, pendulum mass and pendulum length are also chosen to be the same as in §3.8. The linearized dynamics for an individual system then look as follows:

$$\frac{d}{dt}\begin{pmatrix} x_i \\ \dot{x}_i \\ \theta_i \\ \dot{\theta}_i \end{pmatrix} = A \begin{pmatrix} x_i \\ \dot{x}_i \\ \theta_i \\ \dot{\theta}_i \end{pmatrix} + Bu_i$$

where

$$A = \begin{pmatrix} 0 & 1 & 0 & 0 \\ 60.19 & 0 & 0 & 0 \\ 0 & 0 & 0 & 1 \\ -3.12 & 0 & 0 & 0 \end{pmatrix}, \quad B = \begin{pmatrix} 0 \\ -10.57 \\ 0 \\ 2.27 \end{pmatrix}.$$

For the state-space model, the output is chosen to be $(x_i \;\; \theta_i)^T = C(x_i \;\; \dot{x}_i \;\; \theta_i \;\; \dot{\theta}_i)^T$,

where C is the matrix

$$\begin{pmatrix} 1 & 0 & 0 & 0 \\ 0 & 0 & 1 & 0 \end{pmatrix}. \tag{7.1.1}$$

The Q matrix is chosen to be C^TC and R is chosen to be 1. For this choice of Q and R, the LQR feedback gain K is calculated. Therefore, if the cart force for the i^{th} system is chosen to be $u_i = -K(x_i \;\; \dot{x}_i \;\; \theta_i \;\; \dot{\theta}_i)^T$, this control law brings each system asymptotically to the origin.

We now couple the systems using the controls

$$\begin{aligned} u_1 &= -K(x_1 \;\; \dot{x}_1 \;\; (\theta_1 - \theta_2) \;\; \dot{\theta}_1)^T \\ u_n &= -K(x_n \;\; \dot{x}_n \;\; (\theta_n - \theta_{n-1}) \;\; \dot{\theta}_n)^T \\ u_i &= -K(x_i \;\; \dot{x}_i \;\; (2\theta_i - \theta_{i-1} - \theta_{i+1}) \;\; \dot{\theta}_i)^T \end{aligned} \tag{7.1.2}$$

for $i = 2, \ldots, n-1$. The control given by (7.1.2) corresponds to the same communication topology we assumed in §3.8.

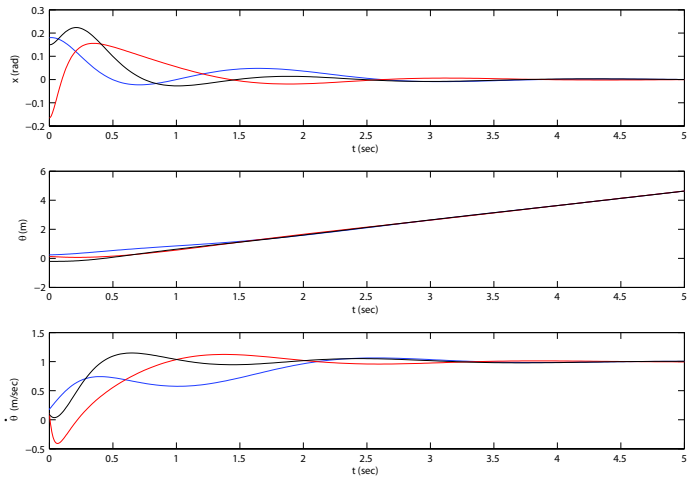

Figure 7.1.1: Simulation of a controlled network of pendulum/cart systems using the LQR technique. The pendulum angle, cart position and cart velocity are plotted as a function of time for each of three pendulum/cart systems in the network.

Two simulation plots are given in Figure 7.1.1 and Figure 7.1.2 for the same initial

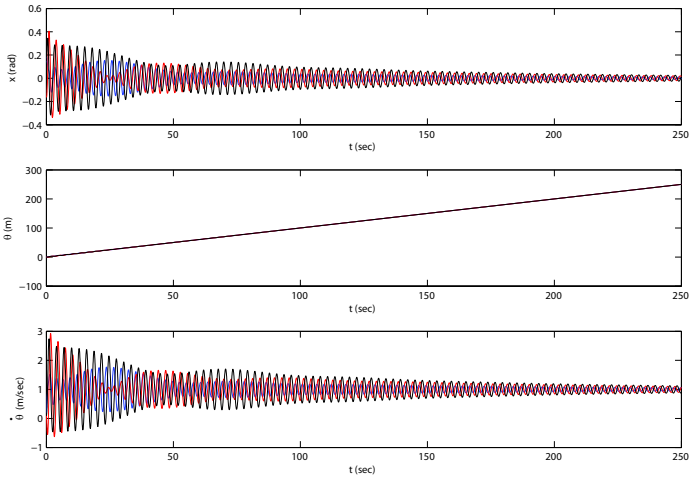

Figure 7.1.2: Simulation of a controlled network of pendulum/cart systems using the control law given in (3.7.2). The pendulum angle, cart position and cart velocity are plotted as a function of time for each of three pendulum/cart systems in the network.

condition given by

$$\begin{pmatrix} x_1(0) & \dot{x}_1(0) & \theta_1(0) & \dot{\theta}_1(0) & x_2(0) & \dot{x}_2(0) & \theta_2(0) & \dot{\theta}_2(0) & x_3(0) & \dot{x}_3(0) & \theta_3(0) & \dot{\theta}_3(0) \end{pmatrix}$$
$$= \begin{pmatrix} 0.18 & 0.06 & 0.24 & 0.18 & -0.17 & 0.03 & 0.12 & 0.11 & 0.15 & -0.10 & 0.21 & 0.10 \end{pmatrix}.$$

Figure 7.1.1 is a simulation with the control law for the individual system given by equation (7.1.2) and Figure 7.1.2 is a simulation with the control law given by (3.7.2). We see in this example that the LQR method has a faster settling time and less overshoot as compared to our method.

Now consider an initial condition further from the equilibrium.

$$\begin{pmatrix} x_1(0) & \dot{x}_1(0) & \theta_1(0) & \dot{\theta}_1(0) & x_2(0) & \dot{x}_2(0) & \theta_2(0) & \dot{\theta}_2(0) & x_3(0) & \dot{x}_3(0) & \theta_3(0) & \dot{\theta}_3(0) \end{pmatrix}$$
$$= \begin{pmatrix} 1.20 & 0.40 & 1.60 & 1.20 & -1.10 & 0.20 & 0.80 & 0.70 & 1.00 & -0.50 & -1.40 & 0.60 \end{pmatrix}.$$

The value of the angles in this initial condition are as high as 1.2 radians. The simulation plot for the above initial condition is shown in Figure 7.1.3. For this initial condition, the LQR approach destabilizes the network, whereas our control law given by (3.7.2) still works fine as shown in Figure 7.1.3.

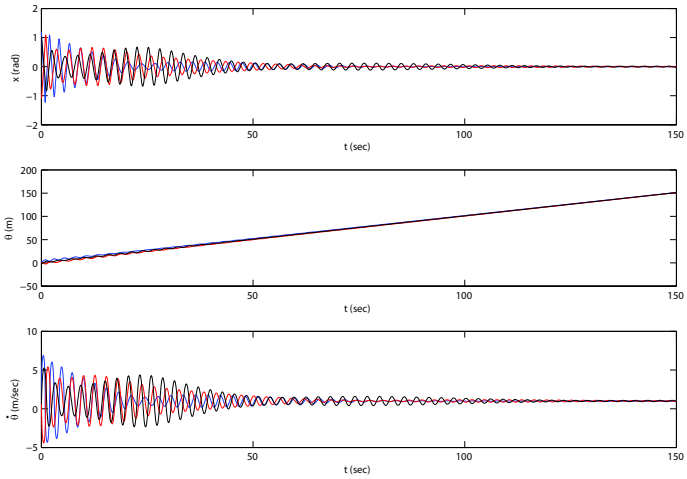

Figure 7.1.3: Simulation of a controlled network of pendulum/cart systems using the control law given in (3.7.2). The pendulum angle, cart position and cart velocity are plotted as a function of time for each of three pendulum/cart systems in the network.

Thus, this example suggests that in the common region of attraction, LQR has better performance features. This is consistent with the principle that LQR is tuned for performance of the linearized dynamics. However, our method, being a nonlinear energy based control method, has a larger region of attraction. In fact, for the inverted pendulum/cart system, if the parameter κ in §3.8 is chosen large enough, the initial angle of the pendulum can be chosen to lie as close to the horizontal plane as one wishes at the expense of having a larger control force. It is intuitively clear that no matter what control law is chosen, if the initial angle of the pendulum is close to the horizontal plane, a huge cart force is required to make sure it does not cross the horizontal plane.

7.1.2 Chapter Summary

We now summarize the main results from Chapter 3 through Chapter 6.

In Chapter 3, we derived control laws to stabilize and coordinate a network of SMC systems which are a class of underactuated systems with symmetry in the

kinetic energy and with no gyroscopic forcing. The control law is derived using energy methods and Lyapunov stability is proven using the Routh reduction criteria. With dissipation included as a term in the control law, we proved two kinds of asymptotic stability. The first case consists of driving the network to a synchronized solution staying on a constant momentum surface that depends upon the initial condition. For the example of a network of planar pendulum/cart systems, these solutions correspond to synchronized oscillatory motions of the cart with a common velocity and with each pendulum also oscillating with the same (tunable) frequency. The second case consists of driving the network to a prespecified relative equilibrium. Again, for the network of planar pendulum/cart systems, this corresponds to the carts moving in synchrony, each along its individual track with a constant velocity and with its pendulum in the upright position.

Each of these cases was proven using an appropriate Lyapunov function and a LaSalle Invariance Principle argument. For each of these cases, the eigenvalues of the linearized system do not lie in the strict left half plane. Hence, the energy functions are critical in proving nonlinear stability.

In Chapter 4, we showed how to derive reduced equations of motion for the case of a network of systems with configuration space $SO(3)^n$ or $SE(3)^n$ coupled using artificial potentials. The symmetry group is $SO(3)$ in the case of a network on $SO(3)^n$ and $SE(3)$ in the case of a network on $SE(3)^n$. The reduced equations make it possible to state explicitly the control laws in Chapter 5 and Chapter 6.

In Chapter 5, we proved stability of relative equilibria for a network of systems in $SO(3)^n$ and $SE(3)^n$. For the $SO(3)^n$ case, these equilibria correspond to the case where each body has the same orientation and is rotating with the same constant angular velocity about its principle axis. For the $SE(3)^n$ case, these equilibria correspond to the case where each body has the same orientation and position in inertial space. Moreover, each body is also rotating about and translating along a particular direction in inertial space.

In Chapter 6, we proved asymptotic stability of relative equilibria for which stability was proved in Chapter 5. Dissipation was designed using appropriate Lyapunov functions which were minimized on the relative equilibrium manifold. This dissipation was added to the control law. The results were illustrated with simulations for a network of three bodies, all in $SO(3)$ or $SE(3)$. The equilibrium angular velocity is tunable using a control parameter. For both $SO(3)$ and $SE(3)$ cases, the first body was chosen as a "leader". In the $SO(3)$ case, the first body was assigned a potential term which makes it orient along the $\boldsymbol{e}_1$ axis in inertial space. In the $SE(3)$ case, the first body was assigned a potential term to align along the $\boldsymbol{e}_1$ axis and translate along the same axis. The choice of which body is leader is arbitrary. It will be an interesting future direction to see if this can be extended to achieve more general tracking maneuvers. One example is where the leader keeps changing its orientation in inertial frame and the remaining systems in the group asymptotically tracks the leader.

7.2 Future directions

Some of the directions in which this thesis can be extended are as follows.

Varying Communication Topology In our approach, the communication topology was fixed for the whole analysis. It will be interesting to see if this can be relaxed. We would like to propose the following approach. Corresponding to each connected communication topology, there exists a coupling potential function which we denote by V_{Ti} where i indexes the topology. A varying communication topology can be modelled by assigning the potential $\tilde{V} = \sum_{i=1}^{k} \rho_i(t) V_{Ti}$ to the closed-loop system. Here k is the number of connected graphs with n nodes. The functions ρ_i could be chosen to be discontinuous square-wave functions or their smoothened versions. The closed-loop Hamiltonian is time dependent in this setting and results from time varying Lyapunov theory need to be used to analyze stability issues. Some very recent works

on time-varying communication topologies are [26, 36]. The goal in these papers is to address network of systems on $\mathbb{R}^n$.

Parameter dependent Lagrangian In Remark 3.6 after Theorem 3.6.1 we stated a control law to make the network of SMC systems converge asymptotically to a prespecified momentum value. Simulations suggest that this can be achieved if the parameter λ is chosen sufficiently small. This seems reasonable since for a large value of λ, the system is driven to a desired momentum value at a "fast" rate which is achieved by pumping energy into the system. If this is not done carefully, it could destabilize the network of SMC systems. This problem raises the following question. Consider a dynamical system whose Lagrangian depends upon a parameter λ, i.e., $L = L(q, \dot{q}, \lambda)$. Suppose for each $\lambda \in [0, \epsilon]$, the system is Lyapunov stable. Is it true that the system is still Lyapunov stable if λ "slowly" evolves in time and goes to a particular value $\bar{\epsilon} \in (0, \epsilon)$? This is an interesting parameter dependency problem. Some of these related problems are addressed in [28, 3] and references therein. The results in [28] for example deals with the case where the system with fixed parameter is asymptotic or exponentially stable. Analytical results are then proven for the case where the parameter is now made to evolve slowly.

Extension of Controlled Lagrangian Another interesting direction is to extend the method of Controlled Lagrangians (CL) itself for SMC systems. For SMC systems, CL gives an algorithm to derive a control law such that the closed-loop system is also Lagrangian. The question is if we could ask for more, i.e., whether there exists a control law such that the closed-loop system is also mechanical with kinetic energy that is strictly definite. For example, in the pendulum/cart example, for a given value of κ in (3.8.2), the determinant of the closed-loop mass matrix is negative, zero or positive depending upon the value of the state of the system. If we could choose controls along the cart direction such that the closed-loop mass matrix has a determinant with fixed sign, then we can design a smooth swing up stabilization and

coordination control law for the pendulum/cart network system. This is because, for an inverted pendulum/cart system without controls, if there is dissipation the system asymptotically goes to the state where velocities are zero and the pendulum is aligned along its stable downward position. This can be considered as the natural swing down phenomena for the system. For this case, the Hamiltonian of the system can be used as a Lyapunov function and along with a LaSalle Invariance principle argument, the conclusion can be obtained. Suppose we could use controls along the cart direction to make the mass matrix negative definite throughout, then the closed-loop Hamiltonian can again be used as a Lyapunov function. And after adding dissipation, the inverted pendulum/cart system will smoothly swing up and asymptotically approach the state where velocites are zero and pendulum is in its upright position.

7.3 Conclusion

This dissertation described how to achieve coordination and stabilization of a network of mechanical systems using energy-based methods. The systems considered were a class of mechanical systems satisfying the Simplified Matching Conditions, free rigid bodies each in $SO(3)$ and rigid bodies following the Kirchhoff's equations of motion, each in $SE(3)$. In this chapter, we compared our results using the example of an inverted pendulum/cart network with LQR based techniques and illustrated the differences. Finally, we discussed a few directions in which this work can be extended.

Appendix A

Calculations for $\dot{E}_1$

We will first write down the equations of motion given by (6.1.2) in inertial coordinates using the fact that $R_i\boldsymbol{\Omega}_i = \boldsymbol{\omega}_i$ and $\dot{R}_i = \widehat{\boldsymbol{\omega}}_i R_i$. The equations of motion in the inertial frame turn out to be

$$\dot{\boldsymbol{\pi}}_i = \sigma(\mathfrak{A}_{i-1} - \mathfrak{A}_i) + R_i \boldsymbol{u}_i^{diss} \tag{A.0.1}$$

where $\mathfrak{A}_i = R_i \boldsymbol{u}_i^{ps}$ for $i = 1, \ldots, n$. Here, $\boldsymbol{u}_i^{ps}$ is given as in (6.1.2) and corresponds to the controls in the i^{th} body frame. Using $I_{li} = R_i I_i R_i^{-1}$ and $\boldsymbol{\pi}_i = I_{li}\boldsymbol{\omega}_i$, we can write the above equation as

$$I_{li}\dot{\boldsymbol{\omega}}_i + \widehat{\boldsymbol{\omega}}_i I_{li}\boldsymbol{\omega}_i = \sigma(\mathfrak{A}_{i-1} - \mathfrak{A}_i) + R_i \boldsymbol{u}_i^{diss}. \tag{A.0.2}$$

Using the expression for E_1 given by (6.1.5), we can calculate its time derivative to be

$$\begin{aligned} \dot{E}_1 &= \sum_{i=1}^{n} \Big((\boldsymbol{\omega}_i - k\boldsymbol{e}_1)^T I_{li}(\dot{\boldsymbol{\omega}}_i + \boldsymbol{\omega}_i \times \boldsymbol{e}_1) + \boldsymbol{e}_1^T (I_{li}\widehat{\boldsymbol{\omega}}_i)\boldsymbol{e}_1 \Big) \\ &\quad + \sum_{i=1}^{n-1} \sigma(\boldsymbol{\omega}_i - \boldsymbol{\omega}_{i+1})^T (\mathfrak{A}_i) + \sigma \boldsymbol{\omega}_1^T ((R_1\boldsymbol{e}_1) \times \boldsymbol{e}_1). \end{aligned} \tag{A.0.3}$$

Plugging in expression for $I_{li}\dot{\boldsymbol{\omega}}_i$ from (A.0.2) into (A.0.3), we get

$$\begin{aligned}\dot{E}_1 &= \sum_{i=1}^{n}\Big((\boldsymbol{\omega}_i - k\boldsymbol{e}_1)^T(-\widehat{\boldsymbol{\omega}}_i I_{li}\boldsymbol{\omega}_i + \sigma(\mathfrak{A}_{i-1} - \mathfrak{A}_i) + R_i\boldsymbol{u}_i^{diss} + I_{li}\widehat{\boldsymbol{\omega}}_i\boldsymbol{e}_1) + \boldsymbol{e}_1^T(I_{li}\widehat{\boldsymbol{\omega}}_i)\boldsymbol{e}_1\Big)\\ &\quad + \sum_{i=1}^{n-1}\sigma(\boldsymbol{\omega}_i - \boldsymbol{\omega}_{i+1})^T(\mathfrak{A}_i) + \sigma\boldsymbol{\omega}_1^T((R_1\boldsymbol{e}_1)\times\boldsymbol{e}_1).\end{aligned}$$

Therefore, we have

$$\begin{aligned}\dot{E}_1 &= \sigma\sum_{i=1}^{n}\boldsymbol{\omega}_i^T(\mathfrak{A}_{i-1} - \mathfrak{A}_i) + \sigma\sum_{i=1}^{n-1}(\boldsymbol{\omega}_i - \boldsymbol{\omega}_{i+1})^T(\mathfrak{A}_i) + \sigma\boldsymbol{\omega}_1^T((R_1\boldsymbol{e}_1)\times\boldsymbol{e}_1)\\ &\quad + \sum_{i=1}^{n}\Big(\boldsymbol{e}_1\widehat{\boldsymbol{\omega}}_i I_{li}\boldsymbol{\omega}_i + \boldsymbol{\omega}_i^T I_{li}\widehat{\boldsymbol{\omega}}_i\boldsymbol{e}_1 - \boldsymbol{e}_1^T I_{li}\widehat{\boldsymbol{\omega}}_i\boldsymbol{e}_1 + \boldsymbol{e}_1^T I_{li}\widehat{\boldsymbol{\omega}}_i\boldsymbol{e}_1\Big)\\ &\quad + \sigma\boldsymbol{e}_1^T\sum_{i=1}^{n}(\mathfrak{A}_{i-1} - \mathfrak{A}_i) + \sum_{i=1}^{n}\Big((\boldsymbol{\omega}_i - k\boldsymbol{e}_1)^T R_i\boldsymbol{u}_i^{diss}\Big). \qquad \text{(A.0.4)}\end{aligned}$$

Rearranging the above equation, we have

$$\begin{aligned}\dot{E}_1 &= \sigma\boldsymbol{\omega}_1^T\mathfrak{A}_0 + \sigma\boldsymbol{e}_1^T\mathfrak{A}_0 + \sigma\boldsymbol{\omega}_1^T((R_1\boldsymbol{e}_1)\times\boldsymbol{e}_1)\\ &\quad + \sum_{i=1}^{n}\Big((\boldsymbol{\omega}_i - k\boldsymbol{e}_1)^T R_i\boldsymbol{u}_i^{diss}\Big). \qquad \text{(A.0.5)}\end{aligned}$$

Using the fact that $\mathfrak{A}_0 = -((R_1\boldsymbol{e}_1)\times\boldsymbol{e}_1)$, the first line in (A.0.5) vanishes. Hence, we get the following expression for $\dot{E}_1$:

$$\dot{E}_1 = \sum_{i=1}^{n}\Big((\boldsymbol{\omega}_i - k\boldsymbol{e}_1)^T R_i\boldsymbol{u}_i^{diss}\Big). \qquad \text{(A.0.6)}$$

References

[1] R. Abraham and J.E. Marsden. *Foundations of Mechanics.* Addison-Wesley, Reading, MA, 2nd edition, 1987.

[2] R. Abraham, J.E. Marsden, and T.S. Ratiu. *Manifolds, Tensor Analysis, and Applications.* Springer-Verlag, New York, NY, 2nd edition, 1988.

[3] V.I. Arnold. *Mathematical Methods of Classical Mechanics.* Springer-Verlag, New York, NY, 2nd edition, 1989.

[4] V.I. Arnold. *Ordinary Differential Equations.* Springer-Verlag, New York, NY, 2nd edition, 1992.

[5] K.J. Astrom and K. Furuta. Swinging up a pendulum by energy control. *Automatica*, 36(2):287–295, February 2000.

[6] D. Auckly, L. Kapitanski, and W. White. Control of nonlinear underactuated systems. *Comm. Pure Appl. Math.*, 53:354–369, 2000.

[7] A. L. Bertozzi, M. Kemp, and D. Marthaler. Determining environmental boundaries: Asynchronous communication and physical scales. In V. Kumar, N. E. Leonard, and A.S. Morse, editors, *Cooperative Control: 2003 Block Island Workshop on Cooperative Control*, pages 25–42. Springer-Verlag, 2005.

[8] A. M. Bloch, D.E. Chang, N. E. Leonard, and J. E. Marsden. Controlled Lagrangians and the stabilization of mechanical systems II: Potential shaping. *IEEE Trans. Aut. Cont.*, 46(10):1556–1571, 2001.

[9] A. M. Bloch, P. S. Krishnaprasad, J. E. Marsden, and G. Sánchez de Alvarez. Stabilization of rigid body dynamics by internal and external torques. *Automatica*, 28(4):745–756, 1992.

[10] A. M. Bloch, N. E. Leonard, and J. E. Marsden. Controlled Lagrangians and the stabilization of mechanical systems I: The first matching theorem. *IEEE Trans. Aut. Cont.*, 45(12):2253–2270, 2000.

[11] A. M. Bloch, N. E. Leonard, and J. E. Marsden. Controlled Lagrangians and the stabilization of Euler-Poincaré mechanical systems. *International Journal of Robust and Nonlinear Control*, 11(3):191–214, 2001.

[12] W.M. Boothby. *An Introduction to Differential Manifolds and Riemannian Geometry*. Academic Press, 2nd edition, 1986.

[13] F. Bullo. Stabilization of relative equilibria for underactuated systems on Riemannian manifolds. *Automatica*, 36(12):1819–1834, 2000.

[14] H. Cendra, J.E. Marsden, and T.S. Ratiu. Lagrangian reduction by stages. *Memoirs of American Mathematical Society*, 152(722), 2001.

[15] D.E. Chang. The extended lambda-method for controlled lagrangian systems. In *Proc. IFAC*, Prague, Czech.

[16] D.E. Chang, A. M. Bloch, N. E. Leonard, J. E. Marsden, and C. Woolsey. The equivalence of controlled Lagrangian and controlled Hamiltonian systems. *ESIAM: Control, Optimisation and Calculus of Variations*, 2001.

[17] D.E. Chang, S.C. Shadden, J.E. Marsden, and R. Olfati-Saber. Collision avoidance for multiple agent systems. In *Proc. IEEE Conf. Decision and Control*, Maui, Hawaii, December 2003.

[18] J. Cortès, T. Martinez, T. Karatas, and F. Bullo. Coverage control for mobile sensing networks. volume 20, pages 243–255, 2004.

[19] J.P. Desai, J.P. Ostrowski, and V. Kumar. Modeling and control of formations of nonholonomic mobile robots. *IEEE Trans. Robotics and Automation*, 17(6):905–908, 2001.

[20] J. Fax and R. Murray. Information flow and cooperative control of vehicle formations. *IEEE Transactions on Automatic Control*, 49(9):1465–1476, 2004.

[21] E. Fiorelli, N.E. Leonard, P. Bhatta, D. Paley, R. Bachmayer, and D.M. Frantonti. Multi-AUV control and adaptive sampling in Monterey Bay. In *Proc. IEEE Autonomous Underwater Vehicles*, Sebasco, ME, June 2004.

[22] E Frazzoli. *Robust Hybrid Control for Autonomous Vehicle Motion Planning.* PhD thesis, MIT, 2001.

[23] E Frazzoli. Motion planning for controllable systems without drift. In *AIAA/IEEE Digital Avionics Systems Conference*, 2002.

[24] J. Hamberg. General matching conditions in the in the theory of controlled Lagrangians. In *Proc. IEEE Conf. Decision and Control*, volume 38, pages 2519–2523, 1999.

[25] H. Hanssmann, N. E. Leonard, and T. R. Smith. Symmetry and reduction for coordinated rigid bodies. *European Journal of Control*, 1, 2006. In press.

[26] A. Jadbabaie, J. Lin, and A.S. Morse. Coordination of groups of mobile autonomous agents using nearest neighbor rules. *IEEE Trans. Aut. Control*, 48(6):988–1001, 2003.

[27] E. Justh and P. Krishnaprasad. Equilibria and steering laws for planar formations. *Systems and Control Letters*, 52(1):25–38, 2004.

[28] H. Khalil. *Nonlinear Systems*. Prentice Hall, Upper Saddle River, New Jersey, 2nd edition, 1996.

[29] H. Lamb. *Hydrodynamics*. Dover, New York, 6th edition, 1932.

[30] N. E. Leonard. Stability of a bottom-heavy underwater vehicle. *Automatica*, 33(3):331–346, 1997.

[31] N. E. Leonard. Stabilization of underwater vehicle dynamics with symmetry-breaking potentials. *Systems and Control Letters*, 32:35–42, 1997.

[32] N. E. Leonard and J. E. Marsden. Stability and drift of underwater vehicle dynamics: Mechanical systems with rigid motion symmetry. *Physica D*, 105:130–162, June 1997.

[33] J. E. Marsden. *Lectures on Mechanics*. Cambridge University Press, New York, New York, 1992.

[34] J. E. Marsden and T. S. Ratiu. *Introduction to Mechanics and Symmetry*. Springer-Verlag, New York, New York, 1994.

[35] Y. Matsumoto. An introduction to Morse theory (translations of mathematical monographs, vol. 208). December 2001.

[36] L. Moreau. Stability of multiagent systems with time-dependent communication links. *IEEE Trans. Aut. Control*, 50(2):169–182, 2005.

[37] S. Nair and N. Leonard. A normal form for energy shaping: Application to the furuta pendulum. In *Proc. of* 41st *IEEE Conf. Decision and Control*, pages 516–521, Las Vegas, NV, December 2002.

[38] S. Nair and N. Leonard. Stable synchronization of mechanical system networks. *SIAM Journal of Control and Optimization*, Dec 2005. Submitted.

[39] K. Nomizu. *Lie Groups and Differential Geometry.* The Mathematical Society of Japan, 1956.

[40] P. Ögren, E. Fiorelli, and N.E. Leonard. Formations with a mission: Stable coordination of vehicle group maneuvers. In *Proc. 15th MTNS*, 2002.

[41] R. Olfati-Saber and R. M. Murray. Graph rigidity and distributed formation stabilization of multi-vehicle systems. In *Proc. IEEE Conf. Decision and Control*, 2002.

[42] R. Ortega, M. W. Spong, F. Gómez-Estern, and G. Blankenstein. Stabilization of underactuated mechanical systems via interconnection and damping assignment. *IEEE Trans. Aut. Control*, 47(4), 2002.

[43] G. Patrick. Relative equilibria in Hamiltonian systems: The dynamic interpretation of nonlinear stability on a reduced phase space. *J. Geom. Phys.*, 9:111–119, 1992.

[44] R. Sepulchre, D. Paley, and N.E. Leonars. Stabilization of planar collective motion, part I: All-to-all communication. *IEEE Transactions on Automatic Control.* Submitted.

[45] M. Spivak. *A Comprehensive Introduction to Differential Geometry.* Publish or Perish, 1976.

[46] M. C. VanDyke. *Decentralized Coordinated Attitude Control of a Formation of Spacecraft.* Master's thesis, Virginia Polytechnic Institute and State University, Blacksburg, VA, 2004.

[47] C. Woolsey. *Energy Shaping and Dissipation: Underwater Vehicle Stabilization Using Internal Rotors.* PhD thesis, Princeton University, Princeton, NJ, January 2001.